

Université de Neuchâtel - Laboratoire Temps-Fréquence (LTF)

---

# Novel Ultrafast High-Power Thin-Disk Laser Oscillators and Applications for Metrology and XUV Generation

---

Thesis presented to the *Faculty of Science* of the University of Neuchâtel  
for the degree of *Doctor of Sciences* by

**Clément Paradis**

*Diplôme d'ingénieur*, ENSTA ParisTech (Paris, France)

*M. Sc. in Applied Photonics*, Imperial College of London (London, UK)

*M. Sc. in Photonics*, Friedrich-Schiller University (Jena, Germany)

Accepted on the recommendation of

Prof. Thomas Südmeyer	Director
Prof. Patrick Georges	Examiner
Dr Antoine Courjaud	Examiner
Dr Valentin J. Wittwer	Examiner

Neuchâtel, December 2017



## IMPRIMATUR POUR THESE DE DOCTORAT

---

La Faculté des sciences de l'Université de Neuchâtel  
autorise l'impression de la présente thèse soutenue par

**Monsieur Clément PARADIS**

Titre:

**“Novel Ultrafast High-Power Thin-Disk  
Laser Oscillations and Applications for  
Metrology and XUV Generation”**

**sur le rapport des membres du jury composé comme suit:**

- Prof. Thomas Südmeyer, directeur de thèse, Université de Neuchâtel, Suisse
- Dr Valentin J. Wittwer, Université de Neuchâtel, Suisse
- Prof. Patrick Georges, Institut d'Optique, CNRS, Paris, France
- Dr Antoine Courjaud, Amplitude Systèmes, Bordeaux, France

Neuchâtel, le 8 mars 2018

Le Doyen, Prof. R. Bshary





“If you saw Atlas, the giant who holds the world on his shoulders, if you saw that he stood, blood running down his chest, his knees buckling, his arms trembling but still trying to hold the world aloft with the last of his strength, and the greater his effort the heavier the world bore down upon his shoulders—What would you tell him to do?”

“I . . . don't know. What . . . could he do? What would *you* tell him?”

“To shrug.”

*Francisco d'Anconia to Hank Rearden in Atlas Shrugged (1957) by Ayn Rand*

# ***Abstract***

Ultrafast lasers have revolutionized research in fundamental physics, chemistry and biology as well as industrial applications. A great number of experiments benefit from the development of Yb-based high-power femtosecond laser sources. These systems typically include a low-power mode-locked oscillator followed by amplifier stages relying on fiber, slab or thin-disk technologies. In many cases, an additional nonlinear pulse compression scheme is necessary to obtain sufficiently short pulse durations. However, external amplification and compression of the pulses add cost and complexity and may degrade the spatial and temporal pulse quality. Moreover, many amplifier schemes are limited in repetition rate which is a challenge for numerous scientific and industrial applications. In contrast, ultrafast thin-disk laser (TDL) oscillators are a simple and compact approach to directly generate powerful ultrashort pulse trains at megahertz repetition rates. State-of-the-art high-power mode-locked TDL oscillators operating around 1  $\mu\text{m}$  central wavelength deliver hundreds-of-watt average power in pulses with hundreds of femtoseconds duration and several tens of microjoule pulse energy. These lasers have already been successfully used to drive initial experiments in high-field science at megahertz repetition rate without any external amplification. Yet, external pulse compression to the sub-100-fs regime was required for these experiments. Generating powerful sub-100-fs pulses directly from ultrafast TDLs would strongly improve their suitability for application fields such as material processing, bio-medical research, or fundamental science. Nevertheless, prior to this work, the power levels achieved by TDL oscillators in the sub-100-fs regime have been limited to 5 W and the minimum pulse duration was 60% longer than for bulk Yb-based oscillators.

This thesis describes the development of novel ultrafast Yb-based TDL oscillators with improved performance at sub-100-fs pulse duration. During the last 17 years, the shortest pulse durations from ultrafast TDLs were obtained by semiconductor-saturable-absorber-mirror (SESAM) mode locking of different Yb-doped gain crystals with broad emission cross sections. In this thesis, the potential of such broadband gain materials is explored in Kerr lens mode locking, which technique provides a faster response and a high modulation depth. The influence of key laser parameters is investigated for the generation of powerful ultrashort laser pulses. This research led to a Kerr lens mode-locked (KLM) TDL based on an Yb:LuO crystal with a record-high average power from any TDL in both sub-100-fs and sub-50-fs pulse duration regimes. With more than 10 W of average output power in 90 fs pulses, the laser

---

emits twice more power than previously achieved by sub-100-fs-class TDL oscillators. This proof-of-principle study opens avenues for average- and peak-power scaling towards the generation of ultrashort pulses from simple single-stage lasers with hundred watts of average power and multi-ten microjoules of pulse energy. These results confirm the potential for compact ultrafast Yb-based TDL oscillators to replace complex amplifier systems and Ti:sapphire-based lasers for an extensive range of applications.

Benefiting from the fruitful combination of the Kerr lens mode locking scheme and the broad emission of the gain materials, TDL oscillators reach new pulse duration limits. Unprecedentedly, two ultrafast TDLs based on Yb:LuO and Yb:CALGO crystals generate shorter pulses than oscillators based on bulk crystals of the same materials. With 30 fs pulse duration, the first KLM Yb:CALGO TDL delivers pulses 60% shorter than any previously reported TDL. This pulse duration is also equally short to the shortest pulses emitted by any Yb-based bulk oscillator. Compared to the standard end-pumping configurations of bulk lasers, it appears that the TDL pumping scheme is advantageous to produce ultrashort pulses since it circumvents the need for an intra-cavity dichroic mirror that could limit the optical spectrum. While the shortest pulses of 35 fs from the Yb:LuO TDL feature optical spectra nearly three times larger than the gain bandwidth, the 30 fs pulses from the Yb:CALGO laser exploit only a fraction of the full bandwidth of the ultra-broadband gain material. These results indicate that further optimization of the mirror optical coatings for a broadband high reflectivity and flat dispersion is paramount to outperform the current 10-cycle pulses delivered by these two lasers.

These novel sources aim at directly driving exciting new applications in the fields of spectroscopy and high-field physics. An initial experiment has been realized to highlight the potential and reliability of these lasers and demonstrates the first fully-stabilized optical frequency comb based on a TDL. The two degrees of freedom of the frequency comb are the carrier-envelope offset (CEO) and the repetition rate frequencies. Both are detected and stabilized to a highly-stable radio-frequency external reference. A tight phase lock of the CEO frequency is achieved with an active feedback to the pump-diode current and the repetition rate is stabilized via a cavity mirror mounted onto a piezo-electric actuator. This approach of TDL-based frequency combs will benefit from the power-scalability capabilities of TDL oscillators resulting in simple high average power frequency combs without the need for any external amplification or nonlinear pulse compression. These sources should open doors to numerous experiments in the areas of metrology and broadband high-resolution

spectroscopy, especially for future extreme ultraviolet (XUV) frequency combs generated via intra-cavity high-harmonic generation (HHG).

Additionally, this thesis reports on the proof-of-principle realization of intra-cavity HHG inside an ultrafast TDL oscillator as a table-top pulsed source of XUV laser light. Using a state-of-the-art SESAM mode-locked TDL, the HHG is driven in a high-pressure gas jet and results in a compact setup operating at megahertz repetition rate. XUV laser light has been detected up to the 17<sup>th</sup> harmonic (61 nm, 20 eV), whereas no severe disturbance of the laser operation from the gas jet and subsequent HHG process was observed. Replacing the current driving laser by the above-mentioned KLM TDLs delivering substantially shorter pulses in combination with optimized phase matching conditions for the HHG process and improved XUV extraction will allow for significantly higher photon flux at even higher harmonics. By stabilization of the repetition rate and CEO frequencies of the KLM driving oscillator, the generation of an XUV frequency comb from a simple single-stage source is within the reach of ultrafast TDL oscillators. Due to the high-photon flux resulting from the high intra-cavity average power of the laser, this class of compact coherent XUV light sources has the potential to become a versatile tool for areas such as attosecond science, nanometer-scale imaging and precision XUV spectroscopy.

**Keywords:** ultrafast lasers, mode-locked lasers, thin-disk laser (TDL) oscillators, high-power lasers, ytterbium-doped (Yb-doped) materials, near infrared, optical frequency combs, carrier-envelope offset (CEO), high-harmonic generation (HHG), extreme-ultraviolet (XUV) laser sources.



# Résumé

Les lasers ultra-rapides ont révolutionné la recherche scientifique en physique fondamentale, en chimie, en biologie ainsi que de nombreuses applications industrielles. Un grand nombre d'expériences bénéficient du développement de sources lasers basées sur l'ytterbium qui émettent des trains d'impulsions femtosecondes de haute puissance. Ces systèmes incluent généralement un oscillateur à verrouillage de modes de basse puissance, suivi par des étages d'amplification basés sur les technologies à fibres, à plaques ou à disques fins. Dans de nombreux cas, une étape additionnelle de compression non-linéaire des impulsions est nécessaire pour obtenir des impulsions suffisamment brèves. Cependant, l'amplification externe et la compression des impulsions ajoutent un coût et une complexité et peuvent dégrader la qualité spatiale et temporelle des impulsions. De plus, beaucoup d'amplificateurs sont limités en termes de taux de répétition, ce qui est un problème pour de nombreuses applications industrielles et scientifiques. En revanche, les oscillateurs lasers ultra-rapides à disques fins (TDL pour « thin-disk lasers » en anglais) représentent une manière simple et compacte pour générer directement de puissants trains d'impulsions ultra-brèves à un taux de répétition dans les mégahertz. Les oscillateurs TDL à verrouillage de modes de haute puissance qui opèrent à une longueur d'onde centrale autour de  $1\ \mu\text{m}$  délivrent une puissance moyenne de plusieurs centaines de watts contenues dans des impulsions d'une durée de quelques centaines de femtosecondes et une énergie de plusieurs dizaines de microjoules. Ces lasers ont déjà été utilisés avec succès pour réaliser des expériences sans amplification externe dans le domaine de la science des champs forts à des taux de répétition dans les mégahertz. Cependant, une étape de compression externe des impulsions à moins de 100 fs était nécessaire pour ces applications. La génération d'impulsions puissantes de moins de 100 fs directement à l'intérieur d'un TDL ultra-rapide améliorerait leur adéquation pour des domaines d'applications comme le traitement des matériaux, la recherche biomédicale, ou la recherche fondamentale. Néanmoins, avant ce travail de thèse, les niveaux de puissance des oscillateurs TDL pour les impulsions de moins de 100 fs était limité à 5 W et les durées d'impulsions les plus courtes étaient 60% plus longues que pour les oscillateurs à cristaux épais dopés à l'ytterbium.

Cette thèse décrit le développement de nouvelles sources TDL ultra-rapides basées sur l'ytterbium qui montrent des performances supérieures pour des durées d'impulsions de moins de 100 fs. Durant les 17 ans passés, les records en termes de durées d'impulsions

étaient obtenus grâce au verrouillage de modes utilisant un miroir à absorbant saturable en matériaux semi-conducteurs (SESAM pour « semiconductor saturable-absorber mirror » en anglais) avec différents cristaux dopés à l'ytterbium présentant des surfaces d'émissions larges spectralement. Dans cette thèse, le potentiel de tels matériaux avec un gain très large est exploré avec le verrouillage de modes par lentille à effet Kerr (KLM pour « Kerr lens mode-locked » en anglais), qui fournit une réponse plus rapide et une large profondeur de modulation. L'influence des paramètres clés du laser est examinée pour la génération de puissantes impulsions ultra-brèves. Cette recherche a conduit à la réalisation d'un TDL KLM basé sur un cristal dopé à l'ytterbium qui délivre une puissance moyenne record pour les TDL dans les catégories de durée d'impulsions inférieures à 100 fs et 50 fs. Avec une puissance moyenne en sortie supérieure à 10 W et des impulsions de 90 fs, le laser délivre plus de deux fois plus de puissance que les autres oscillateurs TDL dans la catégorie de durée d'impulsions de moins de 100 fs. Cette démonstration de principe ouvre les portes à l'augmentation de la puissance crête et de la puissance moyenne en vue de la génération d'impulsions ultra-brèves à partir de lasers simples émettant des centaines de watts de puissance moyenne et des impulsions contenant des dizaines de microjoules d'énergie. Ces résultats confirment que les oscillateurs TDL compacts et ultra-rapides basés sur l'ytterbium ont le potentiel pour remplacer les systèmes complexes d'amplificateurs et les lasers titane-saphir dans une large gamme d'applications.

Bénéficiant de la combinaison avantageuse du verrouillage de modes par lentille à effet Kerr et de l'émission large bande des matériaux de gain laser, les oscillateurs TDL atteignent de nouvelles limites en termes de durée d'impulsions. Pour la première fois, deux oscillateurs TDL ultra-rapides basés sur des cristaux d'Yb:LuO et d'Yb:CALGO génèrent des impulsions plus brèves que les oscillateurs basés sur des cristaux épais de mêmes matériaux. Avec des durées de 30 fs, le premier TDL KLM basé sur un cristal d'Yb:CALGO délivre des impulsions qui sont 60% plus brèves que celles émises par les autres TDL jusque-là. Cette durée d'impulsion est aussi égale à la durée des impulsions les plus brèves délivrées par les oscillateurs à cristaux épais basés sur l'ytterbium. Comparé aux configurations standards de pompage des cristaux épais par la face arrière, il apparaît que le schéma de pompage des TDL est avantageux pour produire des impulsions ultra-brèves puisqu'il permet à des impulsions avec un spectre de fréquences plus large de résonner à l'intérieur de la cavité laser. Tandis que les impulsions les plus brèves (durée de 35 fs) délivrées par un TDL basé sur l'Yb:LuO présentent un spectre optique presque trois fois plus large que la bande passante du gain, les impulsions de 30 fs générées par le laser basé sur l'Yb:CALGO exploitent seulement une fraction de la très large

---

bande passante du gain du matériau. Ces résultats indiquent qu'une optimisation plus poussée des couches optiques des miroirs de la cavité laser pour obtenir simultanément une haute réflectivité qu'une dispersion plate dans une large bande spectrale est capitale pour surpasser les performances des impulsions de moins de 10 cycles optiques actuellement délivrées par ces deux lasers.

Ces nouvelles sources visent à réaliser directement de nouvelles applications attractives dans les domaines de la spectroscopie et de la physique des champs forts. Une première expérience est réalisée pour mettre en valeur le potentiel et la fiabilité de ces lasers. Elle démontre le premier peigne de fréquences optiques entièrement stabilisé basé sur les TDL. Les deux degrés de liberté du peigne de fréquences sont la fréquence du décalage de phase entre la porteuse et l'enveloppe (CEO pour « carrier-envelope offset » en anglais) et celle du taux de répétition. Chaque fréquence est détectée et stabilisée sur un signal de référence externe radiofréquence. Un verrouillage serré de la phase du battement CEO est atteint avec un rétrocontrôle sur le courant d'alimentation de la diode de pompe. Le taux de répétition est stabilisé par un miroir de la cavité monté sur un actuateur piézoélectrique. Cette approche de peignes de fréquences basés sur les TDL bénéficiera des possibilités d'augmentation de la puissance des oscillateurs TDL, réalisant alors des peignes de fréquences de haute puissance sans le besoin d'amplification externe ou de compression non-linéaire des impulsions. Ces sources devraient ouvrir les portes vers de nombreuses expériences dans les domaines de la métrologie et de la spectroscopie large bande de haute résolution, tout particulièrement pour les futurs peignes de fréquence dans l'ultra-violet extrême (XUV pour « extreme-ultraviolet » en anglais) obtenus par génération d'harmoniques d'ordres élevés (HHG pour « high-harmonic generation » en anglais).

De plus, cette thèse expose une démonstration de principe de la réalisation de HHG à l'intérieur de la cavité d'un oscillateur TDL ultra-rapide comme source compacte de lumière laser pulsée dans l'XUV. En utilisant un TDL à verrouillage de modes par SESAM à la pointe de la technologie, la génération d'harmoniques est effectuée dans un jet de gaz à haute pression et donne lieu à un montage compact qui opère à un taux de répétition dans les mégahertz. La lumière XUV est détectée jusqu'à la 17<sup>ème</sup> harmonique (61 nm, 20 eV), alors qu'aucune sévère perturbation n'est observée dans le fonctionnement du laser sous l'effet du jet de gaz et du processus de HHG qui s'ensuit. Combiné avec l'optimisation des conditions d'accord de phase pour le processus HHG et une extraction améliorée de la lumière XUV, le remplacement du laser actuel par l'un des TDL KLM mentionnés précédemment qui émet des impulsions

considérablement plus brèves, permettra une augmentation significative du flux de photons, même à des harmoniques d'ordres plus élevés. En stabilisant les fréquences du taux de répétition et du CEO de l'oscillateur KLM, la génération d'un peigne de fréquences dans l'XUV à partir d'une source simple à une seule étape est à portée de main des oscillateurs TDL ultra-rapides. Etant donné l'intense flux de photons résultant de la haute puissance moyenne présente à l'intérieur de la cavité laser, cette classe de sources compactes de lumière cohérente dans l'XUV a le potentiel pour devenir un outil polyvalent pour des domaines variés comme la science des phénomènes attosecondes, l'imagerie à l'échelle nanométrique et la spectroscopie de précision dans l'XUV.

**Mots clefs :** lasers ultra-rapides, lasers à verrouillage de modes, oscillateurs lasers à disques fins, lasers de haute puissance, matériaux dopés à l'ytterbium, infrarouge proche, peignes de fréquences optiques, fréquence de décalage de phase entre la porteuse et l'enveloppe, génération de hautes harmoniques, sources lasers dans l'ultra-violet extrême.

# ***Table of contents***

<b><i>Abstract</i></b>	<b><i>VI</i></b>
<b><i>Résumé</i></b>	<b><i>IX</i></b>
<b><i>Table of contents</i></b>	<b><i>XIII</i></b>
<b><i>List of abbreviations</i></b>	<b><i>XV</i></b>
<b><i>List of symbols</i></b>	<b><i>XVII</i></b>
<b><i>List of publications</i></b>	<b><i>XIX</i></b>
<b>Chapter 1 High-power femtosecond laser oscillators: achievements and challenges</b>	<b>1</b>
1.1 Technologies for ultrafast high-power laser sources .....	1
1.2 Thin-disk geometry: a versatile concept for laser-light amplification.....	3
1.3 Soliton mode locking of thin-disk laser oscillators .....	5
1.4 Gain materials for powerful ultrashort-pulse thin-disk lasers .....	7
<b>Chapter 2 Cutting-edge sub-100-fs Kerr lens mode-locked thin-disk laser oscillators</b>	<b>13</b>
2.1 Yb:LuO: a gain material well-suited for the generation of powerful sub-100-fs pulses	14
2.2 Evaluation of the capabilities of the TDL crystal in continuous-wave operation.....	16
2.3 Experimental study of the performance of Kerr lens mode-locked thin-disk lasers.....	18
2.4 Performance scaling of Kerr lens mode-locked Yb:LuO thin-disk lasers .....	24
2.5 Towards oscillators delivering sub-100-fs pulses at hundred-watt power levels .....	28
<b>Chapter 3 New pulse-duration limits of ultrafast thin-disk laser oscillators</b>	<b>31</b>
3.1 Yb:CALGO: an ultra-broadband gain material for record-short-pulse generation.....	32
3.2 Evaluation of the performance of the disk crystal in continuous-wave operation.....	34
3.3 Kerr lens mode-locked Yb:CALGO thin-disk laser oscillator .....	36
3.4 Dispersion compensation for ultra-broadband laser pulses .....	40
3.5 Towards few-cycles pulses directly generated by Yb-based laser oscillators .....	43

<b>Chapter 4</b>	<b>Optical frequency combs based on ultrafast thin-disk laser oscillators</b>	<b>45</b>
4.1	High-average-power optical frequency combs for XUV-spectroscopy .....	46
4.2	Carrier-envelope-offset frequency detection and stabilization .....	48
4.2.1	Supercontinuum generation and detection of the CEO frequency .....	48
4.2.2	CEO frequency stabilization .....	49
4.3	Fully-stabilized optical frequency comb .....	52
4.4	Towards applications driven by fully-stabilized thin-disk laser oscillators.....	53
<b>Chapter 5</b>	<b>XUV light source based on HHG inside an ultrafast TDL oscillator</b>	<b>55</b>
5.1	High-repetition-rate high-harmonic generation enabling applications .....	55
5.2	SESAM mode-locked thin-disk laser oscillators for intra-cavity HHG.....	60
5.2.1	Sub-400-fs SESAM mode-locked Yb:LuO TDL at 27-W output power.....	60
5.2.2	Sub-300-fs pulses from a SESAM mode-locked Yb:LuO TDL in air .....	62
5.2.3	Vacuum-environment sub-300-fs SESAM mode-locked Yb:LuO TDL.....	64
5.3	HHG at megahertz repetition rate inside an ultrafast TDL oscillator .....	66
5.4	Enhanced extreme-ultraviolet output coupling methods .....	69
5.5	Towards experiments directly driven by simple XUV laser sources.....	73
<b>Chapter 6</b>	<b>Conclusion and future research</b>	<b>75</b>
	<i>References</i>	<b>79</b>
	<i>Curriculum Vitae</i>	<b>89</b>
	<i>Acknowledgments</i>	<b>91</b>

## ***List of abbreviations***

AAs	aluminum arsenide
Al <sub>2</sub> O <sub>3</sub>	sapphire
AoI	angle of incidence
at. %	atomic percent
AR	anti-reflective
BP	Brewster plate
Ca	calcium
CEO	carrier-envelope offset
CM	curved mirror
CPA	chirp pulse amplification
cw	continuous wave
FM	transverse fundamental mode i.e. Gaussian (TEM <sub>00</sub> ) mode
FN-PSD	frequency noise power spectral density
FWHM	full width at half maximum
Gd	gadolinium
GDD	group delay dispersion
HA	hard aperture
HEM	heat exchanger method
HHG	high-harmonic generation
HR	highly reflective
HT	highly transmissive
IC	intra-cavity
ILP	Institut für Laser-Physik (of the University of Hamburg, Germany)
InGaAs	indium gallium arsenide
KLM	Kerr lens mode-locked
KM	Kerr medium
Lu	lutetium
MgO	magnesium oxide
MM	multi-mode
OC	output coupler
PCF	photonic crystal fiber

## List of abbreviations

---

PID	proportional-integral-derivative
PPLN	periodically-poled lithium niobate
PSD	power spectral density
RF	radio frequency
RIN	relative intensity noise
rms	root mean square
RoC	radius of curvature
SESAM	semiconductor saturable absorber mirror
SiO <sub>2</sub>	fused silica
SNR	signal-to-noise ratio
SPM	self-phase modulation
Ta <sub>2</sub> O <sub>5</sub>	tantalum pentoxide
TBP	time-bandwidth product
Ti:sapphire	titanium doped sapphire (Ti:Al <sub>2</sub> O <sub>3</sub> )
TDL	thin-disk laser
VBG	volume Bragg grating
VUV	vacuum ultraviolet
XUV	extreme ultraviolet
Y	yttrium
YAG	yttrium aluminum garnet (Y <sub>3</sub> Al <sub>5</sub> O <sub>12</sub> )
Yb	ytterbium
Yb:CALGO	ytterbium doped calcium gadolinium aluminate (Yb:CaGdAlO <sub>4</sub> )
Yb:CYA	ytterbium doped calcium yttrium aluminate (Yb:CaYAlO <sub>4</sub> )
Yb:KYW	ytterbium doped potassium yttrium tungstate (Yb:KY(WO <sub>4</sub> ) <sub>2</sub> )
Yb:LuO	ytterbium doped lutetium oxide (Yb:Lu <sub>2</sub> O <sub>3</sub> )
Yb:LuScO	ytterbium doped lutetium scandium oxide (Yb:LuScO <sub>3</sub> )
Yb:ScO	ytterbium doped scandium oxide (Yb:Yb:Sc <sub>2</sub> O <sub>3</sub> )
Yb:YAG	ytterbium-doped yttrium aluminum garnet (Yb:Y <sub>3</sub> Al <sub>5</sub> O <sub>12</sub> )
ZPL	zero-phonon line



## List of symbols

$A_{\text{eff}}$	effective laser mode area
$\beta$	inversion level
$\chi^{(3)}$	third-order nonlinear coefficient
$E_{\text{pulse}}$	pulse energy
$f_{\text{CEO}}$	carrier-envelope offset frequency
$f_{\text{rep}}$	repetition rate frequency
$\gamma$	effective nonlinear coefficient
$L$	resonator length
$\Delta\lambda$	FWHM optical spectrum
$\lambda$	wavelength
$\lambda/2$	half waveplate
$\lambda/4$	quarter waveplate
$M^2$	beam quality factor, also referred to as beam propagation factor
$n_2$	nonlinear refractive index
$\eta_{\text{opt}}$	optical-to-optical efficiency
$P_{\text{out}}$	laser output average power
$P_{\text{peak}}$	laser output peak power
$P_{\text{pump}}$	pump power
$\sigma$	cross section
$T$	(power) transmission
$\Delta\tau$	FWHM pulse duration
$w$	$1/e^2$ mode radius



# List of publications

Parts of this thesis are published in the following journal papers and conference proceedings:

## Journal papers:

1. **C. Paradis**, N. Modsching, V. J. Wittwer, B. Deppe, C. Kränkel, and T. Südmeyer, "Generation of 35-fs pulses from a Kerr lens mode-locked Yb:Lu<sub>2</sub>O<sub>3</sub> thin-disk laser," *Opt. Express* **25**, 14918-14925 (2017), **Editor's Pick**.
2. F. Labaye, M. Gaponenko, V. J. Wittwer, A. Diebold, **C. Paradis**, N. Modsching, L. Merceron, F. Emaury, I. J. Graumann, C. R. Phillips, C. J. Saraceno, C. Kränkel, U. Keller, and T. Südmeyer, "Extreme ultraviolet light source at a megahertz repetition rate based on high-harmonic generation inside a mode-locked thin-disk laser oscillator," *Opt. Lett.* **42**(24), 5170–5173 (2017).
3. N. Modsching, **C. Paradis**, F. Labaye, M. Gaponenko, I. J. Graumann, A. Diebold, F. Emaury, V. J. Wittwer, and T. Südmeyer, "Kerr lens mode-locked Yb:CALGO thin-disk laser," *Opt. Lett.* **43**(4), 879–882 (2018).

## Conference publications:

1. C. J. Saraceno, **C. Paradis**, L. Merceron, M. Gaponenko, S. Schilt, and T. Südmeyer, "Multi-megahertz repetition rate high-power THz sources based on modelocked thin-disk lasers," presented at *NCCR MUST Annual Meeting 2015*, Switzerland, Engelberg, January 12-14, 2015.
2. L. Merceron, A. Diebold, F. Emaury, **C. Paradis**, C. Schriber, M. Gaponenko, C. J. Saraceno, U. Keller, and T. Südmeyer, "Toward intracavity high harmonic generation with thin disk lasers," presented at *NCCR MUST Annual Meeting 2015*, Switzerland, Engelberg, January 12-14, 2015.
3. **C. Paradis**, J. Gateau, B. Debord, F. Gérôme, S. Hermelin, L. Bonacina, C. J. Saraceno, T. Südmeyer, F. Benabid, and J.-P. Wolf, "Beam transmission and spectral broadening of deep-UV femtosecond pulses in Kagome-type hollow-core photonic crystal fibers," presented at *NCCR MUST Annual Meeting 2015*, Switzerland, Engelberg, January 12-14, 2015.
4. C. J. Saraceno, **C. Paradis**, L. Merceron, M. Gaponenko, S. Schilt, and T. Südmeyer, "Multi-megahertz repetition rate high-power THz sources based on modelocked thin-disk lasers," presented at *International school on parametric nonlinear optics*, Les Houches, France, April 20-Mai 1, 2015.
5. **C. Paradis**, N. Modsching, L. Merceron, F. Labaye, M. Gaponenko, V. J. Wittwer, and T. Südmeyer, "Multi-megahertz repetition rate high power THz spectroscopy," presented at *NCCR MUST Annual Meeting 2016*, Switzerland, Engelberg, January 11-13, 2016, poster #68.
6. L. Merceron, F. Labaye, **C. Paradis**, N. Modsching, M. Gaponenko, A. Diebold, F. Emaury, C. J. Saraceno, U. Keller, and T. Südmeyer, "Toward intracavity high harmonic generation with thin-disk oscillators," presented at *NCCR MUST Annual Meeting 2016*, Switzerland, Engelberg, January 11-13, 2016, poster #67.

7. N. Modsching, **C. Paradis**, L. Merceron, F. Labaye, M. Gaponenko, M. Hoffmann, V. J. Wittwer, and T. Südmeyer, "High-power femtosecond mode-locked thin-disk oscillators: from power-scaling towards novel applications," presented at *Swiss Physical Society Annual Meeting*, Switzerland, Lugano, August 23, 2016, talk #722.
8. **C. Paradis**, N. Modsching, L. Merceron, F. Labaye, M. Gaponenko, M. Hoffmann, V. J. Wittwer, and T. Südmeyer, "Multi-megahertz repetition-rate THz generation driven by high-power thin-disk oscillator," presented at *Swiss Physical Society Annual Meeting*, Switzerland, Lugano, August 23, 2016, talk #723.
9. **C. Paradis**, N. Modsching, V. J. Wittwer, B. Deppe, C. Kränkel, and T. Südmeyer, "128-fs Pulses from a Kerr-Lens Modelocked Yb:LuO Thin-Disk Laser," in *Conference on Lasers and Electro-Optics*, OSA Technical Digest (online) (Optical Society of America, 2017), talk SM11.3.
10. N. Modsching, **C. Paradis**, V. J. Wittwer, B. Deppe, C. Kränkel, and T. Südmeyer, "64-fs Pulses from a Kerr-Lens Modelocked Yb:LuO Thin-Disk Laser," in *2017 European Conference on Lasers and Electro-Optics and European Quantum Electronics Conference*, (Optical Society of America, 2017), talk CA\_7\_1.
11. **C. Paradis**, N. Modsching, M. Gaponenko, F. Labaye, F. Emaury, A. Diebold, I. Graumann, B. Deppe, C. Kränkel, V. J. Wittwer, and T. Südmeyer, "Sub-50-fs Kerr Lens Mode-Locked Thin-Disk Lasers," in *2017 European Conference on Lasers and Electro-Optics and European Quantum Electronics Conference*, (Optical Society of America, 2017), **postdeadline talk** PD\_1\_4.
12. M. Gaponenko, F. Labaye, V. J. Wittwer, **C. Paradis**, N. Modsching, L. Merceron, A. Diebold, F. Emaury, I. Graumann, C. Phillips, C. J. Saraceno, C. Kränkel, U. Keller, and T. Südmeyer, "Compact Megahertz Coherent XUV Generation by HHG inside an Ultrafast Thin Disk Laser," in *Nonlinear Optics*, OSA Technical Digest (online) (Optical Society of America, 2017), **postdeadline talk** NTh3A.1.
13. N. Modsching, **C. Paradis**, F. Labaye, M. Gaponenko, V. J. Wittwer, and T. Südmeyer, "Kerr lens mode-locked femtosecond thin-disk lasers: towards powerful sub-50 fs oscillators," presented at *Joint Annual Meeting of the Swiss Physical Society Austrian Physical Society*, Switzerland, Geneva, August 24, 2017, talk #201.
14. M. S. Gaponenko, F. Labaye, V. J. Wittwer, **C. Paradis**, N. Modsching, L. Merceron, A. Diebold, F. Emaury, I. Graumann, C. R. Phillips, C. J. Saraceno, C. Kränkel, U. Keller, and T. Südmeyer, "High Harmonic Generation (HHG) inside a Modelocked Thin-Disk Laser," in *Frontiers in Optics 2017*, OSA Technical Digest (online) (Optical Society of America, 2017), talk FTh2B.1.
15. N. Modsching, **C. Paradis**, M. Gaponenko, F. Labaye, F. Emaury, A. Diebold, I. Graumann, B. Deppe, C. Kränkel, V. J. Wittwer, and T. Südmeyer, "Towards Few-Cycle Ultrafast Thin-Disk Lasers," in *Laser Congress 2017 (ASSL, LAC)*, OSA Technical Digest (online) (Optical Society of America, 2017), poster JM5A.41, **awarded "outstanding student poster presentation prize"**.
16. F. Labaye, M. Gaponenko, V. J. Wittwer, **C. Paradis**, N. Modsching, L. Merceron, A. Diebold, F. Emaury, I. Graumann, C. Phillips, C. J. Saraceno, C. Kränkel, U. Keller, and T. Südmeyer, "SESAM-Modelocked Thin-Disk Laser (TDL) with Intracavity High-Harmonic Generation (HHG)," in *Laser Congress 2017 (ASSL, LAC)*, OSA Technical Digest (online) (Optical Society of America, 2017), talk ATH5A.3.
17. **C. Paradis**, N. Modsching, F. Labaye, M. Gaponenko, F. Emaury, A. Diebold, I. Graumann, B. Deppe, C. Kränkel, V. J. Wittwer, T. Südmeyer, "Kerr lens mode-locked thin-disk lasers delivering 30-fs pulses from Yb:CALGO and 35-fs pulses from Yb:Lu<sub>2</sub>O<sub>3</sub>," presented at *Ultrafast Optics (UFO) XI*, Jackson Hole, Wyoming, United States, 8–13 Oct. 2017, talk Tu7.2

- 
18. F. Labaye, M. Gaponenko, V. J. Wittwer, **C. Paradis**, N. Modsching, L. Merceron, A. Diebold, F. Emaury, I. Graumann, C. Phillips, C. J. Saraceno, C. Kränkel, U. Keller, T. Südmeyer, "Compact megahertz repetition rate coherent XUV light source based on HHG inside a modelocked thin-disk laser," presented at *Ultrafast Optics (UFO) XI*, Jackson Hole, Wyoming, United States, 8–13 Oct. 2017, **Invited (upgraded) talk Tu7.5**.
  19. N. Modsching, **C. Paradis**, M. Gaponenko, F. Labaye, V. J. Wittwer, and T. Südmeyer, "Towards Few-Cycle Ultrafast Thin-Disk Lasers," presented at *NCCR MUST Annual Meeting 2018*, Grindelwald, January 22-24, 2018, poster #55.
  20. F. Labaye, M. Gaponenko, V. J. Wittwer, A. Diebold, **C. Paradis**, N. Modsching, L. Merceron, F. Emaury, I. J. Graumann, C. R. Philips, C. J. Saraceno, C. Kränkel, U. Keller, and T. Südmeyer, "Extreme ultraviolet light source at a megahertz repetition rate based on high-harmonic generation inside a mode-locked thin-disk laser oscillator," presented at *MUST Annual Meeting 2018*, Grindelwald, January 22-24, 2018, poster #56.
  21. V. J. Wittwer, M. Hoffmann, **C. Paradis**, N. Modsching, M. Gaponenko, F. Labaye, T. Südmeyer, "Broadband IBS Coatings for sub-50-fs Pulse Generation from Ultrafast Thin-Disk Lasers," presented at *SPIE Photonics West LASE, Solid State Lasers XXVII: Technology and Devices (Conference 10511)*, San Francisco, California, United States, 27 Jan – 1 Feb. 2018, poster 10511-82.
  22. N. Modsching, **C. Paradis**, P. Brochard, N. Jornod, K. Gürel, C. Kränkel, S. Schilt, V. J. Wittwer, and T. Südmeyer, "Frequency Comb Stabilization of a 4 W, 50-fs Thin-Disk Laser Oscillator," presented at *32<sup>nd</sup> European Frequency and Time Forum (EFTF 2018)*, Torino, Italy, April 10-12, 2018, **awarded "outstanding result prize" in the student paper competition**.
  23. **C. Paradis**, N. Modsching, O. Razskazovskaya, J. Drs, F. Meyer, C. J. Saraceno, C. Kränkel, V. J. Wittwer, and T. Südmeyer, "Broadband THz generation driven by a thin-disk laser oscillator," accepted for poster presentation at *Terahertz Science & Technology*, Berlin, Germany, Mai 6-9, 2018.
  24. N. Modsching, **C. Paradis**, P. Brochard, N. Jornod, K. Gürel, C. Kränkel, S. Schilt, V. J. Wittwer, and T. Südmeyer, "Frequency Comb Stabilization of a 50-fs Thin-Disk Laser Oscillator Operating in a Strongly SPM-broadened Regime," accepted for oral presentation at *Conference on Lasers and Electro-Optics (CLEO) 2018*, San Jose, California, United States, Mai 13-18 2018.
  25. **C. Paradis**, N. Modsching, M. Gaponenko, F. Labaye, V. J. Wittwer, and T. Südmeyer, "Frontiers in Ultrafast Thin-Disk Laser Oscillators," accepted for oral presentation at *Conference on Lasers and Electro-Optics (CLEO) 2018*, San Jose, California, United States, Mai 13-18 2018, **invited presentation**.
  26. N. Modsching, **C. Paradis**, M. Gaponenko, F. Labaye, V. J. Wittwer, and T. Südmeyer, "Towards few-cycle pulses from ultrafast thin disk lasers," accepted for oral presentation at *18<sup>th</sup> International Conference on Laser Optics (ICLO 2018)*, St. Petersburg, Russia, June 4-8, 2018, **invited presentation**.
  27. F. Labaye, M. Gaponenko, V. J. Wittwer, A. Diebold, **C. Paradis**, N. Modsching, L. Merceron, F. Emaury, I. J. Graumann, C. R. Philips, C. J. Saraceno, C. Kränkel, U. Keller, and T. Südmeyer, "Extreme Ultraviolet Light Source by High-Harmonic Generation Inside an Ultrafast Thin-Disk Laser," accepted for oral presentation at *Advanced Photonics 2018 Congress*, Zurich, July 2-5, 2018.
  28. C. Kränkel, E. Castellano-Hernández, A. Uvarova, P. von Brunn, **C. Paradis**, N. Modsching, V. J. Wittwer, T. Südmeyer, and A. M. Heuer, "Advanced Materials for Multi-Wavelength, High Power and Short Pulse Solid State Lasers," accepted for oral presentation at *OPTIQUE Toulouse 2018*, Toulouse, France, 3-6 July, 2018, **invited presentation**.



# Chapter 1 High-power femtosecond laser oscillators: achievements and challenges

These doctoral studies focus on the development of novel ultrafast high-power thin-disk laser (TDL) oscillators and their applications. This first chapter aims at giving the reader a brief introduction to high-average-power lasers with a strong emphasis on the TDL technology. Section 1.1 briefly describes the conventional high-power laser technologies. Section 1.2 concentrates on the specific properties of the TDL geometry for laser-light amplification. Section 1.3 reports on the evolution of the performance achieved from soliton mode-locked TDL oscillators. The key factors for these improvements and the current limitations are presented. Section 1.4 spotlights the two most promising gain materials for the generation of powerful ultrashort pulses from TDL oscillators. Their characteristics are compared to the ones of Yb:YAG the standard gain medium for ultrafast TDLs.

## 1.1 Technologies for ultrafast high-power laser sources

Ultrafast high-power lasers are highly attractive light sources which find applications both in industry and fundamental research [1]. For a given pulse energy, increasing the average power corresponds to increasing the repetition rate, i.e., the number of pulses per second. Laser systems delivering high average power in ultrashort light pulses are beneficial in many ways. They increase the processing quality, speed and precision in industrial applications such as cutting and welding. Additionally, they decrease the acquisition time, and enhance the signal-to-noise ratio for measurements in fundamental science experiments. Unfortunately, the generation of high optical power induces a significant heat load in the gain medium, which mainly originates from the quantum defect and non-radiative decays. The temperature increase of the component and the subsequent temperature gradient are converted into deformation, stress and change of the optical properties of the material, which are quantified

by its thermo-mechanical and thermo-optical coefficients. This affects the laser beam propagation and beam quality, e.g., by creating a thermal lens inside the resonator, and may even lead to damage. Consequently, efficient heat removal from the gain element is paramount for high-power operation.

To minimize the amount of generated heat, laser materials are selected to feature a low quantum defect and good structural quality. Yb-doped materials hold several advantages as gain media for high-power femtosecond lasers [2]. In most cases, they operate in a quasi-three-level system with a quantum defect smaller than 10%. They usually exhibit a relatively large absorption band, typically broader than 3-nm full-width at half maximum (FWHM) in the spectral region 910-950 nm and a zero-phonon line usually narrower than 3-nm located around 960-980 nm, which brings the advantage of a smaller quantum defect. These wavelength ranges are directly accessible by InGaAs-based laser diode systems which are commercially available with kilowatts power levels coupled into a multimode fiber. Moreover, volume-Bragg-grating (VBG) wavelength-stabilization has proven to be a successful way to reduce the diode spectral bandwidth to less than 1-nm FWHM and match the zero-phonon-line absorption peak [3].

Efficient heat removal is a crucial factor to operate the laser at a high average power. The thermal conductivity of the laser gain element controls the cooling efficiency with which the heat can be evacuated from within the volume of the gain element. Gain materials are generally chosen according to distinct laser properties for a given application such as the gain bandwidth or the thermal conductivity. Whereas most physical properties are set by the choice of the laser material, the component geometry can be adjusted for optimal heat management. Excellent heat extraction is achieved in configurations which feature a high surface-to-volume ratio (see Figure 1) [5]. In the slab geometry, the gain component is shaped like a large thick slice. The beam propagates along the longitudinal direction and the heat is removed in the perpendicular direction through the large surface of the gain element. The fiber geometry increases more dramatically the surface-to-volume ratio of the gain medium. The laser beam propagates in the waveguiding structure and the thermal load is efficiently dissipated in the radial direction. Nonlinear effects resulting from the long interaction length of the ultrashort pulses in the gain medium nevertheless compromise the high-amplification capabilities of these two concepts. Due to the difficulties to geometrically relax the laser peak intensity, temporal stretching of the pulses is often required. Therefore, these technologies are mostly used in amplifier architectures for high-power operation. In contrast, TDLs rely on



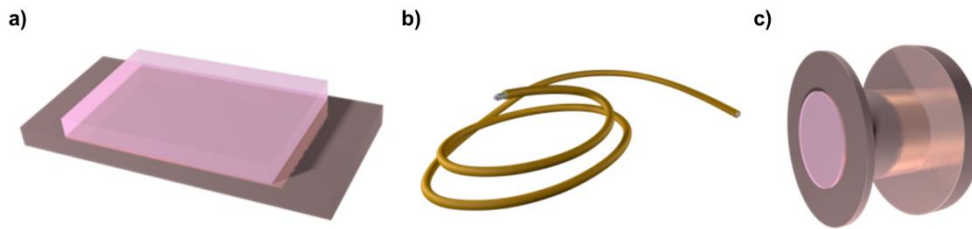


Figure 1. a) Slab, b) fiber and c) thin-disk geometries enable high-average-power operation due to their good heat management resulting from a high surface-to-volume ratio. Figure courtesy of Martin Saraceno [4].

a small interaction length between the gain medium and the laser light, at the expense of a small gain per pass. The beam propagates along the thin direction and the heat is extracted through the large surface of the gain element. This offers the possibility to decrease the laser peak intensity by simply increasing the laser mode size, allowing for reduced nonlinear propagation issues. This technology is therefore compatible with both amplifier and oscillator schemes for the generation of powerful ultrashort pulses.

## 1.2 Thin-disk geometry: a versatile concept for laser-light amplification

The TDL geometry is a scalable concept for diode-pumped solid-state lasers which enables light amplification to high power levels [6,7]. The disk element is generally used in reflection and often referred to as an “active mirror”. The front and back surfaces of the disk are coated to act as an anti-reflective (AR) surface and as a high-reflective (HR) mirror, respectively, for both pump and laser wavelengths. The disk is mounted onto a heat sink, which is cooled from the back side (see Figure 2). The thermal effects are greatly reduced compared to bulk media owing to the thin gain-medium geometry (typically 100-300  $\mu\text{m}$  thickness), used with millimeter- to centimeter-size beam diameters. In combination with a nearly flat-top pump beam, the heat flows homogeneously in the direction perpendicular to the disk surface, along the laser axis. The outstanding heat removal capability combined with efficient laser operation from Yb-doped gain crystals allow for laser operation at kilowatt pump power levels and pump densities exceeding 10  $\text{kW}/\text{cm}^2$ . Geometrical average-power scaling is simply achieved by increasing both pump and laser mode areas on the disk, maintaining a constant intensity on the gain element.

However, the reduced thickness of the gain element provides only a small pump absorption and low gain per single pass. A geometrical configuration with 24-44 passes of the pump through the disk crystal is applied to recycle the pump photons as illustrated in Figure 3. This

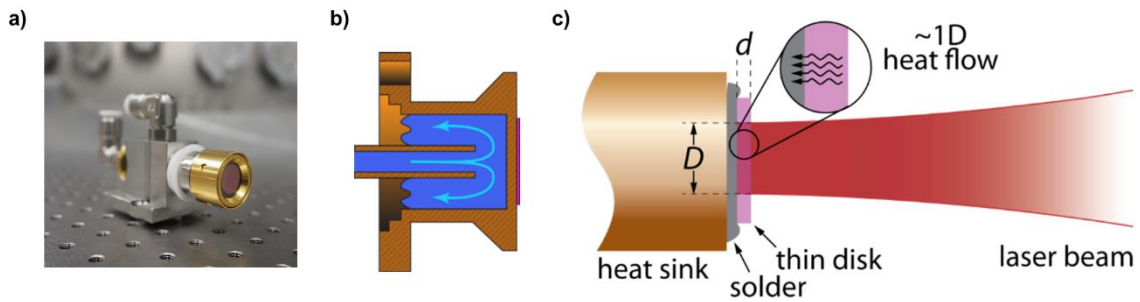


Figure 2. a) Picture of a thin-disk laser crystal contacted onto a diamond heat sink and placed onto a water-cooled mount (Trumpf GmbH). b) The heat generated in the gain crystal is efficiently transferred to the sink owing to the small disk thickness, typically 100-300  $\mu\text{m}$ . The thermal load is then dissipated by water cooling the back side of the heat sink. c) The mm-scale beam diameter on the thin disk favors a quasi-one-dimensional heat flow which limits the detrimental thermally-induced changes of the optical properties of the crystal.

enables efficient pump absorption generally reaching more than 90%. The low single-pass gain of typically 10-15% limits the tolerable total cavity losses. This issue is often mitigated by implementing several bounces of the laser beam on the disk [8] or using setups with a combination of multiple disks [9,10]. Interestingly, the relatively low output coupling degree imposed by the gain can be beneficial and enables intra-cavity experiment benefiting from the high average and peak power present inside the resonator. For example, molecular alignment experiments have been realized using a high-finesse TDL resonator that reached an intra-cavity average power higher than 100 kW from 50 W of pump power [11].

Besides advantageous thermal properties, the TDL technology stands out for ultrafast operation. Ultrashort laser pulses experience only a limited nonlinear phase shift inside the gain medium owing to the small interaction length and the reduced peak intensity exhibited

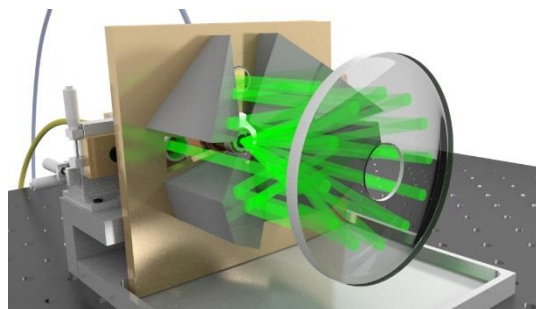


Figure 3. Illustration of the multi-pass pump geometry used to compensate the low absorption per single-pass of the thin gain medium. The pump photons are recycled, allowing for high absorption. 24 pump passes through the disk are shown here. Figure courtesy of Martin Saraceno [4].

by the large-diameter laser beam. In the case of TDL oscillators, the gain is usually not the main contributor to the nonlinear phase shift of the pulse. In contrast to standard laser oscillators based on bulk crystals, the total intra-cavity nonlinearities can thus be adjusted independently from the gain element. This facilitates the laser design, power scaling and optimization of the ultrafast laser performance. In the case of amplifier systems, the reduced interaction length greatly suppresses nonlinear propagation effects and allows, for example, chirp pulse amplification (CPA) with a low stretching factor.

Due to their remarkable properties, TDLs have been developed intensively and used in a large variety of applications. In multi-mode continuous-wave (cw) operation, up to 6 kW of average power have been achieved from a single disk with a high optical-to-optical efficiency<sup>1</sup> of 70% [10]. Additionally, an output power higher than 4 kW has been reported with a high beam quality ( $M^2 < 1.4$ ) [12]. Multi-pass and regenerative TDL amplifiers demonstrated multi-ten GW of peak power, kW of average power and mJ of pulse energy with ps-pulses. The interested reader may refer to [5,9,13,14] for more detailed results from TDL amplifiers.

### **1.3 Soliton mode locking of thin-disk laser oscillators**

Following the demonstration of the first mode-locked TDL oscillator more than fifteen years ago [15], tremendous progress in the area of power scaling has been achieved [16]. In this period, the field of mode-locked TDLs has evolved into being the leading technology for high-power and high-pulse-energy ultrafast laser oscillators. An ultrafast TDL oscillator and conventional mode-locking techniques are illustrated in Figure 4.

State-of-the-art ultrafast TDLs emit nearly 300 W of output power [18,19] and multi-tens of  $\mu\text{J}$  of pulse energy [20] with several hundred femtoseconds pulse duration. Such performance has enabled TDLs to directly drive applications which previously required the use of complex amplifier systems [21–23]. However, reducing the pulse duration of high-power oscillators is a major challenge. The first TDL emitting sub-100-fs pulses has been demonstrated only in 2012 [24] and even today, the power levels in this regime are limited to 5 W [24,25] (see Figure 5). Therefore, many applications in areas such as high-field physics, frequency conversion and frequency-comb generation rely on external nonlinear pulse compression. This introduces an additional stage of complexity to the system and may reduce the beam quality, power level and degrade the temporal pulse profile. Overcoming the trade-

---

<sup>1</sup> The term “optical-to-optical efficiency” is shortened to “optical efficiency” in the rest of the manuscript

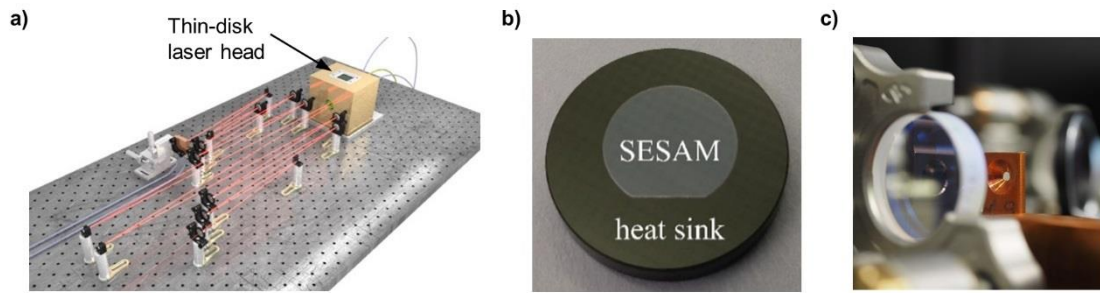


Figure 4. a) Schematic of an ultrafast thin-disk laser oscillator. The thin-disk laser crystal is mounted in the thin-disk laser head which provides a multi-pass pump arrangement (figure courtesy of Martin Saraceno [4]). Passive soliton mode locking is typically achieved by using either b) a SESAM (picture taken from [17]) or c) via the Kerr lensing effect, represented here by a hard aperture.

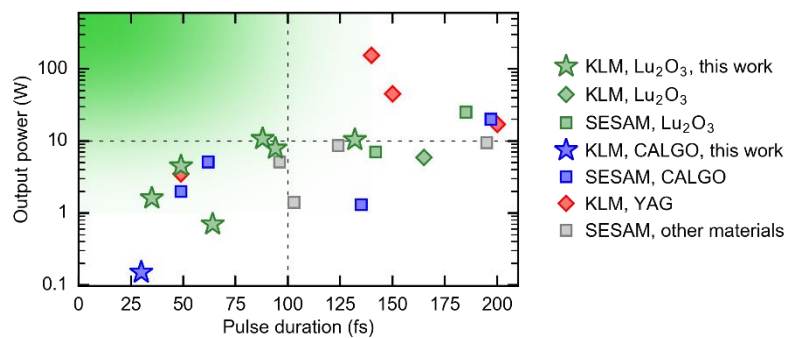


Figure 5. Overview of sub-200-fs thin-disk laser oscillators based on Yb-doped gain materials [24–34]. The colored area spotlights the targeted performances of ultrafast oscillators to directly drive applications such as high-field physics, frequency conversion and frequency-comb generation. The results presented in this thesis are highlighted with star symbols.

off between output power and pulse duration by providing a compact and simple laser oscillator delivering hundred watts and tens of micro-joules in sub-100-fs pulses will simplify many existing experiments and open new application areas.

Initially, all ultrafast TDLs were passively mode-locked using a semiconductor saturable absorber mirror (SESAM, [35]) [36,37]. Besides self-starting pulsed operation and simplicity of the cavity design, the combination of TDLs and SESAMs enables power scalability of the ultrafast laser performance [16]. At constant pump intensity and repetition rate, the average power scales with the laser mode areas on the disk and SESAM, if the dispersion is adapted to the increasing self-phase modulation (SPM). SESAM mode-locked TDLs usually operate at moderate levels of modulation depth (typically in the range of 0.5% to 2%) with a limited spectral bandwidth originating from the spectrally-dependent saturable absorber element, e.g., a quantum well. SESAMs with higher modulation depths usually exhibit higher non-

saturable losses and a higher coefficient of two photon absorption [38,39]. It can cause thermal issues or even damage at typical kW-average powers and peak powers approaching the GW level inside the cavity. These challenges have so far hindered the generation of sub-500-fs pulses from SESAM mode-locked TDLs based on the well-established Yb:YAG gain crystals. One promising direction to overcome this issue is the use of multiple quantum well absorbers and dielectric top coatings [40] in combination with a semiconductor substrate removal method for improved flatness over a large area and better heat extraction [17].

In contrast, Kerr lens mode locking is based on a peak-intensity-dependent  $\chi^{(3)}$ -nonlinearity, and is usually triggered in a bulk crystal [41–43]. The additional lens created by the nonlinear Kerr effect changes the beam propagation inside the cavity. The resonator is designed such that the round-trip losses are reduced for the pulsed operation compared to the cw operation. The scheme is referred to as “hard-aperture mode locking” in case an intra-cavity slit or pinhole is used to block a part of the cw laser beam. This term is opposed to the “soft-aperture mode locking” technique, in which the pulse experiences a better overlap with the pump beam in the active material compared to the cw laser light. The absence of spectrally-dependent losses combined with a high modulation depth and a fast response time of the self-amplitude modulation are beneficial for ultrashort pulse generation. It allows mode-locked operation with very broad pulse bandwidths [33] and operates at different wavelength ranges, e.g., as recently demonstrated around 2  $\mu\text{m}$  from an Ho:YAG laser [44]. The major drawback of Kerr lens mode-locked (KLM) lasers lies in the resonator design that usually requires operation close to a stability edge [45] and couples the spatial and temporal soliton dynamics [46]. Following the demonstration of the first KLM TDL [26], similar scaling laws as for SESAM mode-locked TDLs have been demonstrated. It resulted in average output powers up to 270 W in 330-fs pulses from Yb:YAG gain material [19]. Recently, 140-fs pulses have been generated directly from a KLM Yb:YAG TDL oscillator at an average output power of 155 W and an optical efficiency of 29% [34]. These experiments clearly indicate that KLM is a promising approach for the generation of powerful ultrashort pulses from TDLs based on Yb-doped gain materials.

#### **1.4 Gain materials for powerful ultrashort-pulse thin-disk lasers**

The requirements on the crystal properties for high-power ultrashort TDLs have been thoroughly discussed in [47]. Amongst all, decisive characteristics are a broad gain bandwidth, high thermal conductivity, and reliable manufacturing possibilities granting access to large-diameter high-quality thin-disk crystals. Broad gain materials are typically achieved by

disordered host materials, which however feature a lower thermal conductivity. Therefore, different materials have been investigated to find the best host for Yb-ions. It is important to highlight that it is usually not sufficient to consider only the emission bandwidth of a material to estimate the minimum achievable pulse duration but instead the inversion-dependent gain cross section. Besides, for any given material, the combination of doping concentration and crystal thickness must be carefully selected. While a higher doping enables a higher pump absorption and higher gain, it typically reduces the thermal conductivity. Similarly, thinner crystals offer a lower thermal resistance and reduced thermo-optical effects, which allows for higher pumping densities. However, it then exhibits a lower gain and a higher number of pump passes is necessary for high pump absorption.

While Yb:YAG may be the best choice for high average power, its gain bandwidth of 8 nm (FWHM) does not directly support pulses shorter than 120 fs (see Table 1). In order to generate sub-100-fs pulses from TDL oscillators, numerous Yb-doped laser materials with broader gain bandwidths have been developed [47]. Figure 6 presents the timeline of the evolution of the minimum pulse duration achieved by bulk and TDL oscillators based on Yb-doped gain materials. Benefiting from optimized SESAMs and broad gain bandwidths, the minimum pulse duration from TDL oscillators has been decreased from initially 680 fs [15] to 49 fs, which was delivered by a SESAM mode-locked Yb:CALGO TDL at 2-W average power [32]. However, the multi-watt power level is comparable to state-of-the-art bulk oscillators performance [48] and Yb-based bulk oscillators already demonstrated 40% shorter pulses [49]. Most of the recently demonstrated Yb-based broadband gain materials are still in an early phase of thin-disk development, suffering from growth defects and non-optimized disk processing technologies. Many of the gain media exhibit a comparably low thermal conductivity due to their disordered nature. These factors prevent further power scaling at the moment.

On the other hand, KLM TDL oscillators were exclusively based on the widely-used Yb:YAG gain medium until recently. This material is extremely attractive for ultrafast high-average-power laser applications owing to its excellent thermo-mechanical and spectroscopic properties. The high structural quality, thermal conductivity and gain allow for the generation of sub-ps pulses in more than hundred watts of average power. Yb:YAG crystals are easily produced via the Czochralski growth method [60,61]. Consequently, high-optical-quality crystals are commercially available with large disk diameters, which has been a key element for the rapid progress of the laser performance. Figure 7 reviews the evolution of the

maximum average output power and shortest pulses obtained from Yb:YAG TDL oscillators. Even though SESAM mode-locked and KLM TDLs reach similar output power levels, it turns out that KLM Yb:YAG TDLs enable the generation of much shorter pulses than SESAM mode-locked Yb:YAG TDLs. Although Yb:YAG features a narrow gain bandwidth, KLM Yb:YAG TDL oscillators generated 49-fs pulses at 3.5-W average power [33]. Even shorter pulses of 35 fs have been achieved in bulk oscillators based on this gain material [62]. The large optical bandwidth in excess of 30 nm resulted on intra-cavity pulse spectral broadening, where additional spectral components well beyond the gain spectral limitation are generated via SPM [63].

An extremely promising approach to generate powerful ultrashort laser pulses lies in the combination of KLM TDL oscillators and broadband gain materials. Amongst all Yb-doped gain

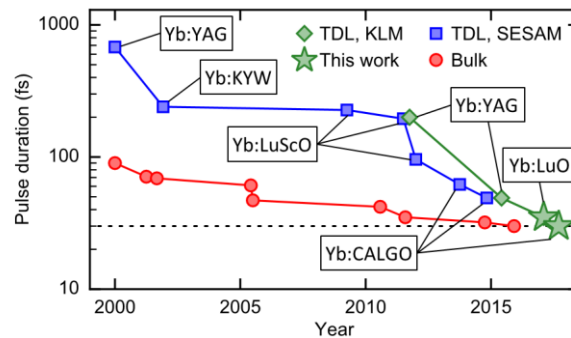


Figure 6. Evolution of the minimum pulse duration generated by ultrafast oscillators based on Yb-doped laser crystals in the bulk and TDL geometries [14,22–25,30,31,41–51]. The gain materials used in the TDL results are shown in boxes for information. Bulk: [49–57]; TDL, SESAM: [15,24,25,27,32,58,59]; TDL, KLM: [26,33]; the results presented in this thesis are highlighted with star symbols.

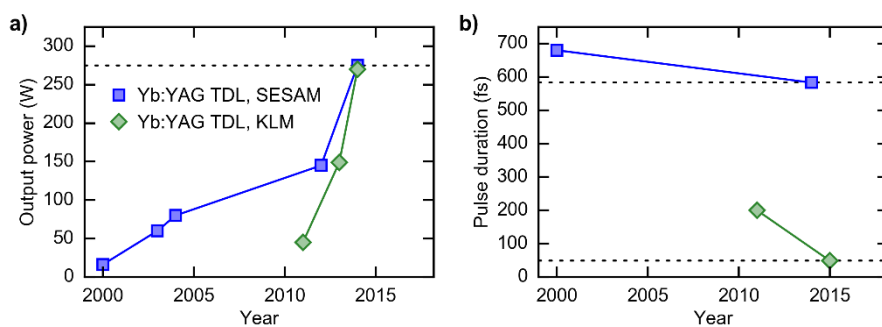


Figure 7. Evolution of the a) maximum average output power and b) minimum pulse duration achieved from ultrafast Yb:YAG TDL oscillators. TDL, SESAM: [8,15,18,64,65]; TDL, KLM: [18, 25,32,66].

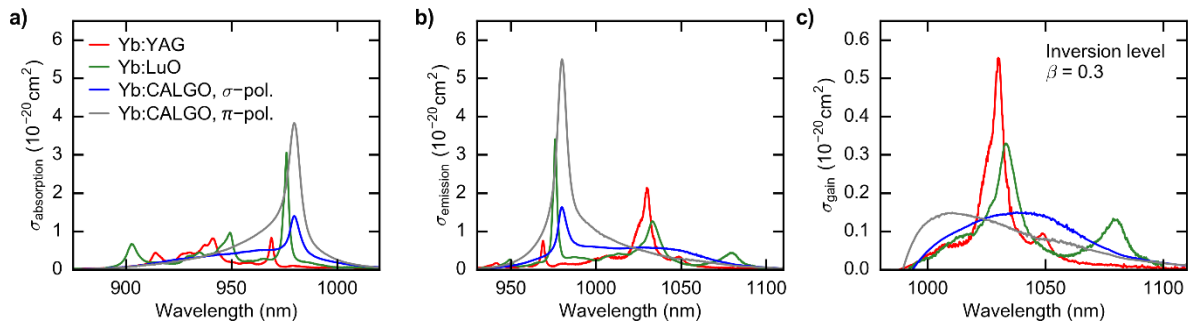


Figure 8. Spectroscopic properties of highly promising Yb-doped gain materials for the generation of powerful ultrashort pulses from TDL oscillators. a) Absorption, b) emission and c) gain cross sections of the different materials. Properties of Yb:CALGO crystals are shown for both  $\sigma$ - and  $\pi$ -polarization. The gain cross sections are calculated for an inversion level<sup>2</sup>  $\beta$  of 0.3 according to  $\sigma_{gain} = \beta \cdot \sigma_{emission} - (1 - \beta) \cdot \sigma_{absorption}$ . Data taken from [2,67].

materials, Yb:Lu<sub>2</sub>O<sub>3</sub> (Yb:LuO) and Yb:CaGdAlO<sub>4</sub> (Yb:CALGO) stand out for their specific properties and advantages over Yb:YAG crystals. Figure 8 shows a comparison of the spectroscopic properties of these gain materials and Table 1 summarizes their main thermo-mechanical and optical characteristics.

The Yb-doped sesquioxide Yb:LuO is an excellent candidate to outperform Yb:YAG as gain material for the delivery of sub-100-fs pulses at hundred-watt average power levels. It features a high thermal conductivity and its gain bandwidth directly supports the sub-100-fs pulse duration. Moreover, average power higher than 140 W has been achieved in mode-locked operation [68] and Kerr lens mode-locking in the TDL configuration has been demonstrated recently [69]. In this proof-of-principle demonstration, the laser delivered sub-200-fs pulses at multi-watt power level. Chapter 2 details successive investigation on KLM TDL oscillators based on Yb:LuO crystals which led to record-high average power generated by TDL oscillators in pulses with sub-100-fs and sub-50-fs duration. This laser enabled the realization of the first fully-stabilized optical-frequency comb based on a TDL oscillator, which is presented in Chapter 4.

On the other hand, Yb:CALGO features by far the broadest spectral gain bandwidth of the Yb-doped materials that have been previously developed for TDL applications. This gain material directly supports sub-50-fs pulse generation and currently holds the record for the shortest pulses emitted from TDL oscillators. Additionally, multi-ten-watt average power has

<sup>2</sup>Reasonable inversion level for TDL oscillators used as a reference value in the manuscript.



been reported from SESAM mode-locked Yb:CALGO TDLs. Owing to their remarkable potential to generate even shorter pulses, KLM TDL oscillators based on Yb:CALGO laser crystals are investigated. A proof-of-concept realization is presented in Chapter 3 and demonstrates record-short pulses of 30 fs from Yb-doped bulk and TDL oscillators.

Table 1. Physical properties at 300 K of few promising Yb-doped gain materials for the generation of powerful short pulses from TDL oscillators. Data taken from [67,70–72].

	Yb:YAG	Yb:LuO	Yb:CALGO ( $\sigma/\pi$ pol.)
Chemical formula	Yb:Y <sub>3</sub> Al <sub>5</sub> O <sub>12</sub>	Yb:Lu <sub>2</sub> O <sub>3</sub>	Yb:CaGdAlO <sub>4</sub>
Melting point (undoped) (°C)	1930	2500	< 1700
Thermal conductivity (undoped) (W/m·K)	9.8	12.2	~10
Thermal conductivity (3 at.% Yb-doped) (W/m·K)	7.1	10.8	6.6
Fluorescence lifetime ( $\mu$ s)	1040	820	445
<b>Zero-phonon line (ZPL):</b>			
Central wavelength (nm)	969	976	979
Absorption bandwidth FWHM (nm)	2.5	2.9	> 5
$\sigma_{\text{abs}}$ ( $10^{-20}$ cm <sup>2</sup> )	0.83	3.1	1.4/3.8
<b>Absorption band:</b>			
central wavelength (nm)	940	950	-
Absorption bandwidth FWHM (nm)	> 10	8	-
$\sigma_{\text{abs}}$ ( $10^{-21}$ cm <sup>2</sup> )	0.82	0.96	-
<b>Gain at inversion level <math>\beta = 0.3</math>:</b>			
Central wavelength (nm)	1030	1033	1042/1010
Bandwidth FWHM (nm)	8	13	> 60
Fourier transform limited pulse duration (fs)	120	90	< 20
$\sigma_{\text{gain}}$ ( $10^{-21}$ cm <sup>2</sup> )	0.55	0.33	0.15/0.15
ZPL quantum efficiency (%)	94	94	94/97
Absorption-band quantum efficiency (%)	91	92	-



## **Chapter 2 Cutting-edge sub-100-fs Kerr lens mode-locked thin-disk laser oscillators**

Given the limited performance or the high complexity of the current laser systems, novel simple laser sources delivering powerful ultrashort pulses are highly attractive to drive a plethora of experiments [73]. As highlighted in Chapter 1, ultrafast TDL oscillators are an ideal technological choice to perform intra- and extra-cavity experiments using a single-stage laser source with an excellent spatio-temporal pulse quality. To extend the performance of these lasers to sub-100-fs pulse durations, numerous Yb-doped broadband gain materials have been investigated in SESAM mode-locked TDLs. On the contrary, little work has been reported on KLM TDLs based on Yb-doped broadband laser crystals, although the narrow gain spectral bandwidth of standard Yb:YAG crystals may be detrimental for operation at sub-100-fs pulse duration. In particular, the average power of sub-100-fs TDL oscillators has been limited to 5 W prior to this work.

This chapter presents state-of-the-art sub-100-fs TDL oscillators which combine the benefits of the broadband Yb:LuO gain material and Kerr lens mode-locking scheme. Section 2.1 discusses the thermo-mechanical characteristics and spectroscopic properties of Yb:LuO crystals. Additionally, previous laser results are reviewed and confirm the potential of this gain medium for the generation of powerful ultrashort laser pulses. Section 2.2 describes cw experiments conducted to evaluate the capabilities of the specific thin-disk crystal later used for mode-locking experiments. Section 2.3 details an investigation into the influence of several laser parameters on the laser behavior. More than 300 laser configurations have been tested to determine the maximum output power achievable at sub-100-fs pulse duration as well as the minimum pulse duration for a given laser mode size on the Kerr medium. Section 2.4 presents the laser performance scaling by enlarging the laser mode size on the Kerr medium. Both higher average output power and shorter pulses are obtained. Section 2.5

concludes and gives an outlook towards further increase of the average and peak power from Yb-based sub-100-fs TDL oscillators.

## **2.1 Yb:LuO: a gain material well-suited for the generation of powerful sub-100-fs pulses**

The Yb-doped sesquioxide Yb:LuO is among the most promising candidates to outperform Yb:YAG in pushing the performance of high-power ultrashort TDL oscillators [2,47]. Yb:LuO exhibits a 60% broader gain bandwidth than Yb:YAG, amounting to 13 nm (FWHM at  $\beta = 0.3$ ), and directly supports sub-100-fs pulse formation. Figure 8 in Chapter 1 shows its absorption, emission and gain cross sections and Table 1 in Chapter 1 summarizes its main properties. The zero-phonon line of Yb:LuO around 976 nm offers 4-times larger absorption cross sections than in the absorption band around 950 nm. It also represents a threefold increase compared to the cross sections of Yb:YAG. Additionally, pumping at the zero-phonon line brings the advantage of an increased Stokes efficiency and thus a lower amount of generated heat due to the quantum defect [74]. The cubic host lutetia ( $\text{Lu}_2\text{O}_3$ ) crystal features a high thermal conductivity of  $12 \text{ W}\cdot\text{m}^{-1}\cdot\text{K}^{-1}$ . Because of the small atomic mass difference between  $\text{Yb}^{3+}$ -ions and  $\text{Lu}^{3+}$ -ions, doping of lutetia leads to only a small distortion of the phonon propagation responsible for heat transport in the crystal. Consequently, the thermal conductivity is nearly independent of the doping concentration [75], in contrast to Yb:YAG in which the thermal conductivity drops by nearly a factor of two down to  $7 \text{ W}\cdot\text{m}^{-1}\cdot\text{K}^{-1}$  at Yb-doping concentrations required in the TDL configuration. Hence, high Yb-ion concentrations up to nearly 5 at.% are achievable in LuO, and result in a high gain without impacting on the heat handling capabilities of the laser crystal. Together with large absorption cross sections, this allows using thinner crystals for an improved heat management and reduced thermal effects.

The larger gain bandwidth and superior thermal behavior favor Yb:LuO over Yb:YAG as ideal gain material for high-power ultrashort pulse generation. However, the high melting point exceeding  $2400^\circ\text{C}$  makes the fabrication of lutetia very challenging. The heat exchanger method (HEM) has proven to be a viable technique for growing large-size high-quality single-crystalline sesquioxide crystals [76]. A picture of a such a crystal produced at the Institut für Laser-Physik (ILP) of the University of Hamburg (Germany) is shown in Figure 9. During the growth process, the crucible is kept at a fixed position and crystallization is performed by a controlled flow of cooling gas blown against the bottom of the crucible. The production of high-quality crystals via HEM requires the use of costly high-purity rhenium crucibles (melting

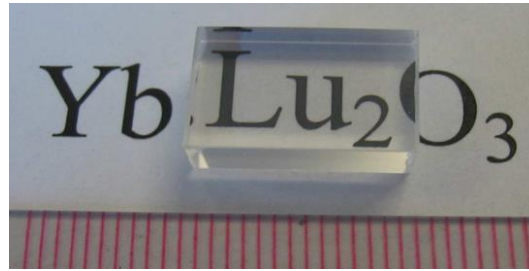


Figure 9. Large-size high-quality Yb:LuO crystal grown by the heat exchanger method (lower scale in mm). Picture taken from [2].

point around 3180°C), high-purity raw material and optimized atmosphere. Due to the technical difficulties and costs, Yb:LuO laser crystals are currently difficult to obtain. However, the improved growth of ceramics might change the situation [77].

Correspondingly, experimental results confirmed the above-mentioned advantages. Figure 10 presents a timeline of ultrafast Yb:LuO laser performance in bulk and TDL configurations. Laser oscillators based on bulk Yb:LuO crystals supported high optical efficiency close to 70% in mode-locked operation [78]. Ceramic-Yb:LuO bulk oscillators delivered pulses as short as 65 fs at 0.3-W output average power [79] and similar results (71 fs pulses at 1.1-W average power) have been obtained from single-crystalline material [80]. The power scalability of Yb:LuO lasers has been demonstrated in the TDL configuration, reaching 500 W of cw output power in multi-mode operation with record-high optical efficiency of nearly 80% and slope efficiency of 90%, approaching the theoretical limit [2]. Even higher average powers have been

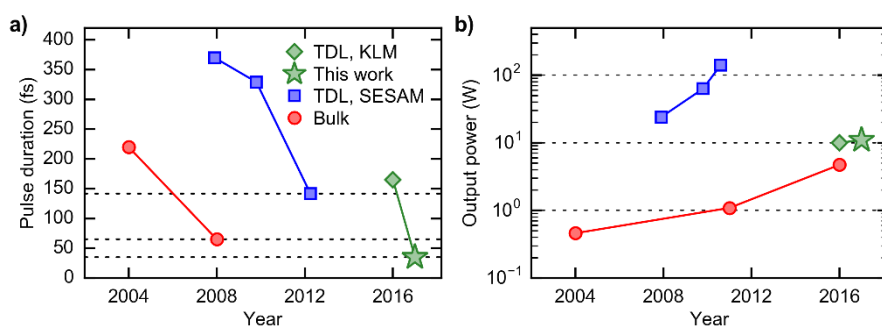


Figure 10. Evolution of the a) minimum pulse duration and b) maximum average output power from ultrafast laser oscillators based on Yb:LuO gain materials in bulk and thin-disk laser geometry. TDL, KLM: [69]; TDL, SESAM: [82,83,68,30]; Bulk: [78–80,84]; the results presented in this chapter are highlighted with star symbols.

achieved with up to 670 W of laser light converted from more than 1 kW of pump power [81]. Pump intensities above 7 kW/cm<sup>2</sup> could be reached without crystal damage, although the crystal was mounted with a sub-optimal indium-tin solder onto a copper heat sink [75]. Diamond heat spreaders offer a higher thermal conductivity and allow for more efficient heat removal from the laser crystal. Consequently, high-quality crystals mounted onto diamond heat sinks with state-of-the-art contacting technologies are expected to withstand even higher pump densities without damage.

SESAM mode-locked Yb:LuO TDL oscillators generated an average power higher than 140 W with sub-ps pulses and an optical efficiency exceeding 40% [68], which has held the record for the highest average power from any ultrafast oscillator for many years. These lasers supported the generation of pulses as short as 142 fs at 7-W average power [30], while improved SESAMs enabled power scaling up to 25-W average power in 185-fs pulses [85]. It is worth noting that Yb:LuO and Yb:ScO crystals have been used together in a dual-gain SESAM mode-locked TDL. In this way, the combination of the two separated emission spectra enabled the generation of 103-fs pulses at watt power level and higher power close to 10 W has been reached at sub-150-fs pulse duration [31]. Recently, the first KLM Yb:LuO TDL achieved 6-W average power in 165-fs pulses [69], making Yb:LuO the second gain material to be Kerr lens mode-locked in the TDL configuration. It is interesting to highlight the promising alternative to single-crystalline Yb:LuO offered by ceramic Yb:LuO. This gain medium can be easily manufactured at low temperature in large size and at relatively low cost, though it has not been widely studied yet. Very recent work demonstrated cw operation at more than hundred-watt power level, and preliminary mode-locking results have been shown at a conference [77]. Altogether, owing to its outstanding laser properties and given the previously reported results demonstrating high-average power levels and short-pulse generation, Yb:LuO is very well suited as TDL gain material for the generation of powerful sub-100-fs pulses.

## **2.2 Evaluation of the capabilities of the TDL crystal in continuous-wave operation**

The laser experiments have been performed with a 12-mm-diameter Yb(3 at.):LuO TDL crystal. It has been cut from a crystal boule grown at the ILP Hamburg and polished to 160- $\mu$ m thickness with a 0.1° wedge, which avoids interaction between residual reflections and the main beam. The front surface is AR-coated while the back surface is coated to be HR at laser and pump wavelengths. The laser crystal is contacted onto a diamond heat sink and exhibits

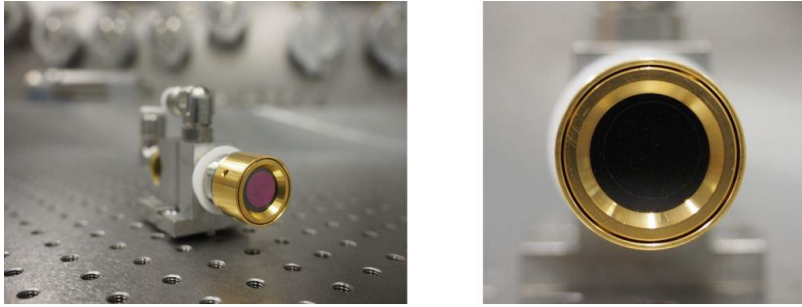


Figure 11. Pictures of the 12-mm-diameter 160- $\mu\text{m}$ -thick Yb:LuO laser crystal mounted onto a diamond heat sink. The combination of the thin-disk geometry and diamond heat sink enables efficient heat removal from the gain medium, which is paramount for high-power laser operation.

a concave radius of curvature (RoC) of 2.1 m. Figure 11 shows pictures of the disk mounted onto its cooling finger by Trumpf GmbH. Water cooling of the diamond backside allows for efficient dissipation of the heat generated in the active material. A 400-W fiber-coupled VBG-wavelength-stabilized diode laser system pumps the laser crystal at the zero-phonon line at a wavelength of 976 nm with a spectral width below 0.5 nm FWHM. The disk is placed in a TDL head designed for 36 passes of the pump through the gain medium to achieve high pump absorption. The pump spot is set to a diameter of 2.8 mm.

The disk was initially tested in cw operation in a linear cavity as shown in Figure 12. The resonator comprises the concave HR-coated backside of the thin-disk crystal and a flat

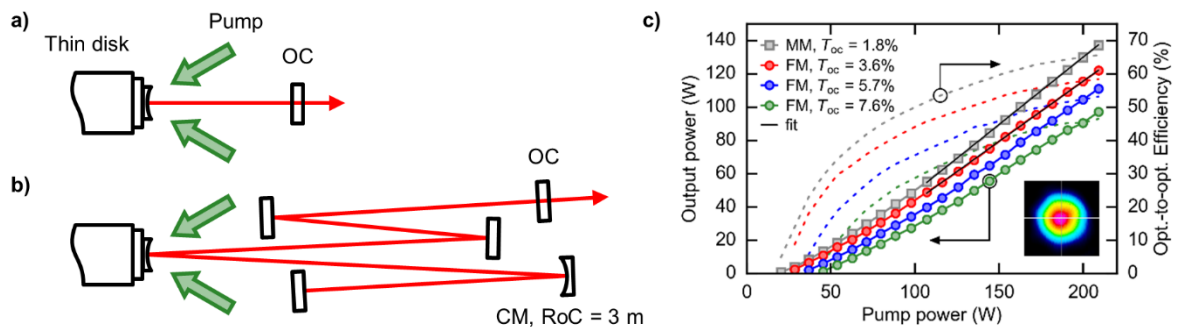


Figure 12. Layouts of a) the multi-mode (MM) and b) fundamental-transverse-mode (FM) resonator cavities. OC, output coupler; CM, curved mirror; RoC, radius of curvature. c) Output power (solid lines) and optical-to-optical efficiency (dashed lines) as a function of the pump power for MM cavity (output coupler transmission  $T_{oc} = 1.8\%$ ) and the FM cavity folded over the disk ( $T_{oc} = 3.6 - 7.6\%$ ), thus experiencing twice higher gain per cavity round trip. The black solid lines show the linear fits used for the calculation of the slope efficiencies. Inset: Mode profile of the output laser beam at 122-W average power ( $T_{oc}$  of 3.6%).

partially-transmissive mirror used as an output coupler (OC) with a transmission  $T_{OC}$  of 1.8%. Given the cavity length of  $\sim 7$  cm, the beam radius of the transverse fundamental mode on the gain crystal was estimated to be  $360 \mu\text{m}$  from ray-transfer matrix calculations. Consequently, the laser operation was highly multi-mode, owing to the 4-times larger pump radius. In such a configuration, highest optical efficiencies can be expected due to the improved overlap of the top-head pump profile and the multi-mode laser beam compared to a diffraction limited Gaussian beam. An output power of 137 W has been obtained from 209 W of incident pump power. The optical efficiency amounted to 66% and the slope efficiency was 81%. These values are close to the best reported results with this gain material in the TDL configuration [2]. To avoid damage, the pump intensity on the disk has been kept below  $3.5 \text{ kW/cm}^2$ , even though no hints for the degradation of the laser efficiency were observed even at the highest pump powers.

In the next step, a 3-m-long linear cavity supporting transverse fundamental mode operation was built, as depicted in Figure 12b). The disk and a concave curved mirror (RoC = 3 m) are placed between two flat end mirrors, of which one is an OC. The ratio between fundamental mode and pump spot was estimated to  $\sim 80\%$ . The beam quality factor  $M^2$  has been measured to be below 1.2 in all experiments, confirming close-to-diffraction-limited laser behavior. In this configuration where the disk is used as a folding mirror, the laser beam passes four times per round trip through the gain medium (accounting 2 passes per bounce), which leads to a twice higher gain and consequently a twice larger optimal output coupling rate compared to the above-mentioned multi-mode resonator. The lasing performance in cw regime has been evaluated for different output coupling rates (see Figure 12c). At  $T_{OC} = 3.6\%$ , the laser emits 122-W average power in fundamental transverse mode with an optical efficiency approaching 60% and a high slope efficiency of 70%. These results reveal that this particular disk features a high optical quality and is therefore very suitable for mode-locking experiments.

### **2.3 Experimental study of the performance of Kerr lens mode-locked thin-disk lasers**

The performance of KLM TDLs depends on several parameters forming altogether a multi-dimensional space. The aim of this section is to explore this parameter space to get insight into the coupling and influence of the different factors. This empirical study focusses on optimizing the laser for maximum output power at sub-100-fs pulse duration or minimum



pulse duration for a given laser mode size on the Kerr medium. In consequence, no attempt has been made to increase the output power level at longer pulse durations.

In order to favor pulsed operation over the cw regime, a laser cavity similar to the first KLM TDL oscillator [26] is used and depicted in Figure 13a). An undoped YAG plate is placed under Brewster angle in the focal region between two HR concave mirrors (CM2 and CM3), which have both a 300-mm RoC. The plate ensures a linear polarization of the laser and serves as Kerr medium for the mode-locking mechanism. The setup for hard-aperture Kerr lens mode locking is completed by a water-cooled pinhole placed in front of an end mirror. The second end mirror is used as an OC. The laser mode radius inside the Kerr medium is estimated to be 70  $\mu\text{m}$  and 125  $\mu\text{m}$  in the sagittal and tangential planes in cw operation. The intra-cavity group delay dispersion (GDD) is adjusted by several dispersive mirrors. Pulsed operation is initiated by a gentle knock on the laser table and a change of the laser mode size is observed as illustrated in Figure 13b). The resonator is operated in ambient air and has a compact footprint of 70 cm  $\times$  40 cm.

In this study, the general cavity design is not changed such that the laser mode size on the Kerr medium is the same in all laser configurations. The parameters under test are the output coupling rate, the intra-cavity dispersion, the hard aperture size, the Kerr medium thickness and the repetition rate of the laser. The associated studied ranges are summarized in Table 2.

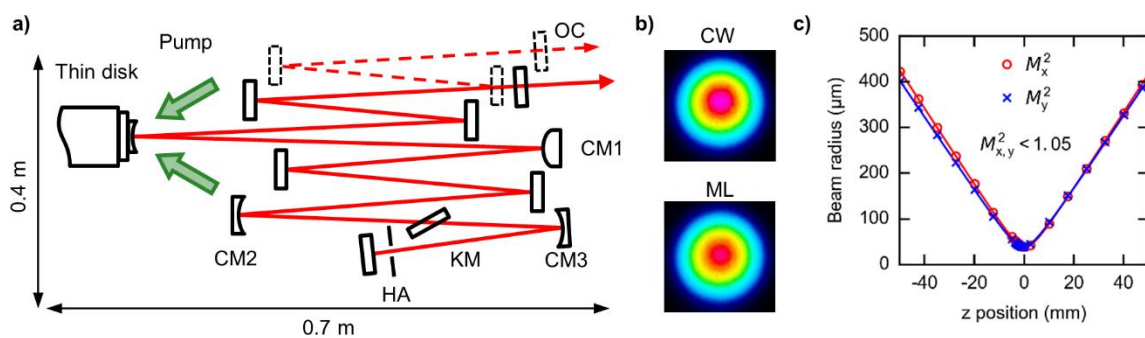


Figure 13a) Schematic of the laser cavity used for the investigation into the performance of Kerr lens mode-locked lasers. OC, output coupler; CM1, highly-reflective (HR) curved mirror with a 2-m convex radius of curvature (RoC); CM2-CM3, HR 300-mm-RoC concave curved mirror; KM, Kerr medium; HA, hard aperture. All other mirrors are HR or dispersive mirrors depending on the configuration. The dashed line shows the extended resonator cavity used to evaluate the influence of the repetition rate on the mode-locking behavior. b) A difference in the size of the output beam profile was observed between cw and mode-locked operation. c) Typical beam quality factor ( $M^2$ ) measurement of the output beam of the mode-locked laser.

For each configuration, the pump power was adapted to produce the shortest pulses in clean single-pulse operation. Increasing the pump power further introduces mode-locking instabilities, and typically a cw breakthrough is observed in the optical spectrum.

For a given resonator design, the Kerr medium determines the strength of the Kerr lensing effect for a given laser peak power. Undoped YAG has been selected as Kerr medium material because of its high nonlinear refractive index  $n_2(6.5 \cdot 10^{-20} \text{ m}^2/\text{W}$  at 1030 nm [86], compared to  $3 \cdot 10^{-23} \text{ m}^2/\text{W}$  for the ambient air [87]) and large thermal conductivity. However, other materials such as fused silica ( $\text{SiO}_2$ ) and sapphire ( $\text{Al}_2\text{O}_3$ ) have also been used in KLM TDLs [26,34]. Besides affecting the Kerr lens focal length, changing the Kerr medium thickness contributes via  $n_2$  to a variation of the effective nonlinear coefficient  $\gamma$  of the laser resonator according to:

$$\gamma = \int_0^L \frac{2\pi}{\lambda} \frac{n_2(z)}{A_{\text{eff}}(z)} dz,$$

where  $L$  denotes the resonator length,  $\lambda$  the laser wavelength,  $n_2(z)$  the nonlinear refractive index of the material at the position  $z$ , and  $A_{\text{eff}}(z)$  the laser mode area at the position  $z$ . In this resonator, a change of thickness of the Kerr medium from 1 to 2 mm increases  $\gamma$  by  $\sim 40\%$  while it provides more than 85% of the total nonlinear phase shift. Moreover, an increase of the repetition rate was evaluated by changing the distance between the disk and OC as shown by the dashed line in the cavity sketch in Figure 13a). According to ray-transfer-matrix calculations, this length shift does not impact on the laser mode size on the disk or inside the Kerr medium for the studied range. As a result of the large beam diameter in this part of the cavity,  $\gamma$  is nearly independent of this length and varies by less than 10% when changing the disk-OC distance by 30 cm. Consequently, the change of repetition rate influences mainly the pulse energy for a given average power.

The systematic study has been limited to the aforementioned parameters which have been found to be the most significant. As expected from the 15-mm Rayleigh length of the 70  $\mu\text{m}$  beam radius at the intra-cavity focus, no significant changes in the mode-locked laser performance were observed when shifting the Kerr medium by a few mm. In contrast, the distance between CM2 and CM3 affected the mode-locking conditions (mode-locking threshold power, tolerable aperture size), however, a thorough investigation of its influence was beyond the scope of this work.

Table 2. Studied parameter ranges for the investigation into the performance of Kerr lens mode-locked thin-disk laser oscillators.

	Min value	Max value
Output coupling rate (%)	0.33	6.5
GDD per round trip (fs <sup>2</sup> )	-1650	-6700
Hard-aperture diameter (mm)	1.5	2.7
Kerr-medium thickness (mm)	1	2
Repetition rate (MHz)	50	66
Pump power (W)	30	160

Stable mode locking was achieved for more than 300 laser configurations and a clear trade-off between the pulse duration, output power and laser efficiency was observed. Figure 14 shows the laser output power and optical efficiency as a function of the achieved pulse duration for the full data set. The graphs highlight the influence of the output coupling rate, the inserted GDD per round trip and the hard-aperture diameter, respectively. For smaller hard-aperture diameters and lower amounts of inserted GDD per round trip, no stable mode locking has been obtained, while for higher values, the pulse duration increased. Besides, increasing both the Brewster plate thickness from 1 mm to 2 mm and the repetition rate from 50 to 66 MHz, which corresponds to a decrease of 20% of the pulse energy at a given average power, did not introduce significant changes in the laser behavior. The beam quality has been measured for numerous configurations and resulted in a  $M^2$  value smaller than 1.05. A typical measurement is shown in Figure 13c).

Several general trends for the optimization of the laser parameters can be extrapolated from this work. For generating the shortest pulses, the output coupling rate, GDD and hard-aperture diameter must be reduced to the smallest value which still allows the laser to operate in stable fundamental cw mode-locking regime. Simultaneously, this leads to a decrease of the optical efficiency and to lower output power levels. To reach higher output powers, a compromise between these parameters should be made. Although the frontiers of the range for stable clean mode locking are clear, any given combination of output power and pulse duration within this region could be obtained by several distinct set of laser parameters. It is also interesting to note that even though a smaller aperture increases the resonator losses and decreases the laser efficiency, it simultaneously enables the generation of both shorter and more powerful pulses. These observation are in good agreement with previous reported studies on mode locking with fast saturable absorbers [34,88–90].

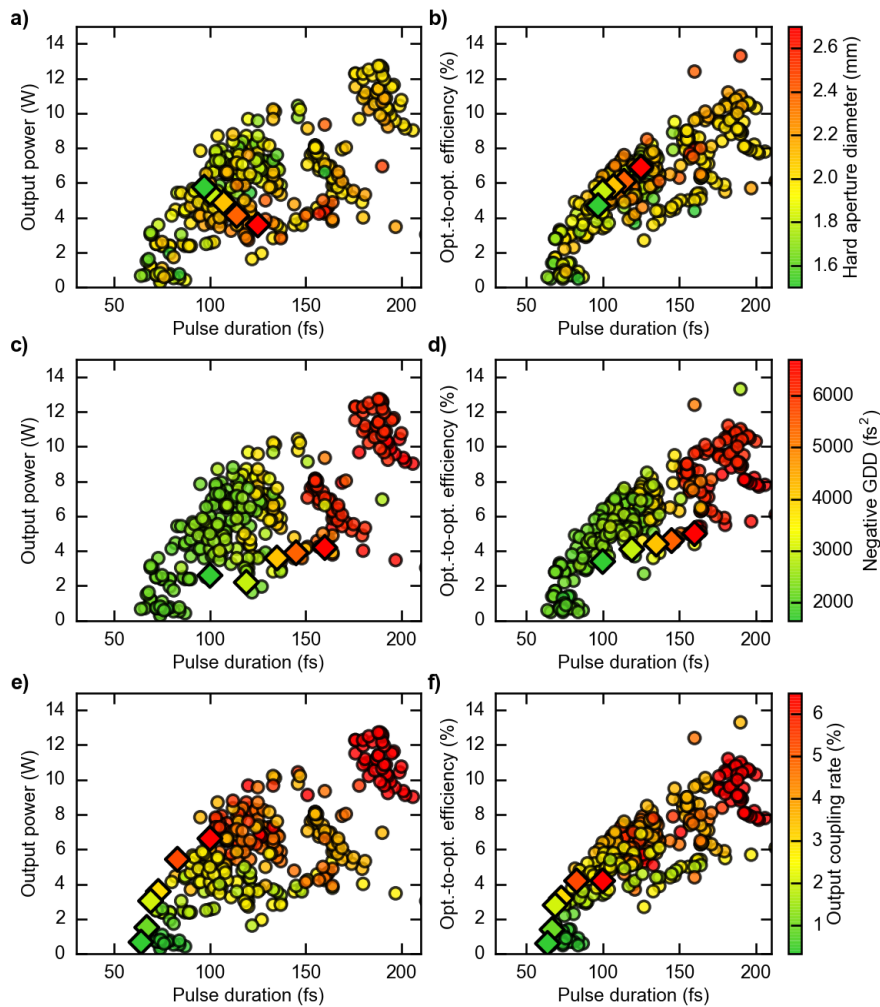


Figure 14: Influence of the laser parameters on the (a, c, e) output power and (b, d, f) optical-to-optical efficiency plotted as function of pulse duration. The individual influence of each specific parameter is highlighted with diamond symbols. In this case, only the parameter under test is varied, and all others are kept constant. Otherwise, (circle symbols) all parameters are varied freely and the value of the parameter under test is given by the color code. The laser parameters shown are (a, b) the output coupling degree, (c, d) the inserted negative group delay dispersion (GDD) per round trip and (e, f) the hard aperture diameter.

Optimization to the shortest pulses led to a duration of 64 fs at 0.7-W average output power. The highest power at sub-100-fs pulse durations has been achieved with 7.9 W in 94-fs pulses, while more than 10 W has been obtained in 132-fs pulses. Table 3 shows the detailed laser parameters and Figure 15 presents the pulse characterization of the three selected configurations. The noise characterization depicted in Figure 15c-d) has been performed with an intermediate cavity configuration which delivered 5-W average power in 94-fs pulses. The

Table 3. Mode-locked performance and laser parameters for the three selected configurations, which achieve the shortest pulse duration, the highest power at sub-100-fs pulse durations, and the shortest pulses with more than 10-W average power, respectively. IC, intra-cavity, HA, hard aperture.

Configuration	64 fs	94 fs	132 fs	Configuration	64 fs	94 fs	132 fs
Output power (W)	0.7	7.9	10.4	GDD per round trip (fs <sup>2</sup> )	-2200	-2200	-3750
Peak power (MW)	0.2	1.1	1.3	HA diameter (mm)	1.7	2.0	2.1
Pulse energy (μJ)	0.01	0.12	0.19	Repetition rate (MHz)	56	65	65
IC average power (W)	233	219	289	Output coupling rate (%)	0.3	3.6	3.6
IC peak power (MW)	57	32	36	Pump power (W)	114	135	135
Central wavelength (nm)	1033	1035	1038	Optical efficiency (%)	0.6	5.9	7.7
FWHM bandwidth (nm)	18.0	12.7	10.0	Time-bandwidth product	0.324	0.334	0.367

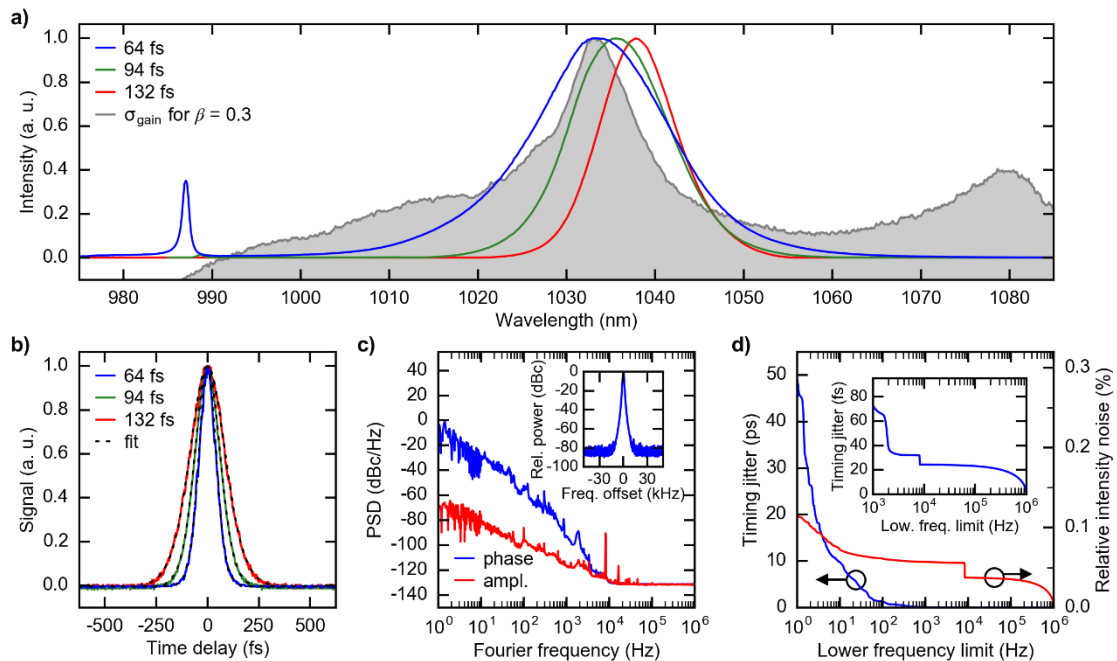


Figure 15. a) Optical spectra of the 64-fs, 94-fs and 132-fs laser configurations. The normalized gain cross section  $\sigma_{\text{gain}}$  of Yb:LuO is calculated for an inversion level  $\beta$  of 0.3 and shown in grey color for reference (data taken from [2]). b) Intensity autocorrelation traces with corresponding  $\text{sech}^2$  fit. c) Phase and amplitude noise power spectral densities (PSD) measured at the 38<sup>th</sup> harmonic of the repetition rate (2.47 GHz) of an intermediate laser configuration delivering 5 W in 94-fs pulses. (inset) Radio-frequency spectrum of the carrier frequency at 65 MHz measured with a 1-kHz resolution bandwidth. d) Left y-axis: Rms timing jitter integrated from 1 Hz and (inset) from 1 kHz up to 1 MHz; right y-axis: rms relative intensity noise.

noise measurement of the 38<sup>th</sup> harmonic of the repetition rate ( $38 \times 65 \text{ MHz} = 2.47 \text{ GHz}$ ) resulted in a 0.1% root-mean-square (rms) relative intensity noise (RIN) (integrated from 1 Hz to 1 MHz) and an rms timing jitter of 50 ps (integrated from 1 Hz to 1 MHz) or 73 fs (integrated from 1 kHz to 1 MHz) for the unstabilized oscillator.

## 2.4 Performance scaling of Kerr lens mode-locked Yb:LuO thin-disk lasers

Following the first demonstration of a KLM TDL [26], Brons *et al.* demonstrated that the intracavity peak power of KLM TDLs scales with the laser mode radius on the Kerr medium inside the resonator cavity [91]. It simultaneously results in an increased average output power of the laser. It is then a logical step to apply this scaling method to the lasers presented in Section 2.3. For this, the curved mirrors around the Kerr medium are replaced by 400-mm-RoC curved mirrors and their separation distance is adapted accordingly, as depicted in Figure 16a). The laser mode radius on the Kerr medium is increased from  $70 \mu\text{m} \times 125 \mu\text{m}$  to  $90 \mu\text{m} \times 150 \mu\text{m}$  in the sagittal and tangential planes in the cw regime. A 2-mm-thick undoped YAG plate is used as Kerr medium, and the cavity length is set to 2.5 m, resulting in 61-MHz repetition rate. The resonator is operated in ambient air and has a footprint of only  $80 \text{ cm} \times 40 \text{ cm}$ .

As observed in Section 2.3, stable mode locking is obtained for a large variety of parameters. The laser has been optimized following the guidelines given in the previous section, and Table 4 summarizes the laser characteristics for three representative

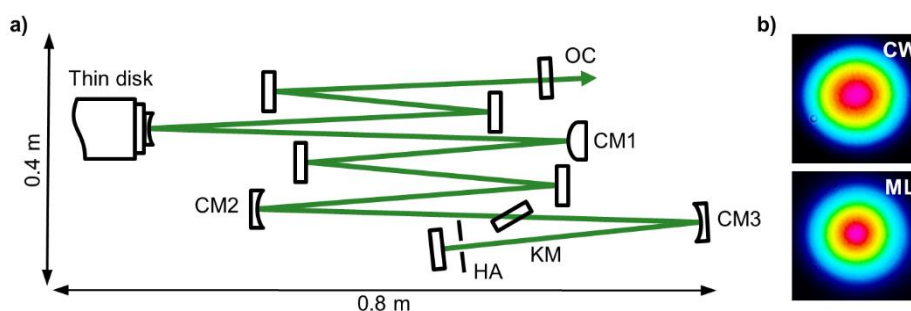


Figure 16. a) Schematic of the cavity used for scaling the performance of Kerr lens mode-locked Yb:LuO thin-disk laser oscillators. CM1, highly reflective (HR) curved mirror with a 2-m convex radius of curvature (RoC); CM2-CM3, HR 400-mm-RoC concave curved mirror; KM, Kerr medium; HA, hard aperture; OC, output coupler. All other mirrors are highly reflective or dispersive mirrors depending on the configuration. b) A difference in size of the output-beam profile was observed between cw and mode-locked (ML) operations (data shown for the 35-fs laser configuration).

Table 4. Mode-locked performance and laser parameters for the selected configurations, which achieved the shortest pulses and the highest average output power at sub-50-fs and sub-100-fs pulse durations, respectively. IC, intra-cavity; HA, hard aperture.

<b>Configuration</b>	<b>35 fs</b>	<b>49 fs</b>	<b>88 fs</b>	<b>Configuration</b>	<b>35 fs</b>	<b>49 fs</b>	<b>88 fs</b>
Output power (W)	1.6	4.5	10.7	GDD per round trip (fs <sup>2</sup> )	-1000	-1100	-2200
Peak power (MW)	0.7	1.3	1.8	HA diameter (mm)	1.9	2.0	2.0
Pulse energy (μJ)	0.03	0.07	0.18	Repetition rate (MHz)	61	61	61
IC average power (W)	178	167	233	Output coupling rate (%)	0.9	2.7	4.6
IC peak power (MW)	73	49	38	Pump power (W)	76	96	186
Central wavelength (nm)	1029	1031	1038	Optical efficiency (%)	2.1	4.7	5.8
FWHM bandwidth (nm)	33.9	24.1	14.4	Time-bandwidth product	0.336	0.333	0.353

configurations. The 88-fs and 49-fs configurations achieve 10.7-W and 4.5-W average output power, respectively, which is the highest average power at sub-100-fs and sub-50-fs pulse durations. The shortest pulses of 35 fs are generated at 1.6-W output power. For each configuration, single-pulse operation is confirmed with a 180-ps long-range autocorrelation and observation of the trace of a fast 18.5-ps photodiode on a 40-GHz sampling oscilloscope. Figure 17a-b) show the optical spectra of the laser output and the intensity autocorrelation traces with the corresponding sech<sup>2</sup> fit for the three configurations. For the measurement of the 35-fs pulses, an extra-cavity dispersive mirror with negative GDD of -250 fs<sup>2</sup> has been used to compensate for the material dispersion of the OC mirror substrate and for the propagation in air. The side peaks observed in the spectra of the ultrashort pulses carry only a minor fraction of the power (about few percent) and are associated with dispersive waves, similar to the sidebands observed in previous work, e.g., [54,57,92]. Their position does not depend on the intra-cavity power but may vary when using distinct sets of intra-cavity mirrors. Moreover, their amplitude is comparably smaller inside the resonator as a result of the 2-fold increase of the OC transmission at the edges of the spectrum. It should be noted that the 35-fs-pulse optical FWHM bandwidth is nearly 3 times broader than the FWHM gain cross section of Yb:LuO. The additional spectral components well beyond the gain limit originate from the SPM in the Kerr medium [63]. Such an intra-cavity spectral broadening has already been reported for Yb:YAG bulk and TDL oscillators [33,93].

The radio-frequency (RF) spectrum of the 35-fs-pulse repetition rate frequency shows a clean spectrum without any side peak at 300-Hz resolution bandwidth (RBW) and 70-dB signal-to-noise ratio (see Figure 17c). The long-term and short-term stability of the 35-fs

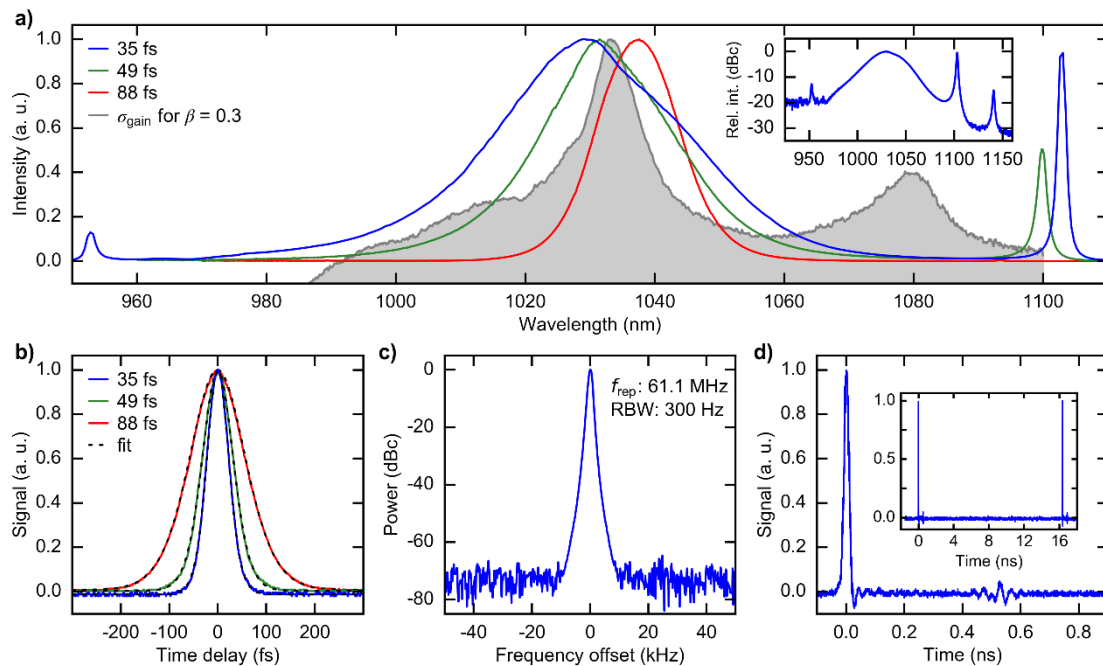


Figure 17. a) Optical spectra of the 35-fs, 49-fs and 88-fs laser configurations. The normalized gain cross section  $\sigma_{\text{gain}}$  of Yb:LuO is calculated for an inversion level  $\beta$  of 0.3 and shown in grey color for reference (data taken from [2]). (inset) Optical spectrum of the 35-fs laser plotted with y-axis in log-scale. b) Intensity autocorrelation traces with corresponding  $\text{sech}^2$  fit. c) Radio-frequency spectrum of the 35-fs-pulse repetition rate frequency ( $f_{\text{rep}}$ ) measured with a 300-Hz resolution bandwidth (RBW). d) Sampling oscilloscope trace in 1 ns and (inset) 20 ns of the 35-fs pulse train. The weak ringing in the signal trace at 0.5 ns is an artefact due to the electronics of the detection setup.

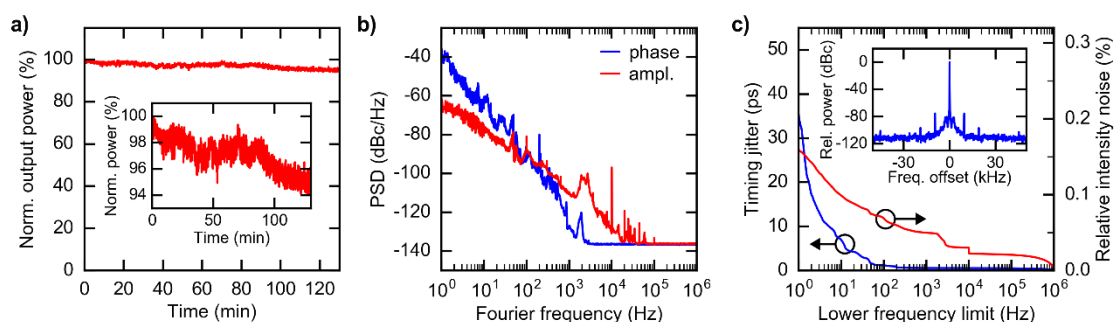


Figure 18. Long-term and short-term stability of the 35-fs Kerr lens mode-locked Yb:LuO thin-disk laser. a) Normalized average output power measured over more than two hours. (inset) Same data plotted with different y-axis limits. b) Phase and amplitude noise power spectral densities (PSD) c) Left y-axis: Rms timing jitter; right y-axis: rms relative intensity noise. (inset) Radio-frequency spectrum of the carrier frequency at 61 MHz measured with a 50-Hz resolution bandwidth.



configuration are presented in Figure 18. Even though no special effort was made to improve the stability of the laser, it operates for hours with considerably stable output parameters. The laser suffers from a small thermal drift, leading to a 5%-decrease of the average output power after two hours of operation and a standard deviation of 1.7%. The short-term noise measurement of the fundamental carrier frequency at 61 MHz shows a RIN smaller than 0.2% (integrated from 1 Hz to 1 MHz) and a timing jitter of 35 ps for an integration from 1 Hz to 1 MHz.

These results demonstrate 35% higher average output power at sub-100-fs pulse durations owing to the  $\approx 30\%$ -enlargement of the laser mode radius on the Kerr medium, compared to the results presented in Section 2.3. The increase of the intra-cavity peak power is in good agreement with the scaling law demonstrated for KLM Yb:YAG TDLs [34] as shown in Figure 19. Besides power scaling, the minimum pulse duration decreased by nearly 50%. However, the impact of the increase of the laser size on the Kerr medium on the pulse duration is not clear yet. The shortening of the pulse duration is mainly attributed to the distinct sets of dispersive mirrors used inside the cavity, the latter ones being more broadband. This point will be discussed in more details in Section 3.4.

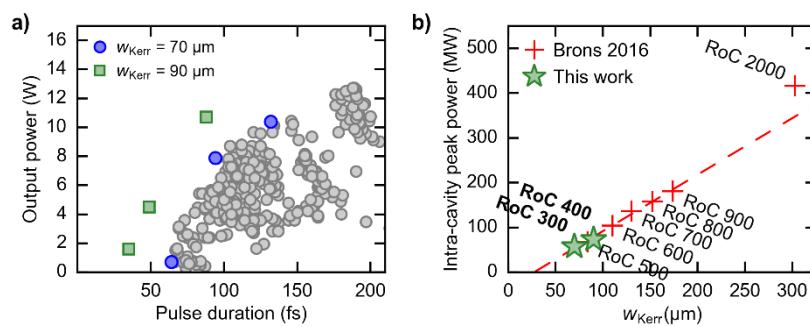


Figure 19. a) Overview of the mode-locked laser performances obtained from two cavities featuring different laser mode radii on the Kerr medium (KM)  $w_{\text{Kerr}}$ . The filled circle symbols (grey and blue) correspond to the lasers presented in Section 2.3; the square symbols correspond to the results presented in this section. b) Intra-cavity peak power as a function of the laser mode radius on the KM. The radius of curvature (RoC) of the concave curved mirrors placed around the KM is given for information. Red cross symbols show the results from [34]. The presented results are highlighted with star symbols.

## 2.5 Towards oscillators delivering sub-100-fs pulses at hundred-watt power levels

This chapter describes an extensive study on the performance of ultrashort KLM TDL oscillators. The maximum average output power at sub-100-fs pulse durations and the minimum pulse duration achievable in soliton mode locking have been investigated. The most influential parameters were the output coupling rate, the intra-cavity GDD, and hard aperture diameter. The results give important guidelines for the generation of ultrashort pulses. The oscillator must be driven at moderate level of inserted GDD and at low inversion of the gain by selecting a low degree of output coupling. A small hard aperture diameter maximizes the modulation depth and allows reaching the shortest pulse durations. Nevertheless, ultrashort pulse durations come at the expense of a low optical efficiency, which is below 10% at sub-100-fs pulse durations in the current systems (see comparison in Table 5). Comparison of the experimental observations with simulations would be beneficial to predict the limits of pulse duration, output power and optical efficiency, especially given the gain narrowing effect and laser reabsorption in the case of ultrabroadband pulses. Higher optical efficiencies are nonetheless expected by refining the cavity design for lower non-saturable losses and using more suitable broadband mirrors. The standard HR-coatings of the mirrors and disk crystal used in these experiments are specified by the manufacturers to exhibit a high reflection (>99.98%) only in the range of 1000-1100 nm, which does not fully support the large pulse spectral bandwidth and may induce detrimental losses. Further details on the optical efficiency of the ultrashort pulse generation are discussed in Chapter 3, Sections 3.3 and 3.4.

Following the suggested scaling law from Brons et al. [91], the intra-cavity peak power of the laser has been scaled by enlarging the spot size on the Kerr medium. This first scaling iteration led to the highest average power in sub-100-fs and sub-50-fs pulses directly emitted from a TDL oscillator with 10.7 W in 88-fs pulses and 4.5 W in 49-fs pulses. These results confirm the advantages of Yb:LuO as ideal gain material for KLM TDL oscillators for the generation of powerful sub-100-fs pulses. As a logical continuation, successive scaling iterations will be performed towards the generation of hundred watts of average power at sub-100-fs pulse durations. Scaling of the output power requires higher pump power levels which may lead to intensities close to the damage threshold of the laser crystal. To avoid this risk, the pump area can easily be scaled on the 12-mm-diameter disk by adapting the pump setup and cavity design. Additionally, previous work reported that the air inside the oscillator has a prejudicial contribution to the total nonlinear phase shift accumulated in lasers featuring

Table 5. Overview of sub-100-fs mode-locked thin-disk laser oscillators.  $P_{out}$ , average output power;  $E_{pulse}$ , pulse energy;  $\Delta\tau$ , pulse duration; Rep. rate, repetition rate;  $P_{peak}$ , output peak power;  $\eta_{opt}$ , optical-to-optical efficiency;  $P_{pump}$ , pump power.

Gain material	$P_{out}$ (W)	$E_{pulse}$ (nJ)	$\Delta\tau$ (fs)	Rep. rate (MHz)	$P_{peak}$ (MW)	$\eta_{opt}$ (%)	$P_{pump}$ (W)	Reference
Yb:LuScO	5.1	66	96	77	0.60	11	46	[32]
Yb:CALGO	5.1	78	62	65	1.11	7	73	[33]
Yb:CALGO	2	31	49	65	0.55	5	40	[34]
Yb:YAG	3.5	18	49	200	0.31	3.5	100	[30]
Yb:LuO	10.7	175	88	61	1.75	5.8	186	Chapter 2
Yb:LuO	4.5	74	49	61	1.32	4.7	96	Chapter 2
Yb:LuO	1.6	26	35	61	0.66	2.1	76	Chapter 2
Yb:CALGO	0.15	1	30	124	0.04	0.1	150	Chapter 3

a high intra-cavity peak power [18,20,34,94,95]. Two different approaches have been used to circumvent this challenge. Firstly, an efficient reduction of the intra-cavity peak power is realized by using a high output coupling degree. To compensate for these losses, a high gain is obtained with a multiple-pass arrangement of the laser beam on the low-single-pass-gain TDL crystal. In SESAM mode locking, 11 bounces per round trip on the disk have been demonstrated and resulted in energetic ps-pulses at an output coupling degree of 72% and an optical efficiency above 25% [94]. In case of Kerr lens mode locking, the resonator must be carefully designed to account for the multiple passes on the disk and the change of the beam size between cw and mode-locked operations. To date, up to 3 passes on the disk have been reported [96] but the influence on the pulse duration of an additional soft aperture or gain narrowing is not yet clear. Secondly, operating the laser in helium or evacuated environment drastically reduces the nonlinearities originating from the air [34,18,95,20]. Nevertheless, the complexity and cost of such a system are greatly increased by the requirements linked to the laser operation under vacuum.

In this work, the key factor for ultrashort pulse generation is the combination of the broadband gain material Yb:LuO and the Kerr lens mode-locking scheme. The 35-fs KLM Yb:LuO TDL achieves 4-times shorter pulses than previously reported from this gain material in TDL configuration [30] and nearly 2-times shorter pulses than generated in the bulk geometry [79]. This is the first demonstration of a TDL oscillator delivering shorter pulses than oscillators based on bulk crystals of the same material. Notably, the 35-fs-pulse FWHM optical

spectrum is 3 times larger than the Yb:LuO gain bandwidth. The pulse duration is currently limited by the optical properties of the intra-cavity components. Further detailed discussion on the limits of the pulse durations are presented in Chapter 3, Section 3.4.

Finally, decisive laser characteristics to drive efficient nonlinear processes are typically the wavelength, the spatio-temporal pulse quality, the pulse duration and the pulse energy (i.e., the peak power). The repetition rate of the driving laser determines in most cases the average power of the generated signal influencing the acquisition time and SNR for a given detection scheme. Ultrafast TDL oscillators based on Yb-doped crystals operate at around 1  $\mu\text{m}$  and deliver trains of ideal soliton pulses at megahertz repetition rates in diffraction-limited laser beams. Therefore, strong effort is given to increase the peak power of these lasers to directly drive experiments. Recently, 500-fs pulses with 10-MW peak power have been reported from a SESAM mode-locked TDL based on Yb:LuO operating at 11-MHz repetition rate in an evacuated environment [97]. Operating the KLM TDLs described in Section 2.4 at 10-MHz repetition rate can easily be achieved by increasing the resonator length to 15 m using a simple telescope in a 4-f arrangement. Assuming similar output power level and pulse duration, the laser would deliver pulses with 10-MW peak power at sub-100-fs pulse durations and exhibit intra-cavity peak power larger than 200 MW. Given the high repetition rate, high peak power and short pulses, this KLM TDL oscillator based on Yb:LuO gain material would be an ideal compact source to efficiently drive both intra-cavity and extra-cavity experiments in the fields of high harmonic generation [23], high-field science [21], THz spectroscopy [98], mid-infrared frequency conversion [22,99] and frequency comb generation [100].

## Chapter 3 New pulse-duration limits of ultrafast thin-disk laser oscillators

During the last decade, Yb-based ultrafast laser oscillators have successfully been replacing conventional Ti:sapphire oscillators in many industrial and scientific areas, especially for applications requiring hundreds of femtosecond long pulses [73,101,102]. However, for operation in the few-cycle regime, Ti:sapphire lasers remain the leading technology. Yet, alternative laser sources delivering few-cycle laser pulses are highly attractive, e.g., ultrafast diode-pumped Yb-doped solid-state laser oscillators feature a high efficiency, compact size, low complexity and relatively low cost. Yb-based bulk oscillators already generated pulses as short as 30 fs, i.e., 10 optical-cycles [49]. However, the graphene-mode-locked laser based on Yb:CaYAlO<sub>4</sub> (Yb:CYA) gain crystal delivered only 26 mW of average power at this pulse duration. Thermal effects and large nonlinearities in the gain medium are severe challenges for significant power increase in the bulk geometry, though it can be solved by reducing the gain medium thickness, i.e., using the thin-disk geometry. In this case, the nonlinearities can be tailored independently from the gain crystal. Nevertheless, as introduced in the previous chapters, the generation of ultrashort pulses at high-power levels is challenging. Chapter 2 demonstrated cutting-edge ultrafast TDL oscillators operating at sub-50-fs pulse duration. These KLM TDL oscillators based on the broadband gain material Yb:LuO emit up to 5-W average power and reach pulse durations down to 35 fs.

This chapter continues to explore the possibilities offered by KLM TDL oscillators based on Yb-doped broadband gain media and reports on new pulse duration limits for these lasers. Record-short pulses from Yb-doped bulk and TDL oscillators are obtained by the unprecedented combination of KLM TDL oscillators with the ultra-broadband gain material Yb:CALGO. Section 3.1 describes the main thermo-mechanical characteristics and the spectroscopic properties of Yb:CALGO. In parallel with a summary of previously reported

results, the advantages and challenges linked to this gain material are highlighted. Section 3.2 presents the initial evaluation of the performance in cw regime of the specific thin-disk mirror later used for mode-locking experiments. Section 3.3 focusses on the first demonstration of a KLM TDL oscillator based on Yb:CALGO. The laser delivers 30-fs pulses which is equally short to the shortest pulses generated by ultrafast Yb-doped bulk oscillators. Section 3.4 discusses the main limitations of the current result. It appears that the dispersion compensation required for soliton mode locking in negative dispersion regime has hindered so far the formation of pulses with a wider optical bandwidth. Finally, Section 3.5 concludes and gives an outlook towards the direct generation of few cycle pulses from Yb-based laser oscillators.

### **3.1 Yb:CALGO: an ultra-broadband gain material for record-short-pulse generation**

Yb:CaGdAlO<sub>4</sub> (Yb:CALGO) offers a nearly-flat extremely-broad smooth gain due to its disordered crystalline structure (see Chapter 1, Figure 8). Its gain bandwidth exceeds 60 nm FWHM at 30% inversion level in both  $\sigma$ - and  $\pi$ -polarizations, which is eight times larger than for Yb:YAG. Such a broad gain profile directly supports the generation of sub-20-fs pulses. Table 1 (in Chapter 1) presents a comparison of the main spectroscopic and thermo-mechanical properties of Yb:CALGO, Yb:YAG and Yb:LuO gain materials. It is interesting to note that the shape and central wavelength of the gain cross section is influenced more consequently by the inversion level in the case of Yb:CALGO than for Yb:YAG and Yb:LuO. Yb:CALGO features a thermal conductivity of  $6.3 \text{ W}\cdot\text{m}^{-1}\cdot\text{K}^{-1}$  along the c-axis at 2-at.% doping concentration, which is comparably high with respect to other Yb-doped broadband gain materials [47,71]. At this doping concentration, the thermal conductivity is nearly half compared to undoped CALGO crystal. A similar behavior is observed in Yb:YAG crystals where the large mass difference amounting to 55% between Y<sup>3+</sup> and Yb<sup>3+</sup> ions strongly affects the thermal properties of the crystal. In Yb:CALGO, the Yb<sup>3+</sup> doping ions substitute either Gd<sup>3+</sup> or Ca<sup>2+</sup> ions, which feature respectively a 10% and 70% mass difference with Yb<sup>3+</sup> ions. Even though Ga<sup>3+</sup> and Ca<sup>2+</sup> occupy the same crystallographic site, substitution of Gd<sup>3+</sup> is greatly predominant since it has the same valence as Yb<sup>3+</sup> ions. This is beneficial for the thermal conductivity which stays above  $5 \text{ W}\cdot\text{m}^{-1}\cdot\text{K}^{-1}$  even at 5 at.% doping concentration [103]. Moreover, pumping at the ZPL at around 979 nm offers large absorption cross sections and a quantum defect smaller than 10%, similar to garnet and sesquioxide crystals. Moreover, Yb:CALGO is easily grown at less than 2000°C using the Czochralski growth method [61] and



Figure 20. Large-size Yb:CALGO crystals grown by the Czochralski method. a) Crystal boule and b) bulk Yb:CALGO crystal. Picture courtesy of C. Kränkel.

processing of laser crystals (cutting, polishing) is not particularly demanding [71]. Nevertheless, the production of high-quality crystals with low scattering losses remains challenging. Figure 20 shows pictures of Yb:CALGO crystals.

The attractive spectroscopic properties of this gain material have been successfully explored in the bulk geometry. In cw regime, 60% optical efficiency and a slope efficiency larger than 70% have been obtained at output powers higher than 3 W [67,104]. An overview of the ultrafast performance (shortest pulse duration and highest average power) obtained by bulk and TDL oscillators is shown in Figure 21. The first mode-locked Yb:CALGO bulk oscillator led to 47-fs pulses at 38-mW average power, which was the shortest pulses from any Yb-based bulk laser at the time in 2006 [54]. Later, the average power has been increased to 12.5 W in 94-fs pulses using SESAM mode locking [105]. KLM oscillators led to the generation of 37-fs pulses in 1.5-W average power and of pulses as short as 32 fs in 90 mW [57]. In the TDL configuration, high optical and slope efficiencies of 56% and 70%, respectively, have been obtained in cw operation at 30-W power level [106]. Mounting the crystals onto diamond heat sinks allowed for pump densities higher than 4 kW/cm<sup>2</sup> without significant astigmatism, leading to 150 W of average power converted from more than 400 W of incident pump power [107]. In transverse fundamental mode operation the performance are slightly reduced, nevertheless 50-W average power has been obtained with an optical efficiency of 25% and excellent beam quality ( $M^2=1.1$ ) [28]. SESAM mode-locked Yb:CALGO TDLs delivered up to 28-W average power in 300-fs pulses with 13% optical efficiency [28]. With the use of optimized SESAMs, the pulse duration was decreased to 62 fs at 5-W average power and 7% optical efficiency [25]. Improvement of the dispersion compensation enabled the generation of 49-fs pulses at 2-W power, realizing the shortest pulses from any TDL oscillator prior to this work [32].

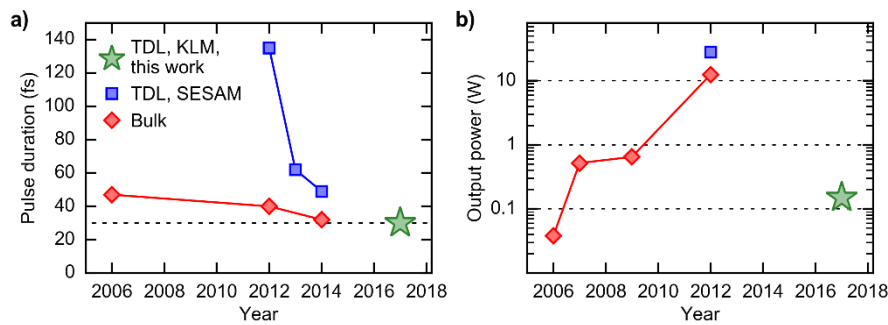


Figure 21. Evolution of the a) minimum pulse duration and b) maximum average output power from ultrafast oscillators based on Yb:CALGO gain material in bulk and thin-disk geometries. TDL, SESAM: [25,32,57]; Bulk: [28,54,72,105,108,109]; the result reported in this chapter is highlighted with a star symbol.

A previous attempt of KLM Yb:CALGO TDL has been reported, but stable mode locking could not be demonstrated [110]. This might have been due to the difficulties to start the mode locking as already observed with other inhomogeneously broadened gain materials [111]. More generally, the use of Yb:CALGO as gain material is challenging due to the strong anisotropy in the lattice, which induces different thermo-mechanical coefficients in the two principal crystal axes [103]. These atypical properties lead to undesirable effects such as astigmatism [28] and polarization switching under high pumping, i.e., under high thermal load [112]. Achieving robust fundamental-mode laser operation at high average power represents a key challenge in the development of high-power diode-pumped solid-state lasers based on Yb:CALGO. Despite these challenges, owing to the demonstration of mode-locked operation at several-ten watts of average power and the ultra-broad gain bandwidth supporting sub-20-fs pulse formation, Yb:CALGO is one of the most promising Yb-doped gain material for the generation of powerful extremely-short pulses.

### 3.2 Evaluation of the performance of the disk crystal in continuous-wave operation

The laser is based on a wedged, 150- $\mu\text{m}$ -thick Yb( $\sim 3.8$  at.%):CALGO disk with a c-cut crystal orientation (FEE GmbH). The disk has a 6-mm diameter and 2-m concave RoC. It is contacted on a diamond heat sink (Trumpf GmbH) and pumped at the zero-phonon line at 979 nm by a 400-W fiber-coupled VBG-wavelength-stabilized diode laser system. The pump light passes 36 times through the disk crystal to achieve high pump absorption. The pump spot is set to 2-mm diameter. Initial tests in cw regime were performed both in transverse multi-mode and fundamental-mode regimes in simple V-cavities (see Figure 22).



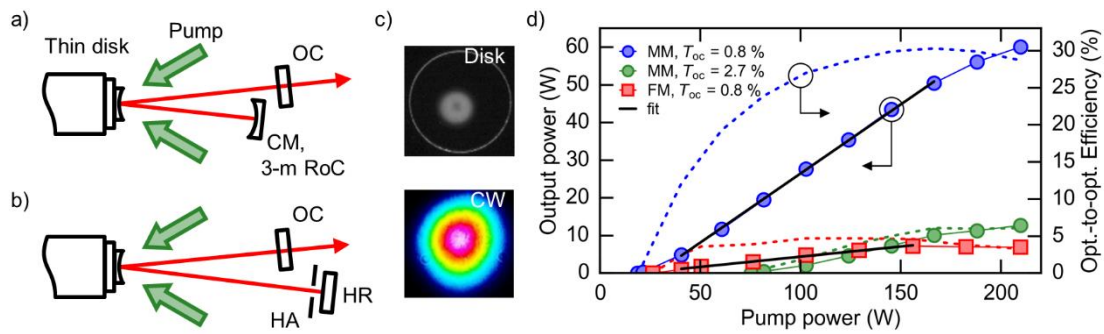


Figure 22. Laser cavity for operation in transverse (a) multi-mode (MM), (b) fundamental mode (FM). OC, output coupler; CM, curved mirror; HA, hard aperture; HR, highly reflective mirror. c) (top) picture of the disk with the pump spot and depletion from the laser operating in FM. (bottom) corresponding mode profile. d) Average output power (solid lines, left y-axis) and corresponding optical-to-optical efficiency (dashed lines, right y-axis) of the disk in MM and FM operations for different output coupler transmissions ( $T_{oc}$ ). The black solid lines show the linear fits used for the calculation of the slope efficiencies.

In highly-multi-mode operation (ratio between the pump and the fundamental laser mode sizes of 4), the laser emits up to 60-W average power with 30% optical efficiency and 37% slope efficiency at 0.8% output coupling rate. Increasing the output coupling rate to 2.7% degraded the optical efficiency to 6% and the slope efficiency to 11%. This indicates a strong limitation of the highest output coupling degree for efficient laser operation, which results from the combination of doping concentration and disk thickness. Moreover, moving the pump spot across the disk showed variations of the extracted power, indicating inhomogeneities in the crystalline structure of the disk. Increasing the overlap ratio between the fundamental laser mode and the pump to  $\sim 80\%$  did not lead to fundamental mode operation as usually expected for TDLs. Transverse fundamental mode operation ( $M^2 < 1.05$ ) was only achieved when inserting a hard aperture in the cavity to suppress the onset of higher order modes. For an overlap ratio of 60% and a 1.8-mm hard-aperture diameter, the laser delivers up to 7-W average power with 5% optical efficiency and 5% slope efficiency at 0.8% output coupling rate. The output power clamps at pump powers higher than 150 W, which probably indicates thermal effects in the disk. It is worth noting that the disk mounted onto a diamond heat sink stood pump power densities of  $6.5 \text{ kW/cm}^2$  without damage. The strong drop of performance from multi-mode to fundamental mode laser operation is attributed to low disk quality which prevents robust transverse fundamental mode operation and extraction of the power over the full pumped area. Due to these difficulties, a multiple-pass of the laser beam on the disk was not attempted. The cw performance of this particular disk

is comparably poor in terms of average output power [107,110], efficiency [106] and gain [113], however further mode-locking experiments have been conducted with this disk.

### 3.3 Kerr lens mode-locked Yb:CALGO thin-disk laser oscillator

For mode locking experiments, the cavity was extended with two 0.25-m-RoC concave mirrors (CM1 and CM2) as shown in Figure 23. A 4-mm-thick undoped YAG plate placed under Brewster angle between CM1 and CM2 serves as Kerr medium for the mode-locking mechanism. The beam radii at this position are estimated from ray-transfer-matrix calculations to be 80  $\mu\text{m}$  and 140  $\mu\text{m}$  in the tangential and sagittal planes, respectively, in cw regime. The setup also comprises a 1.6-mm-diameter pinhole placed near an end mirror. The second end mirror serves as an output coupler with 0.3% transmission. Two dispersive mirrors introduce  $-900\text{-fs}^2$  GDD per round trip. Mode locking is initiated by shifting the position of the mirror CM2, then the pump power is adjusted to produce the shortest pulses in clean fundamental mode-locking operation. Increasing the pump power further introduces mode-locking instabilities, and typically a cw breakthrough is observed in the optical spectrum. The footprint of the overall oscillator operating in air is 90 cm  $\times$  30 cm.

The laser generates 30-fs pulses as shown by the autocorrelation trace in Figure 24a). Extra-cavity GDD amounting to  $-440\text{ fs}^2$  (obtained by two dispersive mirrors and a 3-mm thick fused silica plate) was inserted before the autocorrelator to compensate for the material dispersion of the output coupler mirror substrate and for the propagation in air. Single-pulse operation was ensured by a 180-ps long scan autocorrelation and observation of the trace of a fast 18.5-ps photodiode on a 40-GHz sampling oscilloscope (Figure 24b). The small fluctuations appearing at 0.5 ns are an artefact from the detection electronics. The optical spectrum of the

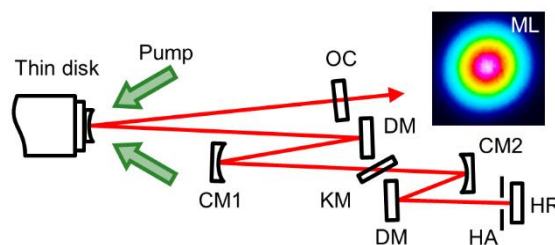


Figure 23. Schematic of the KLM Yb:CALGO TDL cavity. (inset) Output-beam profile of the mode-locked (ML) laser. OC, output coupler; DM, dispersive mirror; CM1-2, curved mirror, 0.25-m RoC; KM, Kerr medium; HA, hard aperture; HR, highly reflective mirror.

laser output is centered around 1048 nm and features a 45-nm FWHM bandwidth. It is shown in Figure 24c) together with the Yb:CALGO gain cross section calculated for an inversion level of 11%. This value is chosen to match the inversion-dependent gain peak with the laser central wavelength, owing to the minor wavelength-dependence of the intra-cavity mirror reflectivity in this wavelength range. At this inversion level, the gain profile presents a 45-nm FWHM bandwidth and sharp edges. The additional peaks in the laser optical spectrum around 950 nm and 1150 nm carry only a minor fraction of the power (less than 5%) and are associated with dispersive waves as already observed in various oscillators, e.g., [54,57,92]. They appear comparably higher in the output spectrum than inside the laser cavity because of the larger output coupler transmission at the edges of the spectrum, e.g.,  $T(\lambda=953 \text{ nm}) = 2.4\%$  compared to  $T(\lambda=1046 \text{ nm}) = 0.3\%$ , which is 8 times smaller. Additionally, this non-uniform transmission might have a detrimental effect limiting the laser optical spectrum, and consequently, output coupler optimized for a flat transmission over a larger spectral might be beneficial for the generation of shorter pulses.

The laser delivers the 30-fs pulses with an excellent beam quality factor ( $M^2 < 1.05$ ) at an average power of 150 mW with an optical efficiency of 0.1%. Stable soliton mode-locking is illustrated by the clean radio-frequency spectra presented in Figure 25a,b). The fundamental repetition rate signal is centered at 123.9 MHz and features no side peak, measured with an 80-dB SNR at 100-Hz resolution bandwidth. Additionally, the harmonic spectrum measured up to 2.9 GHz shows no amplitude modulation. While the laser operates reliably over hours, the short-term stability is confirmed by the amplitude and phase noise measurements (see

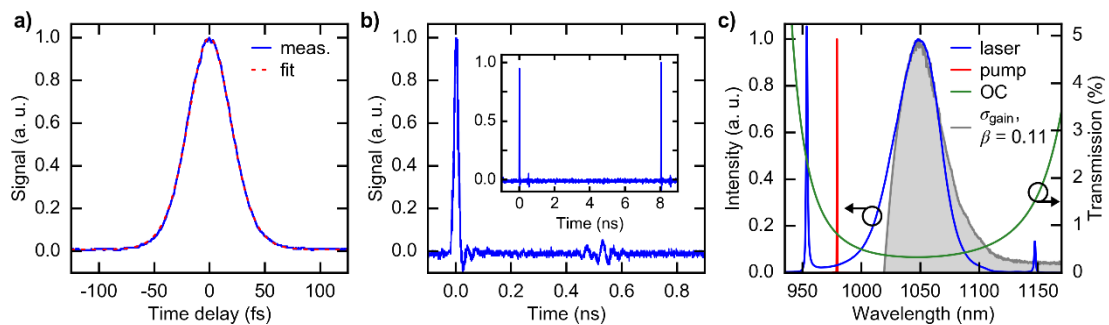


Figure 24. Characterization of the Kerr lens mode-locked Yb:CALGO thin-disk laser oscillator. a) Measured autocorrelation trace of the 30-fs pulses and corresponding sech<sup>2</sup> fit. b) 1-ns and (inset) 9-ns sampling oscilloscope traces. c) Left y-axis: Optical spectra of (blue) laser and (red) pump; right y-axis: Output coupler (OC) transmission (green). The gain calculated for an inversion level  $\beta$  of 0.11 is shown in grey for reference (data from [67]).

Figure 25). The rms RIN amounts to less than 0.2% (integrated from 1 Hz to 1 MHz) which is lower compared to previous ultrafast TDLs [23,34]. The rms timing jitter is  $< 2$  ps (from 100 Hz to 1 MHz, corresponding to an integrated phase noise of 1.5 mrad) and  $< 150$  fs (from 1 kHz to 1 MHz, integrated phase noise of 117  $\mu$ rad). The phase noise in the lower Fourier frequency range is comparably high for a TDL, which though operates at an order of magnitude higher repetition rate. Moreover, it is not actively stabilized, directly mounted onto a laser table, and not built in mechanically stable laser housing. It is expected that the rather high phase noise at Fourier frequencies  $< 1$  kHz can be strongly reduced by active stabilization of the repetition rate.

As for the broadband 35-fs KLM Yb:LuO TDL presented in Chapter 2, the laser optical spectrum contains energy beyond the gain limits (see Figure 24c). These wavelengths are not amplified by the gain medium but generated via SPM inside the laser cavity [63]. In the steady state, the SPM counteracts the reabsorption in the gain medium and other losses (e.g. on the

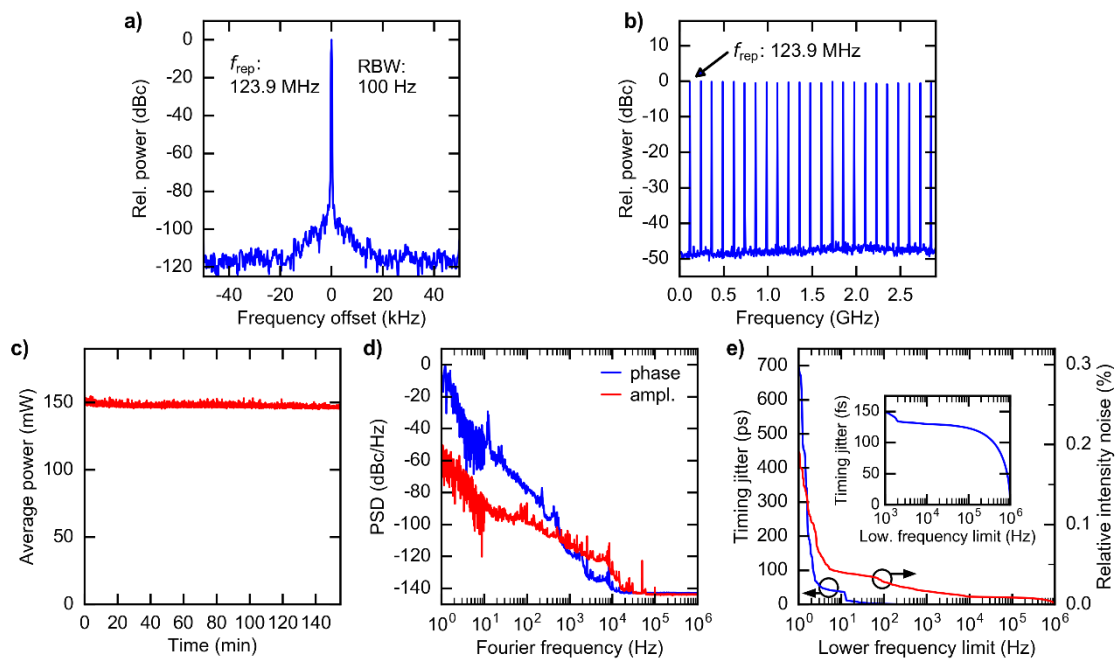


Figure 25. Long-term and short-term stabilities of the Kerr lens mode-locked Yb:CALGO thin-disk laser oscillator. a) Radio-frequency (RF) spectrum of the laser fundamental repetition-rate frequency ( $f_{\text{rep}}$ ) measured with a 100-Hz resolution bandwidth (RBW) and 90-kHz span. b) RF spectrum with a 100-kHz RBW and 2.9-GHz span. c) Average output power measured over more than two hours. d) Phase and amplitude noise power spectral densities (PSD) measured at the fundamental repetition frequency. e) Left y-axis: Rms timing jitter integrated from 1 Hz and (inset) from 1 kHz up to 1 MHz; right y-axis: rms relative intensity noise.

mirrors) for the wavelengths which are not supported by the gain. These additional losses contribute to lower the laser efficiency given the limited available gain. The cw experiments reported in Section 3.2 already demonstrated a strong drop of the laser efficiency at intra-cavity losses of a few percent and showed similar optical efficiency at comparable output power. Therefore, the output power in this result seems to be mainly limited by the available laser gain. Higher gain should lead to substantially higher optical efficiencies and higher output power levels at comparable pulse durations.

Moreover, the laser optical spectrum extends even below the pump wavelength (see Figure 24c). This atypical behavior is enabled by the TDL pumping geometry as depicted in Figure 26. In standard end-pumping geometries for oscillators based on bulk crystals, a resonator mirror has a high transmission at the pump wavelength to inject the pump into the cavity as well as a high reflectivity for the laser wavelength spectrum, which in general is at slightly longer wavelengths. Dichroic mirrors with such properties at closely lying wavelengths are challenging to manufacture, but, most of all, they set a lower limit for the laser optical spectrum, owing to the high transmission at the pump wavelength. Although bulk oscillators already delivered similar pulses durations [49,57], they operated at a slightly longer central wavelength (above 1060 nm) for which the large laser optical spectrum could be supported by the dichroic pump mirror. The generation of significantly shorter pulses appears out of reach in standard end-pumping bulk laser configurations. In contrast, in TDL oscillators, the pump is not delivered collinearly to the laser beam but with a slight angle. In this case, the disk is used in reflection for both pump and laser beams and therefore, it is coated for broadband high reflectance. As a result, the pumping scheme is not limiting the optical spectrum of the intra-cavity pulse and, therefore, allows the generation of even shorter pulses.

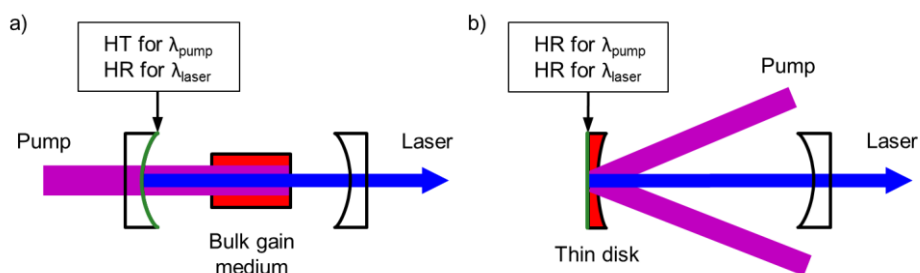


Figure 26. Comparison of a) the standard end-pumping configuration for bulk oscillator with b) the thin-disk laser pumping scheme. For bulk oscillators, a resonator mirror is highly transmissive (HT) at the pump wavelength to inject the pump collinearly to the laser beam. On the contrary, the pump beam is delivered to the thin-disk laser crystal at an angle with respect to the laser beam. Therefore, the disk is coated to be highly reflective (HR) for both laser and pump wavelengths.

### 3.4 Dispersion compensation for ultra-broadband laser pulses

The laser presented in the previous section generates slightly chirped pulses. The time-bandwidth product of 0.368 (ideal  $\text{sech}^2$ : 0.315) indicates that the pulses are 17% longer than their Fourier transform limit of 26 fs. Unfortunately, at the time of the experiment, no diagnostic tool was available to measure the phase of the pulses, which would have been a useful information to confirm the origin of the chirp. Yet, external dispersion compensation has been inserted to correct for the second order dispersion (GDD) for the pulse duration measurement with the intensity autocorrelator. Therefore, the remaining chirp originates most probably from higher-order dispersion. Similar time-bandwidth product has been measured for the 62-fs pulses from a SESAM mode-locked Yb:CALGO TDL [25]. The observed chirp was attributed to uncompensated higher-order dispersion in the laser cavity originating from the spectrally-irregular dispersion profile introduced by the dispersive mirrors. Optimization of the mirrors for a flat dispersion profile led to the generation of 49-fs pulses with a close-to-ideal time-bandwidth product of 0.324 ( $1.03\times$  the ideal  $\text{sech}^2$  value of 0.315) [32].

To illustrate the influence of the dispersion compensation, four laser configurations have been investigated. Table 6 summarizes their parameters while Figure 27 shows the optical spectra of the laser outputs together with dispersion profile introduced by the intra-cavity dispersive mirrors. In the case of the KLM Yb:LuO TDL, the two configurations that delivered the shortest pulses for each mode size on the Kerr medium (see Chapter 2, Sections 2.3 and 2.4) are compared. For the KLM Yb:CALGO TDL, the configuration with the shortest pulses is compared to an intermediate configuration with similar settings, where the main difference is the profile of the introduced dispersion.

Table 6. Laser parameters for the selected laser configurations that are used to illustrate the impact of the dispersion compensation on the pulse duration.  $\Delta\tau$ , pulse duration;  $P_{\text{out}}$ , output power;  $\Delta\lambda$ , FWHM optical bandwidth; TBP, time-bandwidth product (ideal  $\text{sech}^2$ : 0.315); GDD, inserted group delay dispersion per round trip; OC, output coupling rate;  $\eta_{\text{opt}}$ , optical-to-optical efficiency.

Configura- tion	Material	$\Delta\tau$ (fs)	$P_{\text{out}}$ (W)	$\Delta\lambda$ (nm)	TBP	GDD (fs <sup>2</sup> )	OC (%)	$\eta_{\text{opt}}$ (%)
(a)	Yb:LuO	64	0.7	18	0.324	-2200	0.3	0.6
(b)	Yb:LuO	35	1.6	34	0.336	-1000	0.8	2.1
(c)	Yb:CALGO	62	0.24	20	0.342	-1300	0.3	0.3
(d)	Yb:CALGO	30	0.15	45	0.368	-1000	0.3	0.1

Two key effects can be appreciated from the curves presented in Figure 27. First, for a large variation of the dispersion profile within the main part of the pulse spectrum, the pulses are chirped, most probably due the introduced higher-order dispersion. This effect has a stronger impact for lower absolute values of the inserted GDD. Second, the rising edges of the dispersion limits the spectral bandwidth of the mirror and prevents the pulse spectrum to extend further. This effect limited the pulse duration to 64 fs in the configuration (a) for example.

As a result, the pulse durations of the two KLM TDL oscillators based on Yb:LuO and Yb:CALGO, respectively, are mainly limited by the dispersion properties of the intra-cavity components which operate at the edge of their bandwidth and introduce higher-order dispersion. Both lasers demonstrate 10-optical-cycle pulses and further shortening demands for a flat dispersion spanning a wavelength range considerably larger than 100 nm. In TDL oscillators, dispersion compensation for soliton mode locking is generally obtained by intracavity dispersive mirrors because of the reduced thermal aberration compared to prisms. Unfortunately, standard dispersive mirrors operating at around 1  $\mu\text{m}$  exhibit a limited optical

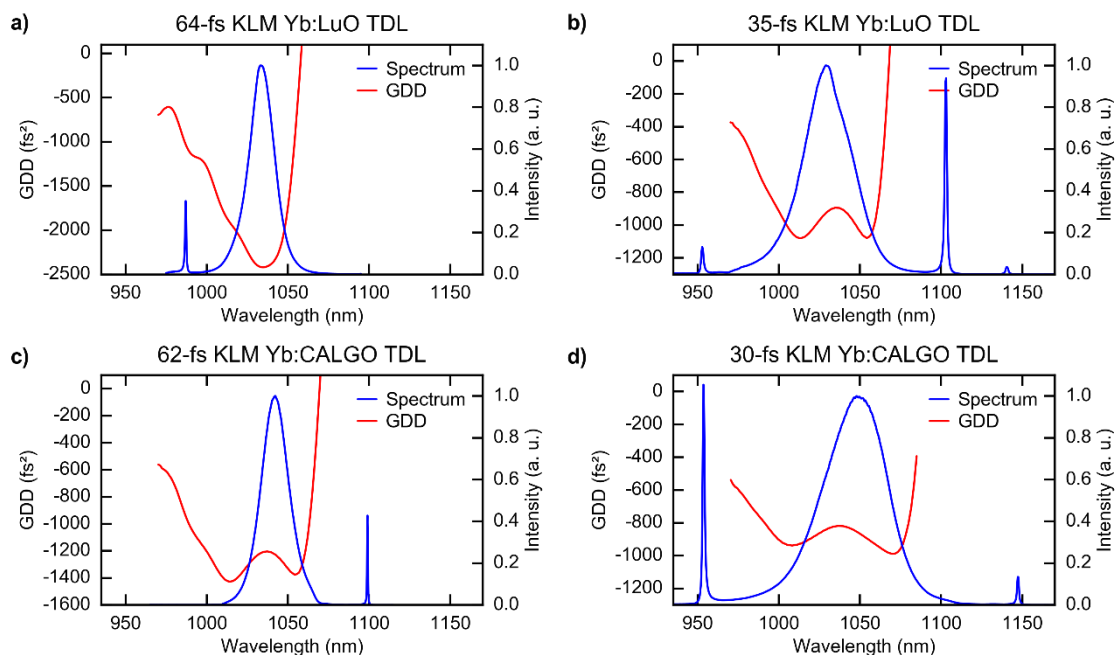


Figure 27. Comparison of four different laser configurations which parameters are given in Table 6. The dispersion profile is plotted as a function of the wavelength (red, left y-axis). The optical spectrum of the laser output is shown in blue (right y-axis). They illustrate the impact of the intra-cavity dispersion profile on the pulse duration. GDD: group delay dispersion.

bandwidth of typically few tens of nm. Optimized non-standard solutions can be designed and manufactured in-house using an ion-beam-sputtering coating machine (Navigator 1100, CEC GmbH). However, processing accurately such complex coatings with very thin layers is challenging due to the sensitivity on growth errors, which is at the limits of the coating-machine accuracy. Figure 28 presents the design and characterization of a broadband dielectric dispersive mirrors recently produced. It also includes an analysis of the influence of growth errors on the reflectivity and dispersion of the mirror. For this, the characteristics of the mirror are computed a hundred times with different growth errors chosen randomly within the growth accuracy of the coating machine (standard deviation of 0.2 nm plus 0.5% of relative error per layer). These mirrors are designed to exhibit a flat GDD and high reflectivity over a broad spectrum ranging from 990 nm up to 1150 nm. As shown in Figure 28d), such a mirror should allow for the generation of unchirped and shorter pulses than in the presented result.

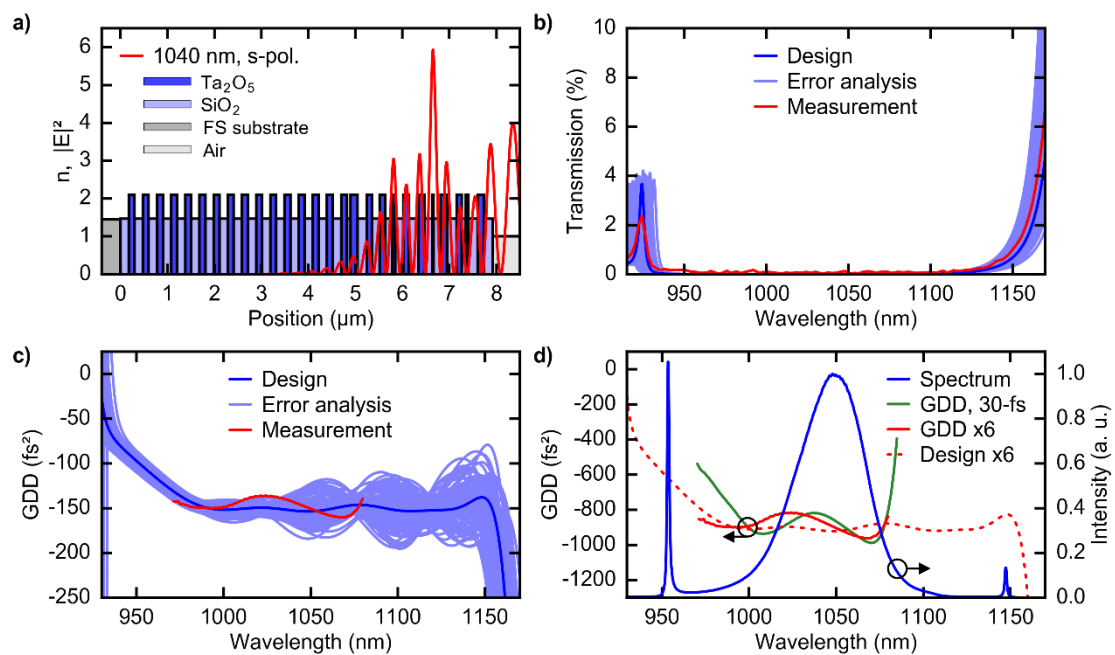


Figure 28. a) Design of new broadband dispersive mirrors, which are grown in-house using an ion-beam-sputtering coating machine. b) Corresponding designed parameters (dark blue), growth error analysis (light blue) and measurements (red) of mirror transmission. c) Group delay dispersion. d) Comparison of the design (dotted red line) and measured (solid red line) dispersion inserted by six bounces on these new dispersive mirrors with the inserted dispersion in the current 30-fs result (green) (left y-axis). The optical spectrum of the 30-fs laser is shown in blue for reference (right y-axis).



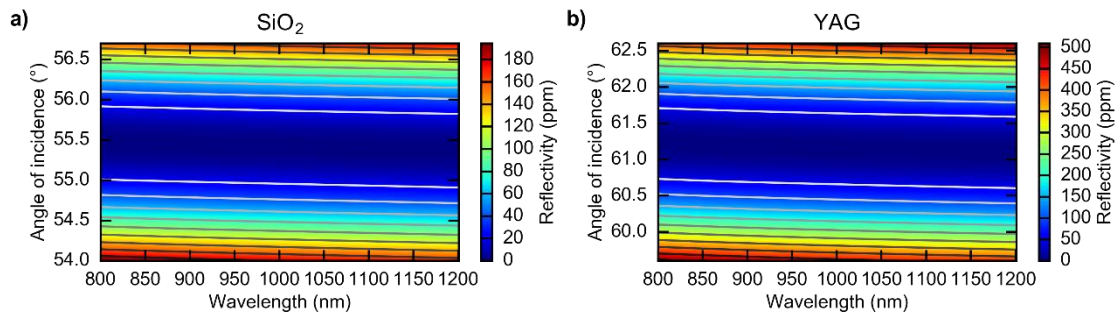


Figure 29. Reflectivity of p-polarized light from (a) fused silica and (b) undoped YAG around their respective Brewster angle. The material properties offer intrinsically a high transmission around the Brewster angle with an extremely broad spectral bandwidth.

Until now, the dispersion introduced by the dispersive mirrors has been exclusively investigated, however all intra-cavity optical components should be considered. The highly-reflective coatings in these lasers are typically specified for a reflectivity larger than 99.98% and zero dispersion from 1000 nm to 1100 nm. In most cases, the reflectivity and dispersion are not controlled outside this range and may give rise to the side peaks observed in the laser optical spectra. Apart from all reflective elements, the Kerr medium used in transmission in KLM TDLs is typically placed under Brewster angle near an intra-cavity focus. The material properties intrinsically induce an extremely broadband high transmission, as shown in Figure 29. Consequently, the losses arising from the parasitic reflections at the Kerr medium surfaces are negligible even for ultrashort pulses.

### 3.5 Towards few-cycles pulses directly generated by Yb-based laser oscillators

In conclusion, this chapter presents the first KLM TDL oscillator based on the Yb:CALGO gain medium. The broadband nature of this gain material combined with the Kerr lens mode-locking scheme enabled the generation of the shortest pulses from any TDL oscillator, being equal to the shortest pulses obtained from Yb-doped bulk oscillators [49].

This work presents the benefits of the thin-disk pumping scheme for the generation of powerful ultrashort pulses. It essentially allows the laser optical spectrum to extend beyond the pump wavelength. The achieved output power of 150 mW and optical efficiency below 1% are unusually small compared to most reported TDLs, yet, the output power is comparably high at this short pulse durations as shown in Figure 30. The laser performance is limited by three main factors. First, the low disk quality makes laser operation in fundamental transverse

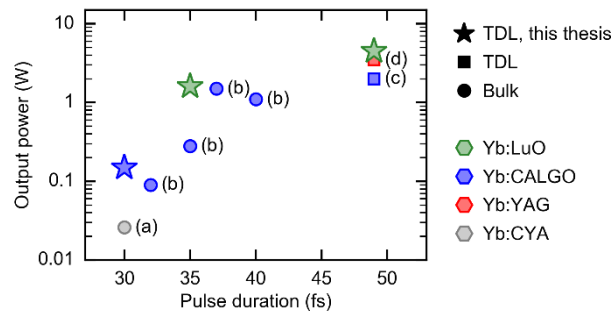


Figure 30. Overview of state-of-the-art ultrafast Yb-doped oscillators based on the bulk and thin-disk laser geometry delivering sub-50-fs pulses. The crystal geometry is indicated with the symbol code and the gain material with the color code. (a) [49]; (b) [57]; (c) [32]; (d) [33]; the results reported in this thesis are highlighted with star symbols.

mode at high average power very challenging. Second, the combination of doping concentration and disk thickness offers a limited single-pass gain and prevents efficient lasing operation at output coupling degrees larger than a few percent for a single bounce on the disk. Third, the losses linked to the ultrashort pulse duration that are due to reabsorption in the gain medium and limited mirror bandwidth contribute to lower the optical efficiency of the laser. It is important to note that even the standard HR coatings for the disk and mirrors are operating at the limit of their bandwidth since the coatings are typically specified for a reflectivity larger than 99.98% from 1000 nm to 1100 nm. Therefore, high-optical-quality high-gain Yb:CALGO disks and ultra-broadband optics should allow the generation of several-ten watts of average power with reasonable optical efficiencies and similar pulse durations.

While KLM TDL oscillators already delivered optical spectra three times larger than their respective gain bandwidth, the presented KLM Yb:CALGO TDL oscillator exploits about 70% of the gain bandwidth. Therefore, further decrease of the pulse duration should be feasible. Next steps require the optimization of the optical properties of all intracavity components towards ultra-broadband high reflectivity and ultra-broadband flat dispersion. Appropriate dispersion engineering should allow the generation of optical bandwidths well beyond the gain limits and thus ultimately outperform the current sub-10-cycle pulses towards the direct generation of few-cycle pulses from Yb-based diode-pumped solid-state lasers.

# Chapter 4    Optical frequency combs based on ultrafast thin-disk laser oscillators

The optical frequency comb technology offers a phase-stable coherent link between optical and microwave frequencies [114–116]. It enabled tremendous progress in various areas [117], e.g., broadband high-resolution spectroscopy [118,119], precision optical-frequency metrology [120], and optical clocks [121,122]. In 2005, the Nobel Prize in Physics was awarded to John L. Hall and Theodor W. Hänsch for their contributions to the development of laser-based precision spectroscopy, which includes the optical frequency comb technique [123,124]. Besides, optical frequency combs with a high average power are attractive for spectroscopy experiments since they offer a high power per comb line and enable performing measurements with high signal-to-noise ratio (SNR).

Any mode-locked laser exhibits a frequency spectrum with a comb structure which has two degrees of freedom: the repetition rate that corresponds to the spacing between the comb modes, and the carrier-envelope-offset (CEO) frequency that is a global frequency shift of the comb modes from exact harmonics of the repetition rate. If both degrees of freedom are stabilized so that all optical lines have an accurately-known frequency, the laser is referred to as an optical frequency comb. This chapter presents the first full stabilization of a high-power ultrafast thin-disk laser oscillator. The frequency-comb generation is based on a KLM Yb:LuO TDL oscillator developed during the framework of this thesis and presented in Chapter 2. Section 4.1 introduces the frequency comb technology and previous work based on TDL oscillators. It also highlights the potential of high-power optical frequency combs for XUV frequency comb generation. Section 4.2 details the detection and stabilization of the CEO frequency. Section 4.3 reports on the stabilization of the repetition rate of the TDL oscillator, leading to the full stabilization of the laser. Section 4.4 concludes and gives an outlook towards future applications.

## 4.1 High-average-power optical frequency combs for XUV-spectroscopy

Mode-locked lasers deliver trains of pulses, which are temporally separated by the cavity round-trip time. Equally said, the lines of the optical spectrum are separated by the repetition rate frequency ( $f_{\text{rep}}$ ). The overall offset of the comb spectrum is given by the CEO frequency ( $f_{\text{CEO}}$ ), which originates from the difference between the phase and group velocities inside the laser cavity, i.e., from the cavity dispersion. If these two frequencies are phase-locked to stable microwave references, then the optical frequency of each comb tooth is accurately known and stable. Figure 31 depicts an optical frequency comb both in the time and frequency domains. The detection of the laser repetition rate is usually straightforward and achieved with a standard photodetector with a sufficient bandwidth. However, measuring the CEO frequency is more challenging. The standard scheme for CEO detection is based on self-referencing using the  $f$ -to- $2f$  interferometry technique [114–116]. It requires a coherent octave-spanning spectrum which is usually generated by spectral broadening in a highly-nonlinear fiber such as a photonic crystal fiber. Yet, the coherence properties of the supercontinuum critically depend on the input pulse parameters (duration typically shorter than 150 fs and high peak power) and the dispersion properties of the nonlinear fiber [126]. The CEO frequency emerges from the beating of the frequency-doubled lower-frequency end of the comb spectrum with the higher-frequency end and can be detected using a photodetector.

On the other hand, a prominent field of research which benefits from the development of high-power Yb-based ultrafast TDL oscillators is the generation of high-order harmonics for attosecond science [127,128] and extreme-ultraviolet (XUV) spectroscopy [129–131]. A crucial aspect for these applications is the accurate control of the comb properties of the XUV train of pulses. Since high-harmonic generation is a coherent process, XUV pulses inherit the comb characteristics of the driving source. Complex high-power CEO-stable laser systems based on amplifier architectures have been intensively developed to seed enhancement cavities for intra-cavity high-harmonic generation at MHz repetition rates [132–134]. However, the necessary input matching of the femtosecond pulses into the cavity is experimentally complex to implement [135]. In contrast TDL oscillators are well suited for the generation of XUV pulses in single-pass configurations [23] or directly inside the cavity of the mode-locked thin-disk oscillator as presented in Chapter 5. Yet, their potential for frequency comb generation has not been entirely exploited. Part of the challenge is the detection of the

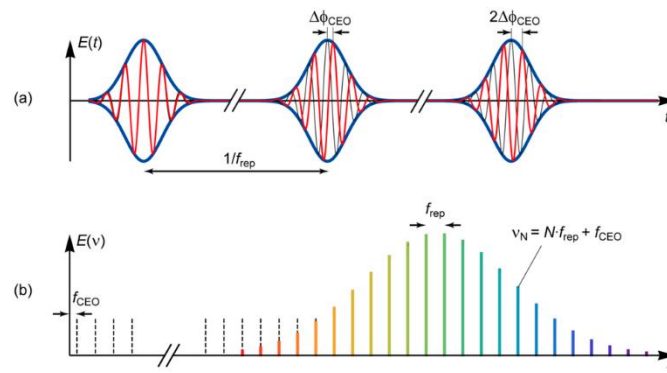


Figure 31. Pulse train emitted from a mode-locked laser a) in the time domain and b) in the frequency domain. The carrier-envelope-offset frequency  $f_{\text{CEO}}$  is at the extrapolated origin of the spectrum and results from the pulse-to-pulse carrier-envelope phase shift  $\Delta\phi_{\text{CEO}}$ . Figure taken from [125].

CEO frequency in an  $f$ -to- $2f$  interferometer, which requires an octave-spanning coherent pulse spectrum generated from pulses with a duration typically shorter than 150 fs.

The first CEO detection of a TDL oscillator has been realized in 2012 with a SESAM mode-locked Yb:LuO TDL delivering 142 fs [30] and shortly after, CEO-stabilization has been achieved concurrently in both KLM and SESAM mode-locked TDLs [136,137]. The stabilization of a 2-W 90-fs-pulse SESAM mode-locked TDL by active feedback to the pump current resulted in an in-loop phase noise of 120 mrad (integrated from 1 Hz to 1 MHz). The CEO frequency of 100-W-class SESAM mode-locked TDL oscillators has been detected after pulse compression from 750 fs down to 60 fs duration, nevertheless the cavity dynamics have prevented its stabilization [138]. Prior to this work, CEO detection of KLM TDLs exclusively relied on an initial pulse compression stage before supercontinuum generation. Subsequent stabilization has been realized either with gain modulation via the pump power of the main diode [136] or of an auxiliary low-power pump diode at a slightly different wavelength [139], or using an intra-cavity acousto-optic modulator [100]. Intra-cavity loss modulator (e.g., acousto-optic) allow for a higher bandwidth of the stabilization loop compared to pump-current modulation which bandwidth is limited by the cavity dynamics of the mode-locked laser, which is largely determined by the long upper-state lifetime of Yb-ions. Although intra-cavity acousto-optic modulators might lead to detrimental thermal effect or nonlinear phase shift hindering the scaling of the average power, the CEO frequency of a KLM oscillator delivering 27 W in 250-fs pulses has been stabilized and featured a phase noise of 180 mrad in-loop and 270 mrad out-of-loop (integrated from 1 Hz to 0.5 MHz). In brief, CEO-detection and stabilization of TDL

oscillators have already been explored, however, no fully-stabilized TDL-based frequency comb has been reported to date.

## 4.2 Carrier-envelope-offset frequency detection and stabilization

### 4.2.1 Supercontinuum generation and detection of the CEO frequency

The experiments are based on a sub-50-fs KLM Yb:LuO TDL presented in Chapter 2, Section 2.4, which delivers among the shortest pulses reported from TDLs. The ultrafast oscillator generates 4.5-W average power in 49-fs pulses at 61-MHz repetition rate, which leads to a pulse energy of 70 nJ and a peak power of 1.3 MW. The laser optical spectrum is centered around 1031 nm and features a 24-nm FWHM bandwidth. This proves nearly transform-limited pulses with a time-bandwidth product of 0.333 (ideal  $\text{sech}^2$ : 0.315).

The short pulse duration enables direct supercontinuum generation in a highly nonlinear fiber for CEO-frequency detection. An external mirror with 2% transmission is placed after the oscillator to extract a small part of the laser power for CEO detection. This power is further reduced with a variable attenuator before being launched into a commercial 2-m-long photonic-crystal fiber (NKT Photonics, SC-3.7-975). The highly nonlinear fiber features a 3.7- $\mu\text{m}$  core diameter leading to a nonlinear parameter  $\gamma = 18 \text{ W}^{-1}\text{km}^{-1}$  (at 1060 nm) and a zero-dispersion wavelength of 975 nm. It is seeded with  $\sim 90 \text{ mW}$  of incident average power and a coupling efficiency higher than 50%. Further optimization of the mode matching should result in a higher coupling efficiency. An octave-spanning supercontinuum spectrum is detected at the output of the fiber as shown in Figure 33a). It is launched into a quasi-

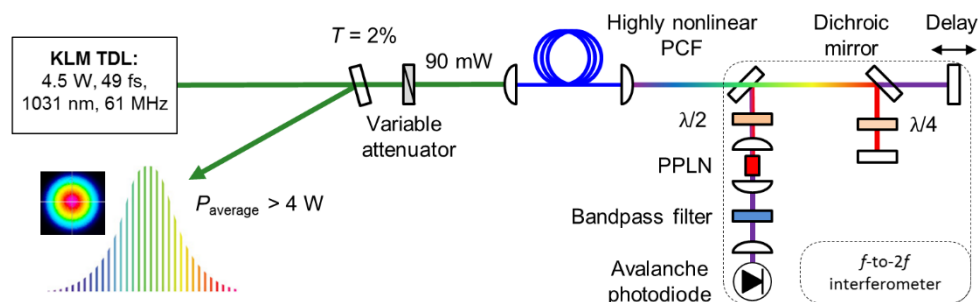


Figure 32. Experimental setup for the detection of the CEO frequency. Only a minor part of the output power is necessary to generate a coherent octave-spanning spectrum in a PCF. The CEO frequency is detected in a quasi-common-path  $f$ -to- $2f$  interferometer.  $T$ , power transmission; PCF, photonic crystal fiber;  $\lambda/4$ , quarter waveplate;  $\lambda/2$ , half waveplate; PPLN, periodically-poled lithium niobate crystal.

common-path  $f$ -to- $2f$  interferometer similar to the one used in Ref. [140]. A long-pass dichroic mirror separates the Raman soliton at around 1360 nm and the dispersive waves at 680 nm and a delay stage controls the relative timing of the two signals in the two distinct optical paths. After their recombination by the same dichroic mirror, both beams are collinearly propagated through an MgO-doped periodically-poled lithium niobate (PPLN) crystal, inside which the long wavelengths are frequency-doubled. By controlling the temporal overlap between the long and short wavelengths, a radio-frequency beat signal can be detected using an avalanche photodiode. The coherence properties of the octave-spanning spectrum are confirmed by the  $>30$  dB SNR of the CEO beat detected at  $\sim 5$  MHz (at 10-kHz resolution bandwidth). The CEO frequency jitter is typically in the order of 200 kHz over a sub-second timescale (see Figure 33c).

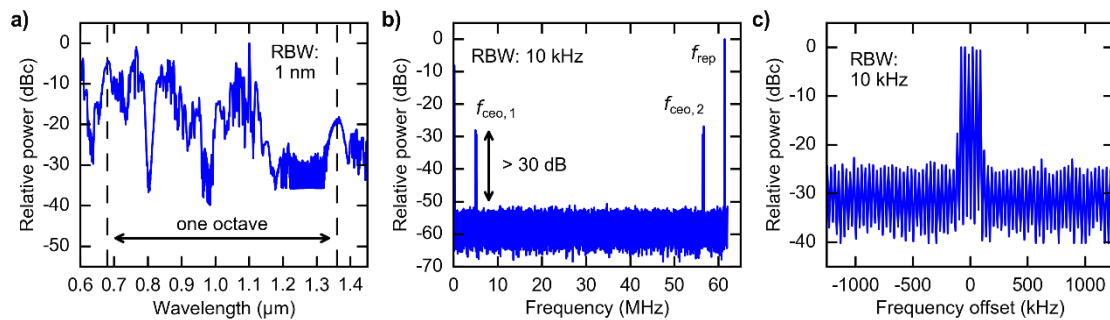


Figure 33. a) Supercontinuum spectrum at the output of the highly nonlinear photonic crystal fiber. b) CEO frequency ( $f_{\text{CEO}}$ ) beat signals are detected with  $>30$ -dB SNR at 10-kHz resolution bandwidth (RBW). c) Free-running CEO frequency at 10-kHz RBW.  $f_{\text{rep}}$ , laser repetition rate frequency.

## 4.2.2 CEO frequency stabilization

The oscillator is pumped at  $\sim 100$ -W average power by a fiber-coupled diode laser system that typically operate at high current (16 A) and voltage (17 V). Because a fast modulation cannot be applied directly to the high current source of the diodes, a high-bandwidth voltage-to-current converter developed in-house is used and enables a fast modulation of the pump power. It is connected in parallel to the high DC driver. A low-pass electrical RC filter inserted between the DC driver and the diode was used to prevent any cross-talk between the two current sources. Additionally, it reduces the current noise induced by the DC source. The transfer functions of the voltage-to-current converter, of the pump power and of the mode-locked laser output power are shown in Figure 34 for a modulation signal applied at the input

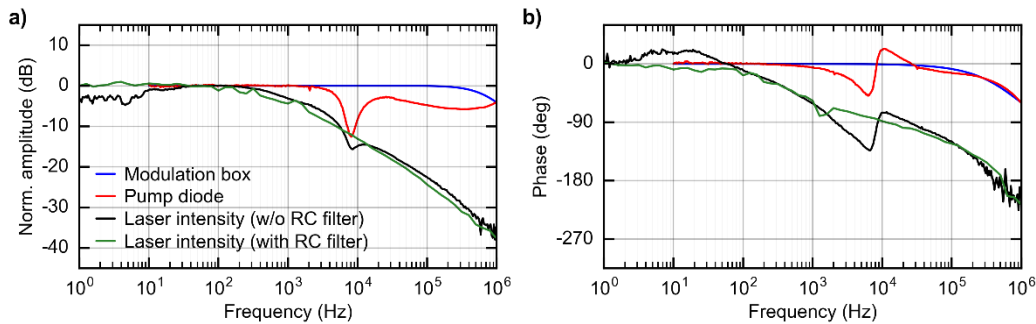


Figure 34. Transfer functions, i.e., (a) relative amplitude and (b) phase, of the current modulation source (blue), pump diode without electrical (RC) filter (red) and laser intensity without (black) and with (green) an RC filter placed between the high DC current driver and the pump diode.

of the modulator. A modulation bandwidth of 2 kHz (cutoff frequency at -10 dB or -90° phase shift) is measured for the laser intensity modulated by the pump power. This value is limited by the laser cavity dynamics and neither by the modulation bandwidth of the electronics nor by the pump diode.

The frequency noise power spectral density (FN-PSD) of the free-running CEO beat is measured using a phase noise analyzer (Rohde–Schwarz FSWP26) and is shown in Figure 35. The linewidth of the free-running CEO frequency calculated using the approximation of the  $\beta$ -separation line [141] is 90 kHz (at 1-s observation time) which is in good agreement with the CEO frequency fluctuations observed in Figure 33b). The required feedback bandwidth for a tight-phase lock of the CEO frequency is estimated to 3 kHz from the crossing point of the CEO FN-PSD with the  $\beta$ -separation line. Stabilization of the CEO beat frequency is achieved with a standard phase-locked loop with feedback applied to the pump current of the ultrafast oscillator. The full setup of the stabilization is depicted in Figure 36. The CEO beat signal from the photodetector is band-pass filtered, amplified and then compared in a digital phase detector to a reference signal from a waveform generator referenced to an H-maser. The error signal is sent to a proportional-double-integrator-derivative (PI<sup>2</sup>D) servo-controller (Vescent Photonics D2-125) and used as a feedback signal to the voltage-to-current converter to modulate the pump power. The FN-PSD of the stabilized CEO beat shows a significant noise reduction compared to the free-running CEO beat signal even at Fourier frequencies higher than few kHz, up to the servo bump at 20 kHz. The frequency noise is reduced below the  $\beta$ -separation line at all frequencies and notably, a 140-dB reduction is achieved at 1-Hz offset frequency. Consequently, and despite the highly-multimode operation of the pump diode ( $M^2 > 200$ ), a tight phase-lock of the CEO beat is achieved, and a coherent peak is observed in the



radio-frequency spectrum with a width limited by the resolution of the RF spectrum analyzer even at the highest resolution of 1 Hz (see Figure 37). The residual in-loop phase noise of the CEO beat note amounts to less than 200 mrad integrated from 1 Hz to 1 MHz. No out-of-loop measurement was realized because no other  $f$ -to- $2f$  interferometer was available at the time of the experiment.

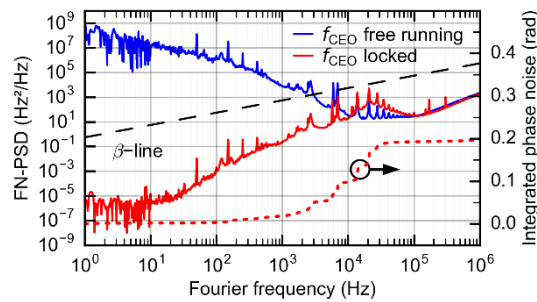


Figure 35. Left axis: Frequency noise power spectral density (FN-PSD) of the CEO beat in free-running mode (blue) and phase-locked to 5-MHz (red). The  $\beta$ -separation line is relevant for the determination of the linewidth [141] and gives an estimation of the necessary feedback bandwidth of the stabilization loop. Right axis: Integrated phase noise of the stabilized CEO signal as a function of the upper cut-off frequency (dashed red line).

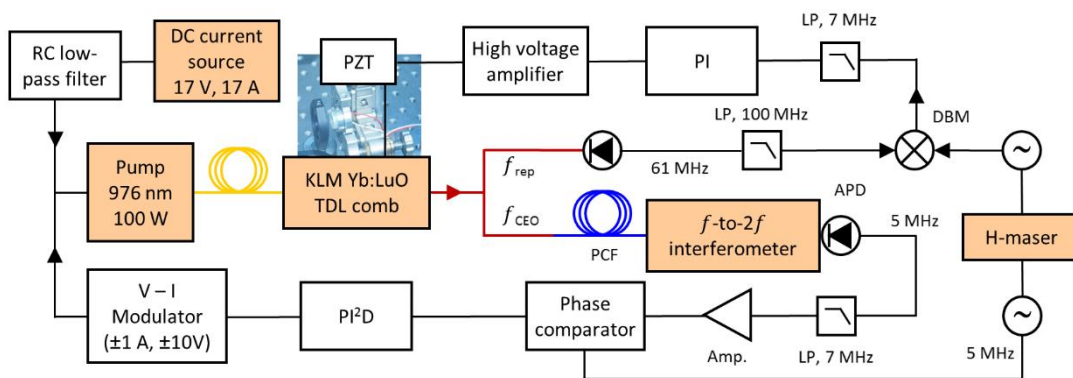


Figure 36. Experimental setup for the stabilization of the CEO frequency ( $f_{\text{CEO}}$ ) and repetition rate frequency ( $f_{\text{rep}}$ ) of the KLM TDL frequency comb. A high DC current source, a 976-nm pump diode system, an RC filter and a V-I modulator are used to pump the TDL oscillator and to stabilize  $f_{\text{CEO}}$  via gain modulation. The generation of the error signal for  $f_{\text{CEO}}$  stabilization is shown in the lower part of the scheme.  $f_{\text{rep}}$  is stabilized by cavity-length control with a piezoelectric transducer (PZT) (upper part). PCF, photonic crystal fiber; PI<sup>2</sup>D, proportional-double-integrator-derivative servo-controller; PI, proportional-integral servo-controller; LP, low pass filter; DBM, double balanced mixer; red lines, free-space optical beams; yellow/blue lines, optical fibers (multimode/PCF); black lines, electrical connections.

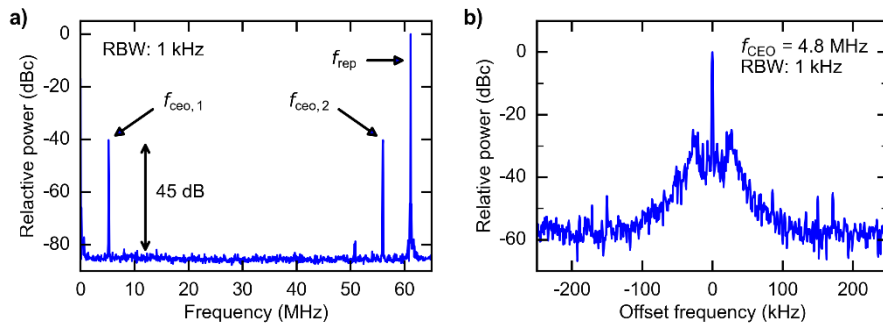


Figure 37. a) Radio-frequency spectrum of the locked CEO beat note. b) Zoom on the coherent peak over a total span of 500 kHz. The large noise originating from the servo bump can be observed at  $\sim 20$  kHz.

### 4.3 Fully-stabilized optical frequency comb

For repetition rate stabilization, the fundamental frequency was detected using a photodiode. The signal was filtered and compared in a double-balanced mixer to a reference signal from a waveform generator, which was referenced to an H-maser for long-term stability (see Figure 36). The resulting phase error signal was low-pass filtered and processed by a proportional-integral (PI) servo-controller (New Focus LB1005) to produce the correction signal to control the cavity length of the laser. This signal was amplified by a high-voltage amplifier (Falco Systems WMA-300, gain of 50) and applied to the piezoelectric transducer supporting an intra-cavity mirror. The resulting FN-PSD of  $f_{rep}$  is shown by the red curve in Figure 38b), together with the noise spectrum of the free-running repetition rate.

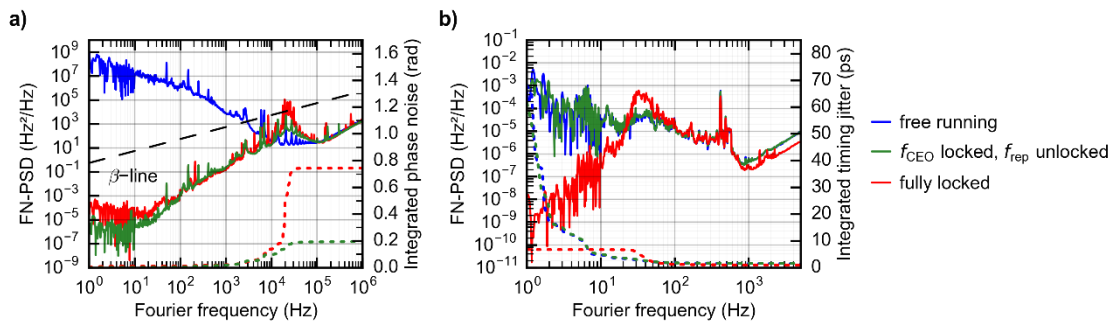


Figure 38. Left y-axis: Noise performance of the fully-stabilized TDL comb. a) Frequency noise power spectral density (FN-PSD) of the CEO beat in free-running (blue) and stabilized (red, green) conditions; Right y-axis: Corresponding integrated phase noise as a function of the upper cut-off frequency. b) Left y-axis: FN-PSD of the free-running (blue, green) and phase-locked (red) repetition rate frequency; Right y-axis: corresponding integrated timing jitter as a function of the lower cut-off frequency.

In this configuration, the noise of  $f_{\text{rep}}$  was reduced at Fourier frequencies up to  $\sim 20$  Hz. This bandwidth might be limited by both the high-voltage amplifier and the piezoelectric actuator combined with the half-inch-diameter 6-mm-thick mirror. Higher stabilization bandwidths should be feasible by reducing the weight of the mirror by using a thin substrate and mounting it on a suitable actuator driven by a high-bandwidth voltage amplifier. The timing jitter was 7 ps in this case (integrated from 1 Hz to 1 MHz). However, this stabilization degraded the CEO noise mainly at around 20 kHz, increasing its integrated phase noise to 745 mrad.

#### **4.4 Towards applications driven by fully-stabilized thin-disk laser oscillators**

This chapter describes the first self-referenced full stabilization of an optical frequency comb based on a TDL oscillator. For this, a coherent octave-spanning supercontinuum was generated after the oscillator using a minor part of the laser output power, without any external pulse compression. Subsequent detection of the CEO frequency was realized in a standard self-referencing  $f$ -to- $2f$  interferometer. The CEO beat signal was phase-locked to an external reference via pump current feedback using home-built modulation electronics. A loop bandwidth of  $\sim 20$  kHz was achieved and resulted in a tight CEO lock with a residual phase noise less than 200 mrad (integrated from 1 Hz to 1 MHz). The repetition rate is controlled via an intra-cavity mirror mounted onto a piezoelectric actuator. It was stabilized to a reference synthesizer with a residual timing jitter of 7 ps (integrated from 1 Hz to 1 MHz).

In this preliminary investigation, the repetition rate stabilization loop achieved a small stabilization bandwidth of  $\sim 20$  Hz. To further improve the performance, the transfer function of the loop will be evaluated as well as the static and dynamic tuning rates of the piezoelectric actuator and optimization of the servo-controller will follow. A low-pass filter inserted between the PI servo-controller and the high-voltage amplifier before the piezoelectric transducer could help reducing the parasitic influence of the  $f_{\text{rep}}$  stabilization loop onto the CEO frequency noise. Moreover, non-optimal components will be replaced. Using a thin light-weight mirror will allow the use of faster piezoelectric transducers with a suitable high bandwidth voltage amplifier, which should increase the stabilization bandwidth of  $f_{\text{rep}}$ . Besides, improvement of the performance will rely on the reduction of the intrinsic laser noise. In this experiment, the laser was directly mounted onto the laser table. Building the laser with highly-stable opto-mechanical components in a mechanically-stable laser housing, isolated from the mechanical noise (including decreasing the impact of the water cooling of the disk [100]) will help reducing the laser free-running noise. Moreover, it has been reported

in [100] that the position of the Kerr medium inside the cavity has a strong impact on the CEO behavior, which parameter has not been investigated yet in this experiment.

This approach of TDL-based optical-frequency comb could benefit from the power-scalability capabilities of TDL oscillators since the system requires only a low-current modulator in parallel to a high DC current source to modulate the pump power and retro-act on the CEO frequency. In the case of a high-power (> 100 W) SESAM mode-locked TDL, the CEO frequency could not be stabilized due to cavity dynamics probably linked to the SESAM [138]. In the present experiment, the laser is Kerr lens mode-locked and might not suffer from this issue. This approach in combination with the development of the performance of the KLM TDLs based on broadband gain materials could lead to the generation of optical frequency combs with hundreds of watts and sub-100-fs pulse duration. Nevertheless, stabilization with active feedback to the pump power has a cut-off frequency of ~20 kHz due to the cavity dynamics of the laser. In case higher bandwidths for CEO-frequency stabilization are required, other techniques compatible with high-power operation could be implemented and should result in even lower noise operation. They include the promising opto-optical modulation of a semi-conductor mirror which combines a fast modulation with power-scalability [142,143].

Finally, the fully-stabilized TDL oscillator delivers more than 4-W average power in sub-50-fs pulses at 61-MHz repetition rate and central wavelength of 1031 nm. This initial experiment proves the suitability of KLM TDLs to be used for CEO-sensitive experiments. This high-power optical-frequency comb will benefit to XUV frequency comb generation but also to various application areas such as high-field and attosecond science [128], optical frequency metrology [120], atomic clocks [121], or broadband high-resolution spectroscopy [118,119].

# Chapter 5 XUV light source based on HHG inside an ultrafast TDL oscillator

Coherent extreme-ultraviolet (XUV) light sources offer numerous new inspiring opportunities for science and technology [127,128]. Femtosecond-laser-driven high-harmonic generation (HHG) in gases is the most successful method for table-top coherent XUV-pulse generation. While initial HHG laser systems were limited to low repetition rates, the last years have seen the rapid development of MHz-repetition-rate XUV light sources providing a high photon flux. Such apparatus can strongly reduce the measurement time, improve the signal-to-noise ratio, and enable XUV frequency-comb metrology. However, current MHz XUV sources rely on complex and costly multi-stage laser systems.

This chapter presents a promising alternative to directly produce MHz-repetition-rate XUV-pulse trains from simple ultrafast TDL oscillators. Section 5.1 describes the benefits and challenges of HHG at high repetition rates. Section 5.2 details the development of a SESAM mode-locked TDL oscillator with suitable performance to drive intra-cavity highly-nonlinear processes. Section 5.3 focuses on HHG experiments unprecedentedly performed inside the cavity of a mode-locked TDL oscillator. Section 5.4 discusses enhanced XUV output coupling techniques for increased XUV-extraction efficiency. Finally, Section 5.5 concludes and gives an outlook towards an increased photon flux for future applications.

## 5.1 High-repetition-rate high-harmonic generation enabling applications

Focusing intense femtosecond pulses into a gas target enables the generation of high-order harmonics of the fundamental laser frequency [144,145] (see Figure 39). This highly-nonlinear process occurs at optical peak intensities above  $10^{13}$  W/cm<sup>2</sup> and results in a highly inefficient

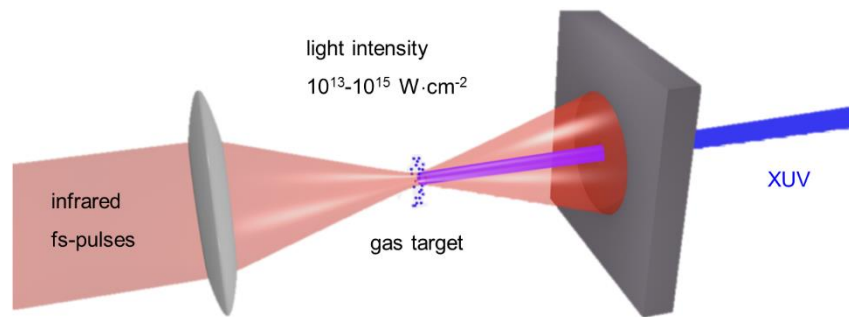


Figure 39. Focusing intense femtosecond pulses into a gas target enables the generation of high-order harmonics of the fundamental laser frequency. The high-harmonic spectrum typically extends down to the XUV-wavelength range. Figure courtesy of Martin Saraceno [4].

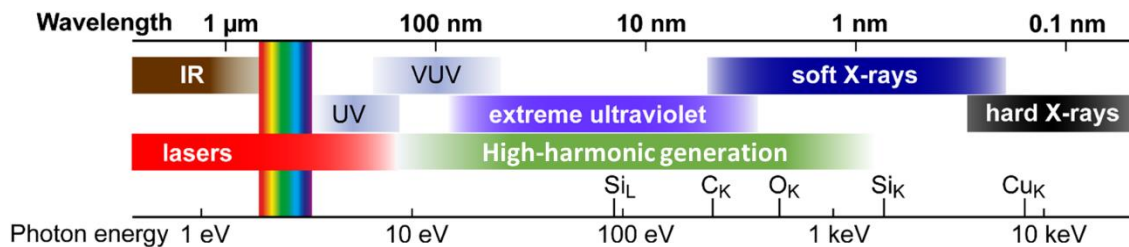


Figure 40. Electromagnetic spectrum. The wavelength range accessible via high-harmonic generation is highlighted with the green area. In this highly-nonlinear process, photons are upconverted from the driving laser frequency to higher energy levels ( $10\text{-}10^3$  eV), into the vacuum and extreme ultraviolet (VUV and XUV) regions, and up to the soft X-ray domain.

photon conversion [146,147] ( $7 \times 10^{-5}$  at maximum for a single harmonic [148]). The high-harmonic spectrum typically covers the vacuum and extreme ultraviolet (VUV and XUV) regions (10-200 nm) but can also extend to soft X-ray (0.1-10 nm), corresponding to photon energies ranging from 10 eV to a few keV, as illustrated in Figure 40. Such table-top high-harmonic sources can be used for applications instead of synchrotron radiations [127].

Standard HHG systems are based on a Ti:sapphire CPA laser, which usually operates at kHz repetition rate and average power of a few watts (e.g., [149]) and consequently, limits XUV photon flux and XUV pulse repetition rate. However, a high photon flux enables shorter measurement time and enhanced resolution for high resolution imaging [150,151]. Furthermore, the low repetition rate is a challenge for experiments in which the energy or momentum of photoelectrons must be precisely measured [21]. A prominent example is photoelectron emission microscopy [152], which can be used to explore ultrafast dynamics in nanostructured surfaces with simultaneous hundred-attosecond temporal and nanometer spatial resolution. Since low-pulse-energy operation is required to mitigate space charge

effects, high-repetition-rate sources are required to achieve a realistic acquisition time. Similarly, for coincidence detection, integration over a large number of shots is necessary to achieve sufficient signal-to-noise ratio and high-quality statistical data [153,154]. Moreover, a kHz-spaced comb is too dense for direct frequency comb spectroscopy which requires mode separation. In contrast, MHz frequency combs allow for the identification of the exact mode number and offer more power per single comb line. Therefore, MHz XUV frequency combs are highly attractive for high-resolution spectroscopy [129–131].

Given the large scientific potential, the last years have seen a tremendous increase in research efforts to optimize HHG sources for high photon flux and MHz repetition rate [155,156]. It has been shown that HHG is possible even with relatively low pulse energies in the micro-joule level and conditions for efficient generation in tight-focus geometries have been derived [157].

One straightforward approach to improve the current XUV sources has been to increase simultaneously the pulse energy and repetition rate of the driving laser system, i.e., to use high-average-power lasers as driving sources [156]. As already presented in Chapter 1, three laser architectures allow for high-power operation. They are based on the fiber, slab and TDL geometries. Due to their distinct benefits and challenges, each type of technology has been used to drive single-pass HHG. In 2009, a fiber-CPA laser system enabled the first single-pass HHG at MHz repetition rate, generating harmonics up to the 15<sup>th</sup> order (68.7 nm, 18 eV) [158]. Recent results based on fiber amplifiers include photon flux at ~25-eV photon energy of 50  $\mu$ W and up to the milliwatt level at 0.1-MHz and 10-MHz repetition rate, respectively [148,156]. However, these systems feature a high degree of complexity owing to the multi-stage amplification and necessary pulse compression. In 2011, the temporally-compressed output of a slab-amplifier achieved HHG at 20.8-MHz repetition rate in a chirp-free pulse amplification system [159]. Harmonics up to the 17<sup>th</sup> order (60.6 nm, 20.5 eV) have been generated at nW average power level. Amplification-free ultrafast oscillators offer a simpler way to generate high harmonics. The proof-of-concept has been demonstrated by a commercial Ti:sapphire oscillator delivering only 2.6-W average power at 4-MHz repetition rate [160]. In contrast, Yb-based ultrafast TDL oscillators operate at much higher average power and achieved single-pass HHG at 2.4-MHz repetition rate from the compressed laser output [23]. 46-W average power of the TDL oscillator enabled HHG up to the 25<sup>th</sup> order (41.3 nm, 30 eV) with 0.18-nW average power in the 19<sup>th</sup> harmonic (53.9 nm, 23 eV).

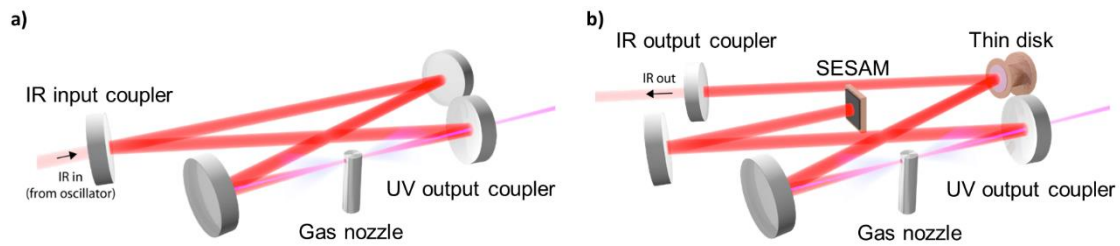


Figure 41. a) Enhancement cavities operate at enhanced field strength inside the cavity. When seeded with energetic femtosecond laser pulses, passive enhancement cavities enable high harmonic generation at MHz repetition rate with an improved overall efficiency since the unconverted photons are “recycled” inside the cavity. b) Placing the HHG interaction inside a mode-locked oscillator results in a simple approach to operate at enhanced field strength without the need for input matching of fs-pulses. Figure courtesy of Martin Saraceno [4].

The second approach to increase both photon flux and repetition rate of the XUV light is based on intra-cavity HHG (see Figure 41) [135,161,162]. The operation at enhanced field strength inside the cavity reduces the constraints on the driving-laser performance and increases the overall conversion efficiency by “recycling” the unconverted light. In the case of passive enhancement cavities, ultrashort pulses are coherently superimposed in the resonator and the effective peak power is enhanced by a factor ranging from ten to thousands. Therefore, high peak intensities at high repetition rate can be achieved from a moderate laser average power in the order of 1-10 W. Stable coupling of the driving field requires careful control of both the repetition rate and the CEO frequency. The comb properties of the driving laser are transferred to the high harmonics and lead inherently to XUV-frequency-comb generation.

Enhancement cavities enabled the first HHG at MHz repetition rates already in 2005, demonstrated concurrently in two distinct research groups [163,164]. In both systems, the cavity was seeded by a standard low-power ( $< 1$  W) Ti:sapphire laser oscillator. The development of powerful frequency combs based on fiber-CPA systems pushed this method further by combining state-of-the-art high-power lasers with enhancement cavities [132,133,165]. It resulted in the generation of XUV photon fluxes up to several hundred  $\mu$ W in a given harmonic up to 150-MHz repetition rate [166–168]. In 2012, the first direct frequency comb spectroscopy in the XUV region was demonstrated [130]. One year later, it was shown that such systems can generate XUV light with a coherence time longer than 1 second for sub-hertz-precision spectroscopy [169]. Recently, intra-cavity HHG allowed for the generation of photon energies exceeding 100 eV at a repetition rate of 250 MHz from



10 kW of intra-cavity average power and 30-fs pulses [170]. Efforts are currently made to push the performance of femtosecond enhancement cavities even further: increasing the tolerable intra-cavity average power using robust cavity designs and large mode size on the mirrors [171–173]; increasing the bandwidth of high-finesse enhancement cavities to support few cycle pulses [174], which should allow for efficient generation of MHz-repetition-rate isolated extreme ultraviolet attosecond pulses via intra-cavity HHG [175]. However, the experimental realization of enhancement cavities is highly complex. The requirements on the phase stability of the driving laser system are stringent. Stable coupling of fs-pulses from an amplified frequency comb into a high-finesse resonator containing the HHG interaction is very demanding and maintaining a high enhancement disregarding the linear and nonlinear phase shifts is challenging [176–178].

To avoid the need for the input matching of ultrashort pulse trains, the HHG process can be realized directly inside a high-power ultrafast oscillator. This results in a simple approach for which the complexity is reduced to only one stage, namely the oscillator, as shown in Figure 41. Yet, this approach shares several challenges with passive enhancement cavities, which are linked to the resonator stability under the high-pressure gas jet, the intra-cavity plasma and the XUV output coupling element. In contrast to passive cavities where input matching is critical for a high enhancement factor, the circulating femtosecond pulse inside a mode-locked oscillator can adapt to the nonlinearities and the dispersion originating from the HHG, the extraction method and the propagation inside the cavity. In 2012, HHG inside a mode-locked oscillator has been demonstrated in a Ti:sapphire laser [179], though the intra-cavity average power was limited to 10 W due to thermal effects and nonlinearities in the bulk crystal, limiting the XUV photon flux.

In contrast, ultrafast TDL oscillators are power-scalable. They operate at megahertz repetition rate (currently  $\sim 2\text{--}260$  MHz) [20,180] and achieve the highest average power and pulse energy from any mode-locked oscillator with intra-cavity performance reaching kW average power and tens to hundreds  $\mu\text{J}$  of pulse energy [18,20,34]. State-of-the-art ultrafast TDLs generate perfect soliton pulses with durations typically ranging from 30 fs to 1 ps and intra-cavity peak powers up the GW level have been reported with 500-fs pulses [66]. In this case, a tight focus inside the resonator allows reaching sufficiently high peak intensities to drive HHG processes [157]. Furthermore, TDL oscillators can run with low noise and the stabilization of the CEO and repetition-rate frequencies has been demonstrated in Chapter 4, showing the suitability of TDL oscillators for XUV-frequency-comb applications.

## 5.2 SESAM mode-locked thin-disk laser oscillators for intra-cavity HHG

This section describes the development of an ultrafast TDL oscillator with the required performance to drive intra-cavity HHG. To reach high optical intensity of  $3 \times 10^{13}$  W/cm<sup>2</sup> in a reasonable focus ( $> 10$   $\mu$ m radius), an intra-cavity peak power higher than 50 MW is necessary. One of the main challenge is to operate the laser at high power level under a vacuum level well below  $10^{-3}$  mbar, which creates thermal issues due to the lack of convective air [34] but is necessary to avoid the reabsorption of the XUV light in the ambient environment.

Owing to the fact that short pulse durations are extremely advantageous for HHG since they increase both the conversion efficiency and the saturation intensity [156,181], Yb:LuO was selected as gain medium for the oscillator given the previously demonstrated results of high average power operation [68] and ultrashort pulse duration [30]. At the time of this work, ultrafast Yb:LuO TDLs were exclusively mode-locked with SESAMs, and therefore SESAM mode locking was a more reasonable approach for a proof-of-principle experiment. First, the laser has been developed and tested in ambient air and later transferred to a vacuum chamber. Building the laser in air was more convenient than in vacuum environment since it allows for a lot of flexibility, rapid changes and tests of the different laser configurations. On the contrary, the evacuation time of the chamber ( $\sim 10$  minutes) prevents extensive study and optimization of the laser parameters such as the one presented in Section 2.3.

### 5.2.1 Sub-400-fs SESAM mode-locked Yb:LuO TDL at 27-W output power

The laser oscillator is based on the Yb:LuO TDL crystal used for the Kerr lens mode-locking experiments presented in Chapter 2. The cw performance has been presented in Section 2.2. The 12-mm-diameter 160- $\mu$ m-thick Yb(3 at.):LuO disk delivers up to 122 W of average power at 3.6% output coupling rate with an optical efficiency approaching 60% and an excellent beam quality. During the optimization of the mode-locking parameters, numerous damages of the mirrors and of the SESAM have been observed (see Figure 42). The damages are attributed to Q-switched pulses or Q-switch mode-locking and to the high optical intensity and potential contamination on the mirrors [16]. Consequently, the resonator design has been tailored to prevent damage from Q-switched pulses and from large intensity due to small spot sizes on the optics, especially dispersive mirrors which are more prone to damage due to the field enhancement inside the dielectric structure. The cavity is optimized to operate at the center of the stability zone, to be robust against the thermal lens of the disk and SESAM and

to consider the Kerr lens effect inside the Brewster plate (see Figure 43a). The beam diameter of the transverse fundamental mode on the disk is set to about 2.2 mm to optimize the overlap with the 2.8-mm-diameter flat-top pump profile. The large-scale high-power SESAM used for mode locking has been manufactured at the FIRST cleanroom facilities at ETH Zürich (picture shown in Figure 42b and Figure 43b). It was manufactured using the standard fabrication technique [182] and was glued to a copper heat sink using a thermally-conducting adhesive. The SESAM comprises three quantum wells and three pairs of dielectric top-coating. Due to the top-coating, a very high saturation fluence larger than  $100 \mu\text{J}/\text{cm}^2$  is achieved, together with a modulation depth of around 1% and non-saturable losses smaller than 0.2% (characterized with 1-ps laser with central wavelength around 1030 nm). In this result, the SESAM is operated at a fluence about 20 times its saturation value. A 4-mm-thick undoped YAG plate is inserted under Brewster angle near the output coupler. It induces SPM that is balanced by two dispersive mirrors, resulting in an inserted GDD of  $-4000 \text{ fs}^2$  per round

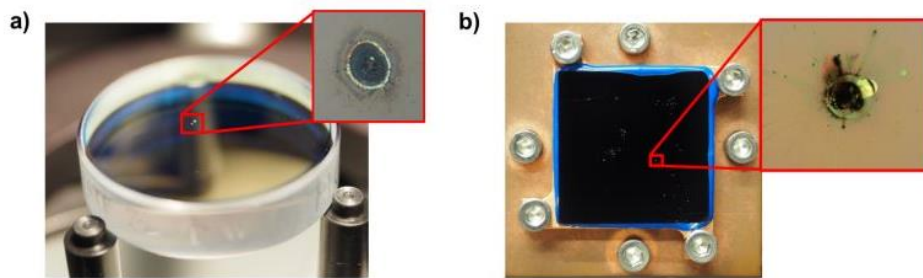


Figure 42. Pictures of typical damage spots on (a) a highly reflective mirror and (b) a SESAM.

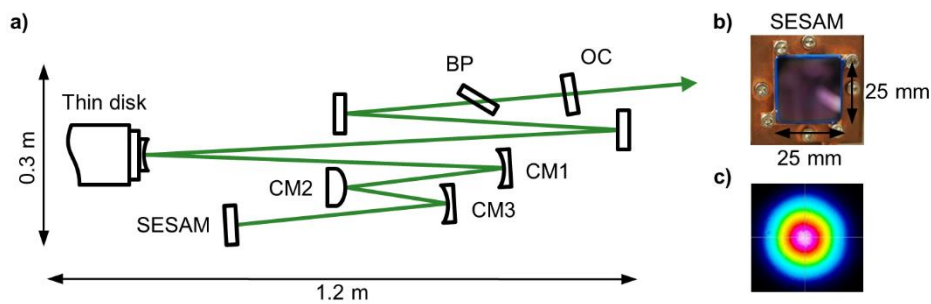


Figure 43. a) Schematic of the SESAM mode-locked laser oscillator. BP, Brewster plate; OC, output coupler; CM1, concave mirror with a 3-m radius of curvature (RoC); CM2, 0.4-m-RoC convex mirror; CM3, 0.75-m-RoC concave mirror. Other mirrors are dispersive mirrors. b) Picture of the large-size high-power SESAM. c) Output-beam profile of the mode-locked laser at 27-W average power.

trip. Self-starting stable passive soliton mode locking is achieved for several combinations of laser parameters. At 5.7% output-coupling rate and 98-W pump power, 27 W of average output power are obtained in 380 fs pulses at 43.4-MHz repetition rate.

The autocorrelation trace, optical spectrum and radio-frequency spectrum measurements are shown in Figure 44. The optical spectrum is centered at 1035 nm and has a FWHM of 3.4 nm, leading to a close to ideal time-bandwidth product of 0.362 (ideal  $\text{sech}^2$ : 0.315). The laser generates pulses with more than half a microjoule of pulse energy leading to 1.4-MW peak power and 25-MW intra-cavity peak power with a high optical efficiency amounting to 28%. Stable operation of the laser is achieved daily for more than two months with nearly no realignment. This result proves the suitability of the here-presented oscillator to drive experiments.

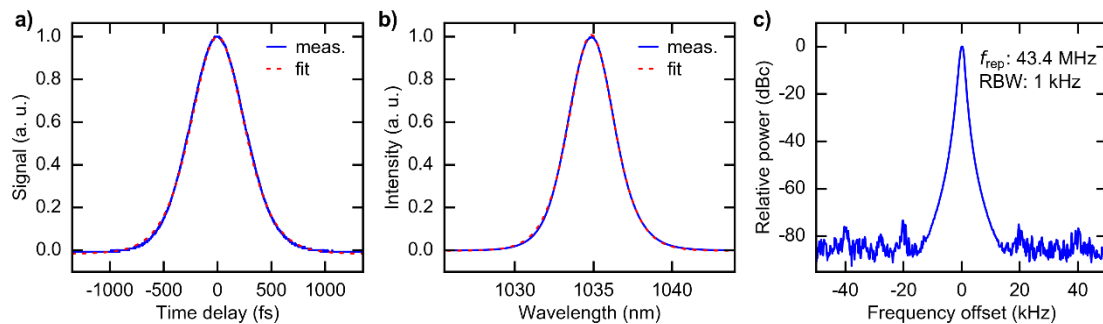


Figure 44. Characterization of the SESAM mode-locked Yb:LuO laser. a) Measured autocorrelation trace and corresponding  $\text{sech}^2$  fit. b) Laser optical spectrum. c) Radio-frequency spectrum of the fundamental repetition-rate frequency measured with a 1-kHz resolution bandwidth (RBW) and 90-kHz span.

### 5.2.2 Sub-300-fs pulses from a SESAM mode-locked Yb:LuO TDL in air

In a second step, the focus was given on the realization of a laser source operating in ambient air with shorter pulse durations. This laser is based on a different disk crystal shown in Figure 45a). In this case, the wedged Yb:LuO disk has a 7-mm diameter and a 200- $\mu\text{m}$  thickness. It is mounted onto a water-cooled diamond heat sink and exhibits a 2.15-m concave RoC with no measurable astigmatism. A 600-W fiber-coupled VBG-wavelength-stabilized diode laser system pumps the gain material at the zero-phonon line at a wavelength of 976 nm with a spectral width below 0.5 nm FWHM. High absorption of the pump power is achieved via 36 passes of the pump light through the gain crystal with a 2.8-mm diameter (Figure 45b). The resonator design is very similar to the one presented in the previous section, however a

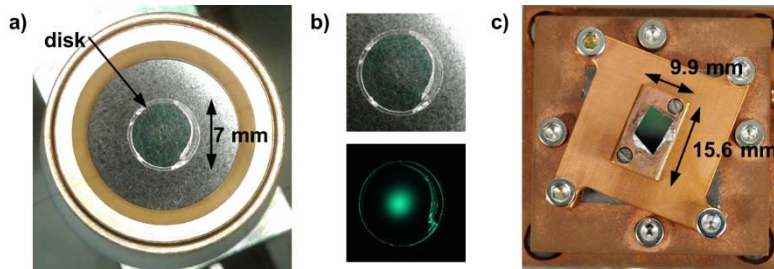


Figure 45. a) Picture of the 200- $\mu\text{m}$  Yb:LuO thin-disk laser crystal. b) Picture of the (top) unpumped disk and (bottom) disk fluorescence at 13-W pump power. c) Picture of the SESAM used in the mode-locking experiments.

different SESAM with higher modulation depth was used to generate shorter pulses. Processed with two dielectric top-coatings, it features a saturation fluence of  $38 \mu\text{J}/\text{cm}^2$ , a modulation depth of  $\sim 1.8\%$  and non-saturable losses smaller than  $0.4\%$  (characterized with a 1-ps laser at a central wavelength around 1030 nm). Stable passive soliton mode locking is self-starting. At 4.6% output coupling rate and 100-W pump power, an average output power of 19.5 W is obtained in 284-fs pulses at 44.8-MHz repetition rate and a high SESAM saturation parameter of 50. The autocorrelation trace, optical spectrum and radio-frequency spectrum measurements are shown in Figure 46. The optical spectrum is centered at 1035.5 nm and has a FWHM of 5.1 nm, leading to a time-bandwidth product of 0.405. The laser operating in ambient air generates sub-300-fs pulses with close to 30-MW intra-cavity peak power. This result shows the potential of this laser to reach the required performances to drive intra-cavity HHG when operating in evacuated environment at a lower repetition rate.

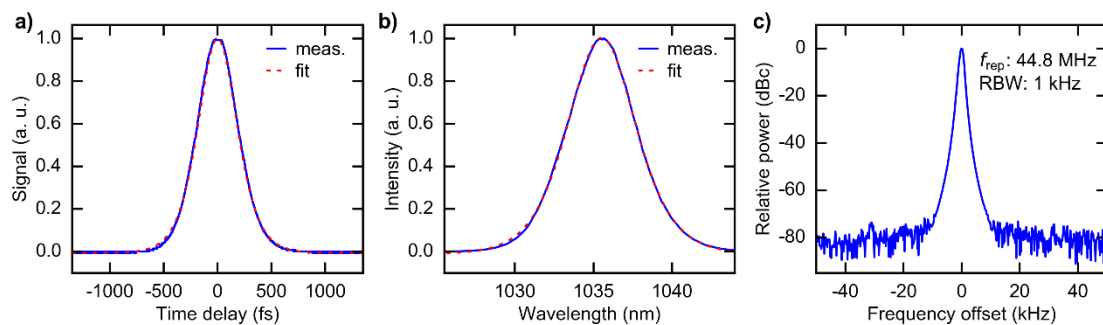


Figure 46. Characterization of the SESAM mode-locked Yb:LuO laser oscillator. a) Measured autocorrelation trace with corresponding  $\text{sech}^2$  fit. b) Laser optical spectrum. c) Radio-frequency spectrum of the fundamental repetition rate frequency at a 1-kHz resolution bandwidth (RBW).

### 5.2.3 Vacuum-environment sub-300-fs SESAM mode-locked Yb:LuO TDL

Following the success of the preliminary study on the SESAM mode-locked Yb:LuO TDL operating in ambient air, the full resonator including the TDL head was transferred to a compact vacuum chamber with dimensions of 80 cm × 150 cm (see Figure 47b). The laser oscillator is built onto an inner breadboard, which is independent from the laser housing. The vacuum chamber is evacuated to a pressure of  $\sim 10^{-4}$  mbar using two turbomolecular pumps directly connected to the chamber with standard ISO-K flanges. The modified laser cavity is shown in Figure 47a). The beam radius of the transverse fundamental mode is estimated to be 1.15 mm on the disk. A 4-mm-thick undoped-YAG plate is used at Brewster angle to enforce linear p-polarization and to introduce SPM for soliton mode locking. The SPM is balanced by three dispersive mirrors inserting  $-3000\text{-fs}^2$  of GDD per round trip. An output coupler with 0.7% transmission is used as a folding mirror. The SESAM was replaced by a another sample containing four InGaAs quantum wells, placed in pairs into two subsequent antinodes of the electric field. An embedment of the quantum wells in AlAs layers ensures full strain compensation of the epitaxial structure [183]. A dielectric top-coating is added to reduce the field enhancement and multi-photon absorption related effects [182]. The SESAM has a 1.6% modulation depth, 0.3% nonsaturable losses and a  $47\text{-}\mu\text{J}/\text{cm}^2$  saturation fluence (measured with 100-fs pulses centered at 1030 nm). The laser mode radius is adjusted to 0.95 mm on the SESAM for an operation with a saturation parameter of the absorber around 30 in mode-locked regime.

A simple extension consisting of two concave mirrors of 1 m and 3 m RoC is inserted after the output coupler to lower the repetition rate, i.e., to increase the pulse energy for a given average power. An intra-cavity focus is created between two curved mirrors of 100-mm and 150-mm RoC (the latter one is used as an end mirror). The waist size is estimated from ray-transfer-matrix calculations to be 12  $\mu\text{m}$  in radius. The calculations are calibrated with the measurement of multiple transmitted beams through the cavity mirrors and the error is estimated to be in the order of 10%. To extract the generated XUV light, a wedged 250- $\mu\text{m}$  sapphire plate is placed 2 cm behind the focus under Brewster angle for the laser wavelength. This outcoupling method has often been used in cavity-enhanced HHG experiments [163,164,169]. While the Brewster plate reflection is negligible at the laser wavelength, the refractive-index difference between the infrared and the XUV allows for about 7% reflection at 100-nm wavelength and up to 15% at 60 nm.

observed, most likely due to operation close to the roll-over of the SESAM reflectivity in combination with the finite gain bandwidth of the gain material [97]. The laser autocorrelation trace, optical spectrum, radio-frequency spectrum and  $M^2$  measurements are shown in Figure 50. With 63-MW intra-cavity peak power, this laser realizes state-of-the-art intra-cavity average- and peak-power performance from SESAM mode-locked TDL oscillators operating at sub-500-fs pulse durations, as depicted in Figure 48. It is to be noticed that other oscillators which operate in vacuum environment are evacuated to a pressure of about 1-100 mbar, while the presented laser operates at  $10^{-4}$  mbar. The high intra-cavity peak power leads to a peak intensity of  $\sim 2.8 \times 10^{13}$  W/cm<sup>2</sup> at the focus, which is sufficient for first HHG experiments inside a mode-locked TDL oscillator.

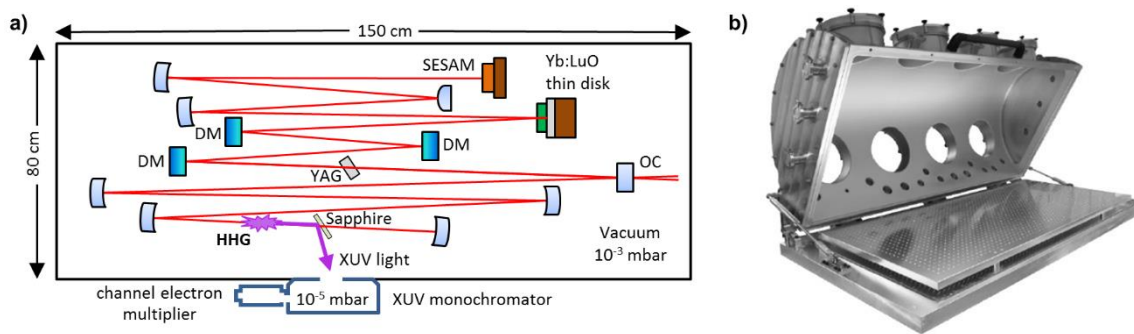


Figure 47. a) Schematic of the resonator cavity and experimental setup used for intra-cavity high-harmonic generation. OC, output coupler; DM, dispersive mirror. All other mirrors are coated for high reflectivity. b) Picture of the vacuum chamber in which the entire laser resonator was built.

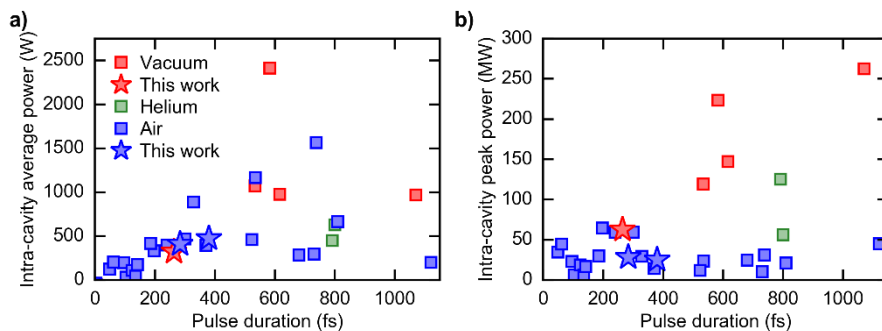


Figure 48. Overview of SESAM mode-locked thin-disk laser oscillators. The intra-cavity (a) average and (b) peak powers are plotted as a function of the pulse duration. The laser environment is indicated as reference in the legend. Vacuum: [18,20,97]; Helium: [40,95]; Air: [14,23,24,27–31,39,57,63,65,68,82,95,161]; the results reported in this chapter are highlighted with star symbols.

### 5.3 HHG at megahertz repetition rate inside an ultrafast TDL oscillator

A quartz nozzle with  $\sim 100\text{-}\mu\text{m}$  opening diameter is inserted and delivers the gas into the focus inside the laser resonator. To maintain the chamber pressure below  $5 \times 10^{-3}$  mbar while a high-pressure gas jet is used, a gas-jet dump is placed below the nozzle [73]. Figure 49 shows a schematic view of the generation setup. When the xenon gas jet is emitted into the focus, HHG is observed and detected with a channel electron multiplier (Photonis Magnum 5900). The XUV light is directed by an unprotected gold mirror to a wavelength-calibrated monochromator (Acton VM-502) equipped with a 1200-g/mm iridium-coated grating. The slit width was set for a 3.4-nm spectral resolution.

Using 3.4 bar of backing pressure in the nozzle leads to a pressure estimated to  $\sim 400$  mbar at the laser focus. At this gas pressure, the average output power of the laser slightly drops, and increasing the pump power from 49 W to 51 W achieves the same intra-cavity average power of 320 W as without gas jet. The TDL oscillator with HHG operates with slightly shorter 255-fs pulses. Its intra-cavity peak power is 65 MW, which leads to a peak intensity of  $\sim 2.9 \times 10^{13}$  W/cm<sup>2</sup> at the focus. The corresponding autocorrelation trace, optical spectrum, radio-frequency spectrum, and  $M^2$  measurements are shown in Figure 50 with and without gas jet for comparison.

High harmonics up to the 17<sup>th</sup> order (60.8 nm, 20.4 eV) are detected in accordance with the prediction from the cutoff formula ( $\lambda_{\text{cutoff}} = 58$  nm) [186]. XUV spectra are acquired with and without a 0.2  $\mu\text{m}$  thick aluminum filter to check the validity of the measurement (see

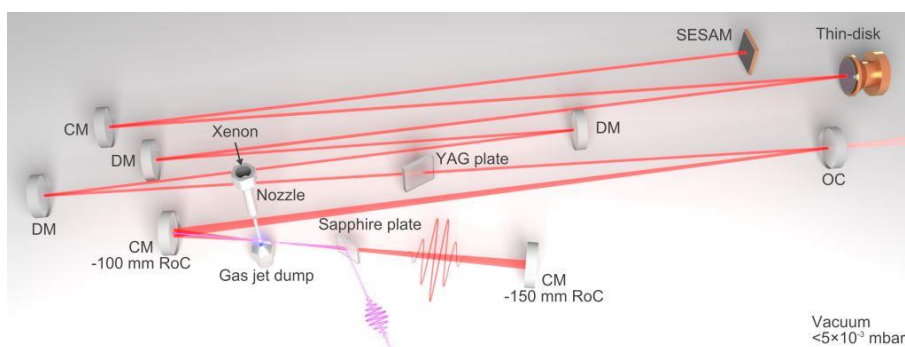


Figure 49. Experimental setup for high-harmonic generation inside the cavity of a mode-locked thin-disk laser oscillator. This new approach is a simple and compact way to provide MHz-repetition-rate XUV sources. For clarity, two intra-cavity telescopes were omitted in this sketch. DM, dispersive mirror; CM, curved mirror; RoC, radius of curvature; OC, output coupler. Figure created by Martin Saraceno [4].



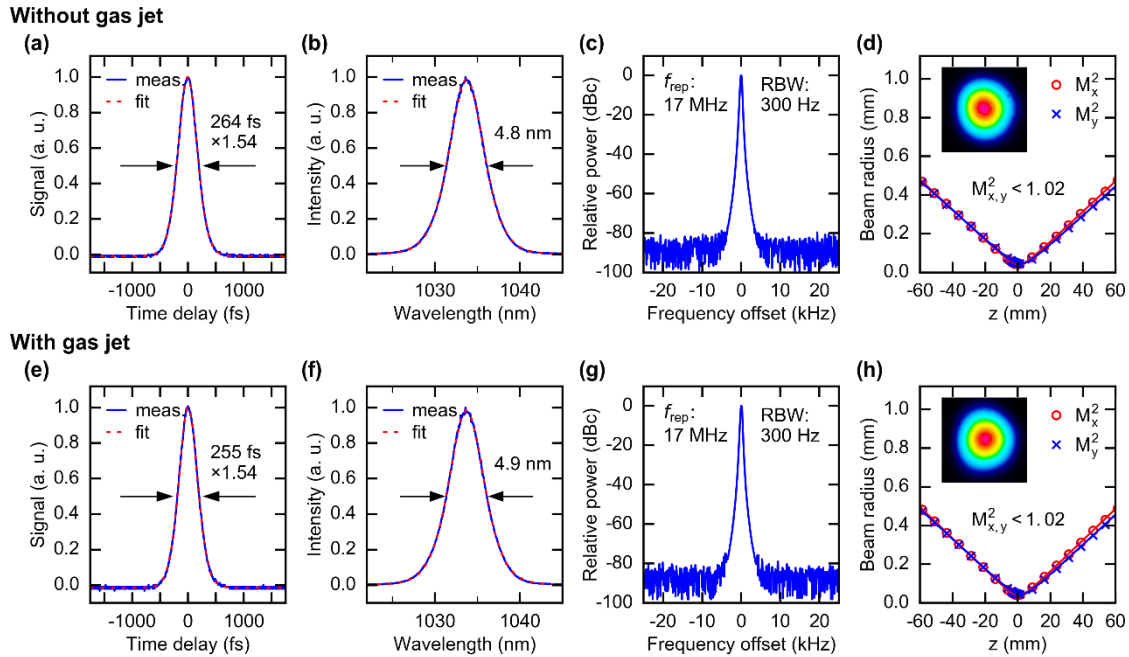


Figure 50. Comparison of the SESAM mode-locked TDL oscillator output parameters (a-d) without gas jet and (e-h) with high pressure gas jet. (a,e) Measured autocorrelation trace and corresponding sech<sup>2</sup> fit, (b,f) laser optical spectra, (c,g) radio-frequency spectra of the fundamental repetition rate frequency at a 300-Hz resolution bandwidth (RBW) and 50-kHz span, (d,h)  $M^2$  measurements and (insets) output beam profiles.

Figure 51). Both curves were taken with similar gas pressure, pulse duration and pulse energy. However, to insert the aluminium filter, the system had to be put to atmospheric pressure and then to vacuum again, and the laser was slightly realigned. Therefore, the nozzle position had to be re-optimized. Yet, the aluminium cuts the 11<sup>th</sup> harmonics, so the optimization was done while seeing only the 15<sup>th</sup> and 17<sup>th</sup> harmonics. Therefore, for that second measurement, the nozzle was placed in such a way that phase matching was optimized for those orders, leading to a stronger flux at these harmonics. Harmonics below the 11<sup>th</sup> order (94 nm, 13.2 eV) were not detected, most likely due to reabsorption in xenon for the 9<sup>th</sup> harmonic [167] and to the low quantum efficiency of the detector for wavelengths longer than 140 nm.

Using the measured spectra and an additional measurement of the total XUV flux in all the detected harmonics with the channel electron multiplier placed before the monochromator and without aluminum filter, the average power and photon flux generated at the 11<sup>th</sup> harmonic are estimated with a similar method as described in [23]. A very conservative estimation results in a generated flux  $\gtrsim 2.6 \times 10^8$  photons/s. This corresponds to an average

power  $\geq 0.55$  nW and a conversion efficiency  $\geq 1.7 \times 10^{-12}$  with respect to the intracavity average power and  $\geq 1.1 \times 10^{-11}$  with respect to the diode pump power.

To evaluate the influence of the gas jet and plasma on the operation of the ultrafast laser oscillator, the transverse beam quality and laser noise were compared with and without HHG. The laser operates in both cases in a fundamental transverse mode with an  $M^2$  factor smaller than 1.02 (Figure 50.d,h). The noise of the TDL oscillator output was measured in free-running operation on the passively filtered 4<sup>th</sup> harmonic of the repetition rate using a phase noise analyzer (Rohde & Schwarz FSWP26). The measured power spectral densities of the amplitude and phase noise are shown in Figure 52. Although the vacuum chamber is connected to two turbomolecular pumps and the opto-mechanical components were not optimized for high stability, the laser features a RIN of only 0.78% and 0.76% (integrated from 1 Hz to 1 MHz) with and without gas, respectively. The phase noise integrated in the same frequency range amounts to less than 1.5 mrad (1.33 mrad with gas and 1.25 mrad without gas). Both turbomolecular pumps were running at their maximum speed during these measurements and the nozzle backing pressure during the measurement with gas was 3.4 bar as during the XUV light spectra acquisition. The laser noise is comparable to the typical values of free-running ultrafast TDL oscillators [23,138]. Therefore, CEO stabilization of this system should be feasible and would lead, together with the intra-cavity HHG process, to the generation of an XUV frequency comb directly from a mode-locked oscillator. The measurements of the laser stability confirm that in the current conversion regime, the phase distortion caused by plasma inside the cavity does not degrade the oscillator stability.

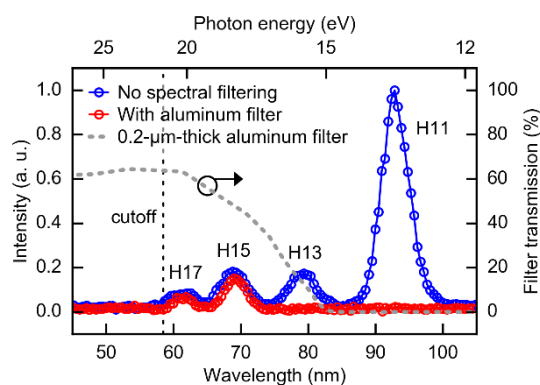


Figure 51. Left y-axis: Measured spectrum of the generated XUV light (blue). The vertical dashed line shows the calculated cutoff wavelength [186]. Placing a 0.2- $\mu\text{m}$ -thick aluminum foil in the beam enables removing the uncertainty of the harmonic number (red). Right y-axis: The theoretical transmission of the aluminum filter is shown for reference (grey dashed line).

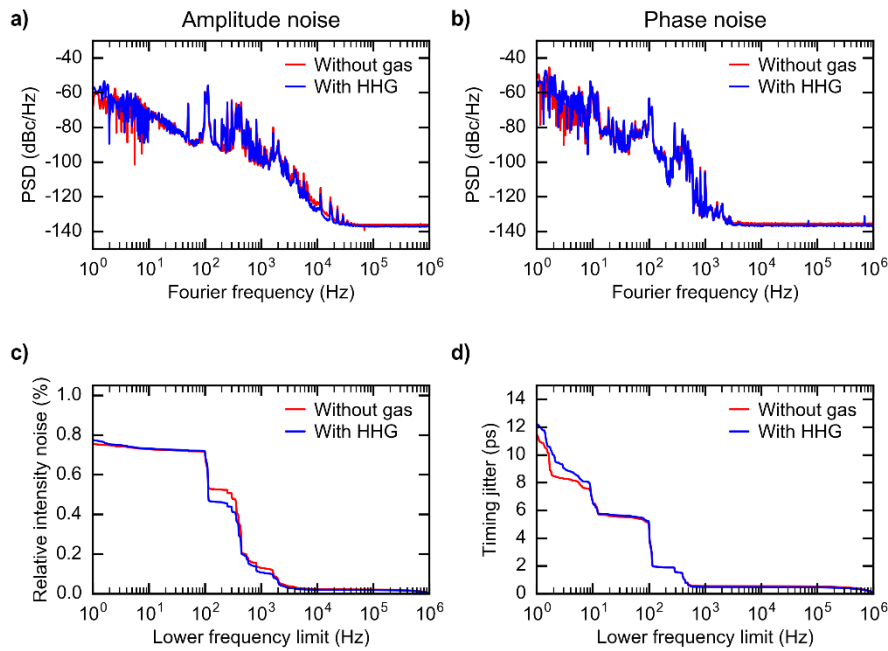


Figure 52. a) Amplitude and (b) phase noise power spectral density (PSD), (c) rms relative intensity noise, (d) rms timing jitter measurements of the TDL oscillator output in free-running operation with and without gas. Nearly no difference of the noise performance is observed with and without intra-cavity high-pressure gas jet.

## 5.4 Enhanced extreme-ultraviolet output coupling methods

The previous section proposed a proof-of-concept for XUV generation inside an ultrafast TDL oscillator. The XUV light was coupled out with an efficiency below 20% using a sapphire plate placed under Brewster angle for the driving laser. However, in many XUV experiments, the photon flux is a decisive performance [135,156]. Therefore, the separation of the XUV from the driving IR field is a critical step since the harmonics are generated collinearly with the fundamental light in this presented experiment. The output coupling of the high harmonics from the laser cavity should be as efficient and broadband as possible. Since materials typically exhibit strong absorption at XUV wavelengths, the XUV light cannot pass through a cavity mirror substrate to be extracted without being absorbed. For single-pass HHG, the unconverted light from the high-average-power driving laser can conveniently be dumped and extraction through a pinhole or using a plate under a large angle of incidence ( $>60^\circ$ ) is commonly done. In the case of XUV generation inside a passive or active resonator cavity, the separation should result in low losses, low nonlinearities and limited perturbation of the driving laser. Different approaches were explored for femtosecond enhancement cavities.

Extraction of the XUV beam can be achieved from a plate placed under Brewster angle for the p-polarized IR laser light. It results in negligible losses for the driving laser while the Fresnel reflection due to the index difference at the vacuum/plate interface offers a reflection of a few percent for the XUV as shown in Figure 53. Due to the simplicity of this technique and the intrinsic broadband properties at the driving wavelength, it was chosen for the proof-of-principle demonstrations of HHG inside an enhancement cavity and a mode-locked oscillator [163,164,179]. However, the efficiency and XUV bandwidth are rather limited.

Other techniques include the use of an intra-cavity small-period diffraction grating etched directly onto the surface of a dielectric mirror [130,189]. This component is highly reflective for the fundamental light and acts as a diffracting grating for the higher harmonics with an efficiency up to 20% [190]. Unfortunately, nonlinear effect originating from the nanostructure might be detrimental. Moreover, HHG in a noncolinear geometry using two colliding pulses has also been proposed [191,192]. It results in IR and XUV beams propagating in different directions but temporal and spatial overlapping of two pulses in a tight focus configuration are stringent requirements. Therefore, this approach is extremely challenging to apply for HHG inside an ultrafast oscillator.

For most materials, the reflection of XUV wavelengths increases with the angle of incidence and it is greater for s-polarized light than for p-polarized light (see Figure 54). Therefore, a higher XUV reflectivity is observed for angle of incidence larger than the Brewster angle though the reflectivity is simultaneously increased at the driving laser wavelength. Deposition

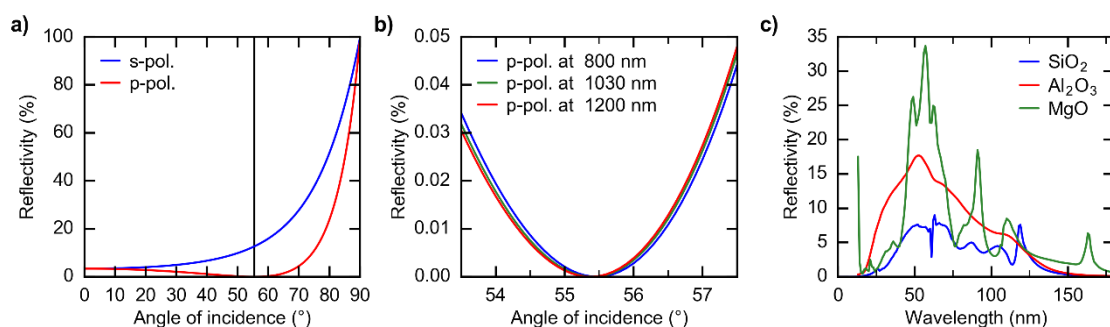


Figure 53. a) Reflectivity of fused silica ( $\text{SiO}_2$ ) at 1030 nm with respect to the angle of incidence of the light. At Brewster angle, the p-polarized light undergoes no reflection as depicted by the vertical black line. On the contrary, the s-polarized light always experiences a larger reflection than the p-polarized light. b) Reflectivity of  $\text{SiO}_2$  near the Brewster angle. c) Reflectivity of  $\text{SiO}_2$ , sapphire ( $\text{Al}_2\text{O}_3$ ) and magnesium oxide ( $\text{MgO}$ ) at XUV wavelengths for an incident 1030-nm p-polarized light at Brewster angle ( $55^\circ$  for  $\text{SiO}_2$ ,  $61^\circ$  for  $\text{Al}_2\text{O}_3$  and  $60^\circ$  for  $\text{MgO}$ ). Data taken from [188].

of a broadband anti-reflection coating on a substrate enables to drastically reduce the losses for the driving laser field [193,194]. As the plate must be placed after the focus, the entire spatial beam profile hits the plate under different angles of incidence. Consequently, the coating must exhibit low losses over a certain range of incidence angles and support the entire driving pulse spectrum. These criteria make the design and manufacturing of broadband coatings with low sensitivity to growth errors very challenging. Besides, a compromise for the substrate thickness should be realized. While a thin substrate might bend due to the stress induced by the coating, a thick substrate could lead to excessive peak-power-dependent nonlinear phase shift and thermal effects under the vacuum environment. The design and simulated reflectivity of coatings operating around  $60^\circ$  and  $70^\circ$  of incidence angle are shown in Figure 55. As a next step, substrates will be processed with such AR-coatings using our ion-beam-sputtering coating machine. Once placed inside the cavity under grazing incidence, no significant loss for the laser and high extraction efficiencies above 30% at around 90 nm are expected. Owing to the material properties, this extraction method is limited to photon energies up to about a few hundred eV, which is sufficient for the targeted experiments.

An efficient approach to extract high harmonics from the cavity is realized with an HR-mirror with a clear aperture of a few-ten to hundred microns [191] (see Figure 56). This method takes advantage of the fact that higher harmonics have a smaller divergence than the driving field. The high harmonics are extracted through a hole inside the mirror while the large IR beam is reflected on the mirror with only minor losses (<1%). This technique was successfully implemented in enhancement cavities operating with either transverse fundamental mode [170,195] or higher-order modes in combination with a slotted mirror (slit opening) [196]. Since the XUV light travels undisturbed, efficient outcoupling of the low wavelengths is possible (theoretically > 80% below 10 nm). Harmonics with wavelengths down to 11 nm have already been coupled out from an enhancement cavity through a hole in the mirror following the HHG focus demonstrating the most broadband XUV output coupling method to date [170]. Key parameters for low loss and good extraction efficiency are the laser-to-hole radius ratio, the amount of lost area due to chipping of the dielectric coating and surface deformation near the edge of the hole. Even though the drilling process of such a dielectric mirror is not straightforward, it is possible to obtain good quality holes, e.g., by using inverse laser drilling technique and post-processing with tempering the substrates [197]. To date, operation of a mode-locked laser with a pierced mirror has not been demonstrated and mode-locking might be prevented by the onset of higher order modes due to the losses at the

center of the mirror. However, this recent development of intra-cavity HHG might motivate efforts in this direction.

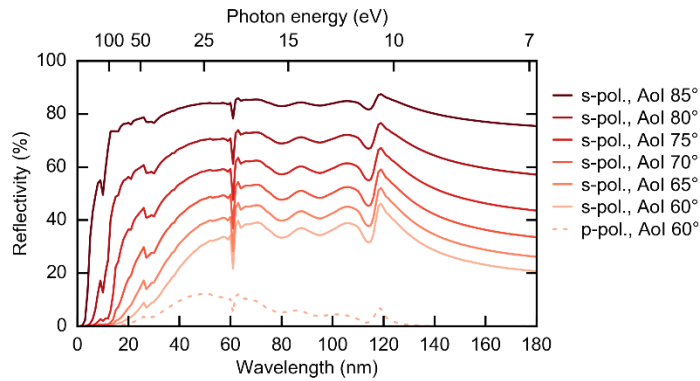


Figure 54. Fused silica ( $\text{SiO}_2$ ) exhibits a broadband high reflectivity for the XUV s-polarized light under a large angle of incidence (AoI).

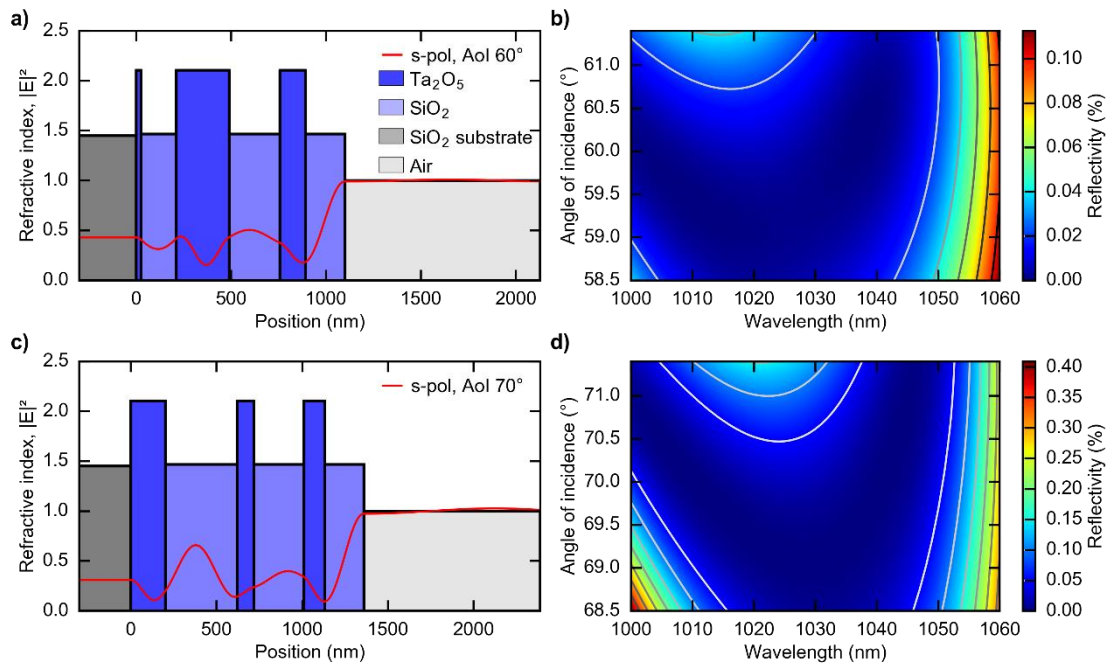


Figure 55. a,c) Coating design and (b,d) simulated IR-reflectivity of broadband anti-reflection coatings operating at (a,c)  $60^\circ$  and (b,d)  $70^\circ$  of incidence angle. Centered at 1030 nm, the coatings exhibit less than 0.1% of reflection over a bandwidth larger than 50 nm supporting sub-100-fs pulses. At these angles of incidence, the reflection of the top layer ( $\text{SiO}_2$ ) is above 30% for the XUV.

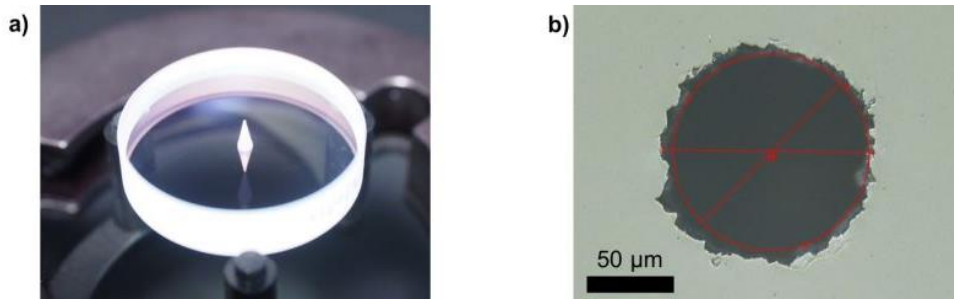


Figure 56. a) Picture of a 1-inch mirror substrate with a hole manufactured by the inverse laser drilling method [197]. The free aperture has a diameter of about  $110\ \mu\text{m}$  in the front surface. It was drilled with an undercut of a few degrees, resulting in an opening larger than 1 mm in the back surface. b) Magnified picture of the hole in the center of the mirror. The chipping of the hole is very small, and the lost area has a diameter only  $10\ \mu\text{m}$  larger than the clear aperture.

## 5.5 Towards experiments directly driven by simple XUV laser sources

This chapter described HHG experiments realized directly inside the cavity of a SESAM mode-locked TDL oscillator. The XUV light was generated down to a wavelength of 61 nm (17<sup>th</sup> harmonic, 20.4 eV) at 17-MHz repetition rate from a compact and simple setup. HHG is driven in a high-pressure xenon gas jet with an intra-cavity peak intensity of  $2.9 \times 10^{13}\ \text{W}/\text{cm}^2$  and 320 W of intra-cavity average power. The system is driven with only 51 W of pump power and generates an estimated average power of 0.5 nW in the 11<sup>th</sup> harmonic (94 nm, 13.2 eV), i.e., a photon flux of  $\sim 2.6 \times 10^8$  photons/s.

The conversion efficiency of  $10^{-11}$  with respect to the pump power and the photon flux are limited in this proof-of-concept experiment by the long pulse duration ( $> 250$  fs) and the moderate peak power ( $< 70$  MW). However, TDL oscillators already operated at GW intra-cavity peak-power levels [66] and sub-100-fs pulse durations [25]. Chapter 2 demonstrated the generation of 35-fs pulses with 73-MW intra-cavity peak power from a cutting-edge KLM Yb:LuO TDL oscillator operating in air. Operation with shorter pulse durations should lead to a substantial increase of the conversion efficiency and saturation intensity. Therefore, further optimization of the laser parameters to reach performances similar to state-of-the-art HHG systems at the MHz repetition rate [170,198] appears feasible. In combination with phase matching optimization of the HHG process [147,155,157], this should significantly increase the conversion efficiency and allow for generating higher-energy photons. Furthermore, more efficient extraction schemes [191,193,195] should significantly increase the XUV flux available in future experiments. The implementation of a grazing incidence plate seems straightforward and should lead to a 5-fold increase of the extraction efficiency. In case a larger XUV

bandwidth is required, a pierced output-coupler mirror can be inserted in the cavity instead. However, operation of a mode-locked oscillator with a hollow mirror has not yet been demonstrated.

In addition, the CEO and repetition frequencies can be stabilized as already presented in Chapter 4. Because HHG is a coherent process, the comb properties of the driving source are transferred to the XUV pulses. This fully-stabilized XUV frequency comb will enable performing various XUV spectroscopy experiments.

Since the HHG process does not affect the laser behavior, multiple ports for HHG can be inserted inside the laser cavity to obtain multiple high-harmonic beams with different wavelengths or to simultaneously run multiple experiments. It might also be possible to insert a second output coupler on the other side of the gas target to get a second XUV beam from the backward propagating pulse, though phase matching conditions are not optimal. A recent result presented at a conference reported on HHG inside a TDL oscillator with two HHG ports [199]. Though, insertion of more gas targets and output couplers inside the laser resonator might lead to challenges of the spatial arrangement, the source might be suitable for 1- and 2-D pump-probe spectroscopic measurements in the IR, VUV and XUV domains.

This new approach of HHG inside a TDL oscillator can lead to a novel class of coherent XUV light sources driven by only few-tens- to hundreds-watt pump diode systems, and which combine efficient MHz-repetition-rate operation at high XUV flux with a compact design. Such simple systems will be highly attractive versatile tools to drive many applications ranging from high-resolution imaging and structural analysis of matter to XUV spectroscopy and attosecond science.



## Chapter 6 Conclusion and future research

In this thesis, novel achievements in the field of high-power ultrashort Yb-based oscillators were reported and discussed. Most of the results presented in this manuscript are based on three key ingredients: the thin-disk laser (TDL) technology, the Kerr lens mode locking scheme and broadband gain materials. Using this highly promising combination, new frontiers in laser performance are reached. Record average power levels from TDL oscillators are achieved in pulses with sub-100-fs and sub-50-fs durations. In addition, 30-fs pulses are generated from a Kerr lens mode-locked (KLM) TDL for which the duration is 60% shorter than previously reported ultrafast TDL oscillators. The results achieved in this thesis and the recommendations for further steps are important milestones for the development of a compact simple laser technology that is suitable to directly drive applications demanding ultrashort pulses, with multi-ten to hundred watts average power levels and excellent spatio-temporal properties. These cutting-edge laser sources have the potential to become a versatile tool for scientific research, enabling measurements with high signal-to-noise ratios and short acquisition times. The attractiveness of ultrafast TDLs delivering ultrashort pulses is confirmed with two proof-of-concept experiments: the full-stabilization of an optical frequency comb based on TDLs, and the generation of extreme ultraviolet (XUV) light inside the cavity of an ultrafast TDL oscillator.

While state-of-the-art ultrafast Yb-based TDL oscillators emit up to 300-W average power in pulses with hundreds of femtoseconds duration, a maximum of only 5 W has been achieved in pulses with sub-100-fs duration prior to this work. To date, Yb:YAG crystals are the standard gain element for ultrafast TDLs because they are commercially available in high quality and large disk diameters, but their gain bandwidth is a limit for the achievable pulse duration. Yb:LuO is one of the most promising gain material for high-power ultrashort-pulse operation since it features favorable thermo-mechanical properties and a 30% broader gain bandwidth

that directly supports sub-100-fs pulse formation. In this thesis, KLM TDLs based on Yb:LuO crystals are thoroughly investigated. The key laser parameters for the generation of sub-100-fs pulses have been investigated with more than 300 distinct laser configurations experimentally evaluated. The results highlight that operating at a small output coupling degree, with a low amount of inserted group delay dispersion and a small intra-cavity hard aperture allows for the shortest pulses. This extensive study is supplemented by a power scaling iteration, which is achieved by increasing the laser mode size on the Kerr medium. As a result, the laser delivers more than 10 W of average power in 90-fs pulses, which represents a two-fold increase of the average power emitted by ultrafast TDL oscillators at sub-100-fs pulses durations. Given the repetition rate of 60 MHz, the laser operating at 1040-nm central wavelength produces 0.2- $\mu$ J pulse energy and a peak power close to 2 MW. Additionally, by decreasing the output coupling rate and the amount of inserted group delay dispersion, up to 4.5 W of average power are emitted in 49-fs pulses. Further average- and peak-power scaling was discussed. It should lead to the direct generation of hundred-watt average power and tens of MW peak-power levels directly from simple and compact sub-100-fs TDL oscillators, without the need for external amplification and temporal compression, thus preserving an excellent spatio-temporal pulse profile. This outstanding performance hold great promises for ultrafast TDL oscillators to enable ground-breaking research in various areas such as nonlinear optics, high field science and high-precision spectroscopy.

Furthermore, KLM TDLs based on broadband gain materials strike new limits for the minimum pulse duration generated by TDL oscillators. A KLM Yb:LuO TDL delivers 1.6-W average power in 35-fs pulses, which is four times shorter than previously obtained from a SESAM mode-locked Yb:LuO TDLs and two times shorter than obtained in bulk Yb:LuO oscillators. Besides, the first KLM TDL based on an Yb:CALGO crystal is demonstrated. Beneficiating from the ultra-broad gain bandwidth offered by the gain material, the laser emits 150-mW in 30-fs pulses at 124-MHz repetition rate and 1050-nm central wavelength and achieves record-short pulse durations from TDL oscillators, which is equal to the shortest pulses produced by Yb-doped bulk lasers. It appears that in contrast to the standard end-pumping of bulk oscillators, the TDL pumping geometry does not limit the pulse spectrum on the short wavelength side. Yb-based TDLs combine advantages for ultrashort pulse generation and high-power operation, owing to the pumping geometry, low quantum defect and efficient heat removal from the gain material. Scaling the average power to several tens of watts with reasonable optical efficiencies and similar pulse durations was discussed. It will rely on high-optical-quality high-gain broadband disks and ultra-broadband optics. Indeed, the current

limitations mainly originate from the low laser gain and from the insufficient bandwidth of the intra-cavity components. Optimization of the optical coatings for a broadband high reflectivity and a flat dispersion is necessary to outperform the current results. While the 34-nm-FWHM optical spectrum of the 35-fs Yb:LuO TDL is nearly three times broader than the crystal gain bandwidth, the Yb:CALGO laser features a 45-nm FWHM optical spectrum that does not exploit the full ultra-broad gain bandwidth of Yb:CALGO. Consequently, further decreasing the pulse duration should be feasible and could result in few-cycle pulses directly emitted from diode-pumped Yb-based TDL oscillators.

Moreover, this thesis presents the first fully-stabilized optical frequency comb based on a TDL. The self-referenced fully-stabilized laser delivers more than 4-W output power in 50-fs pulses at a central wavelength of 1030 nm and a repetition rate of 61 MHz. A coherent octave-spanning supercontinuum is generated in a photonic crystal fiber using only few mW average power picked up from the laser output. The carrier-envelope offset (CEO) frequency is detected in a standard  $f$ -to- $2f$  interferometer and stabilized to an external radio-frequency reference by active feedback applied to the current driving the laser diode pump system. The repetition rate is detected with a photodetector and stabilized via a mirror mounted onto an intra-cavity piezo-electric actuator. A tight phase lock of the CEO frequency is achieved at 5 MHz leading to a residual in-loop phase noise of less than 200 mrad (integrated from 1 Hz to 1 MHz). The stabilization of the repetition rate leads to residual timing jitter of 7 ps (integrated from 1 Hz to 1 MHz) and was limited by the sub-optimal components used in this proof-of-concept experiment. Due to cross talks of the two stabilization loops, the phase noise of the CEO frequency was increased to 745 mrad for the fully-stabilized optical frequency comb. This initial experiment exploits the remarkable performance of the above-mentioned lasers that allow for CEO detection without any external compression and validates the suitability of sub-100-fs KLM TDL oscillators for metrology applications and high-precision spectroscopy.

Although state-of-the-art femtosecond TDL oscillators operate with up to GW intra-cavity peak power levels, their potential to drive intra-cavity nonlinear experiments has remained unexplored until now. A prominent application is the generation of coherent XUV light via high-harmonic generation (HHG) at megahertz repetition rate. In case of intra-cavity HHG, the unconverted photons are recycled inside the cavity, which increases the overall efficiency of the process, and high photon fluxes can be produced owing to the high intra-cavity driving-laser average power. The last part of the manuscript describes HHG driven inside a mode-

locked TDL oscillator. The XUV light is extracted with a sapphire plate placed under Brewster angle for the driving laser wavelength and harmonics up to the 17<sup>th</sup> order (60.8 nm, 20.4 eV) are detected. The photon flux is estimated to be  $\sim 2.6 \times 10^8$  photons/s for the 11<sup>th</sup> harmonic (94 nm, 13.2 eV). The TDL oscillator and the HHG setup are housed in a single vacuum chamber, resulting in a simple and compact system. Remarkably, the system is pumped with only 51 W of laser diode power. The driving SESAM mode-locked laser produces 250-fs pulses at a wavelength of 1034 nm and a repetition rate of 17 MHz in an environment evacuated down to  $10^{-4}$  mbar. HHG is driven in a high-pressure xenon gas jet with an intra-cavity peak intensity of  $2.9 \times 10^{13}$  W/cm<sup>2</sup> and an average power of 320 W, which leads to an intra-cavity peak power of about 60 MW. The noise properties of the near-infrared driving laser have been evaluated and no disturbance from the intra-cavity high-pressure gas jet and subsequent HHG was detected. Further scaling of the performance was discussed and will rely on improved laser parameters, better phase matching conditions and enhanced XUV output-coupling efficiency obtained from an AR-coated plate under a large angle of incidence. Since HHG is an extremely nonlinear process, several orders of magnitude higher photon fluxes and higher photon energies can be expected by upgrading the driving oscillator to, e.g., the KLM TDLs developed in the framework of this thesis, which already demonstrated substantially shorter pulse duration of 35-fs with an intra-cavity peak power of 70 MW in air. Owing to the fact that HHG is a coherent process, the full frequency stabilization of the driving laser should lead to the generation of an XUV frequency comb from a simple and compact setup. This experiment confirms the benefits of using an ultrafast TDL oscillator for intra-cavity HHG at megahertz repetition rates. Such a class of compact and simple coherent-XUV-light sources will be highly attractive for driving numerous applications ranging from high-precision spectroscopy to attosecond science and high-resolution imaging.

# References

1. W. Sibbett, A. A. Lagatsky, and C. T. A. Brown, "The development and application of femtosecond laser systems," *Opt. Express* **20**(7), 6989 (2012).
2. C. Kränkel, "Rare-Earth-Doped Sesquioxides for Diode-Pumped High-Power Lasers in the 1-, 2-, and 3- $\mu$ m Spectral Range," *IEEE J. Sel. Top. Quantum Electron.* **21**(1), 250 (2015).
3. B. Köhler, T. Brand, M. Haag, and J. Biesenbach, "Wavelength stabilized high-power diode laser modules," *Proc SPIE* **7198**, 719810 (2009).
4. Martin Saraceno, contact: martin@saraceno.info.
5. W. S. Brocklesby, "Progress in high average power ultrafast lasers," *Eur. Phys. J. Spec. Top.* **224**(13), 2529 (2015).
6. A. Giesen, H. Hügel, A. Voss, K. Wittig, U. Brauch, and H. Opower, "Scalable concept for diode-pumped high-power solid-state lasers," *Appl. Phys. B Lasers Opt.* **58**(5), 365 (1994).
7. A. Giesen and J. Speiser, "Fifteen Years of Work on Thin-Disk Lasers: Results and Scaling Laws," *IEEE J. Sel. Top. Quantum Electron.* **13**(3), 598 (2007).
8. D. Bauer, I. Zawischa, D. H. Sutter, A. Killi, and T. Dekorsy, "Mode-locked Yb:YAG thin-disk oscillator with 41  $\mu$ J pulse energy at 145 W average infrared power and high power frequency conversion," *Opt. Express* **20**(9), 9698 (2012).
9. H. Fattahi, H. G. Barros, M. Gorjan, T. Nubbemeyer, B. Alsaif, C. Y. Teisset, M. Schultze, S. Prinz, M. Haefner, M. Ueffing, A. Alismail, L. Vámos, A. Schwarz, O. Pronin, J. Brons, X. T. Geng, G. Arisholm, M. Ciappina, V. S. Yakovlev, D.-E. Kim, A. M. Azzeer, N. Karpowicz, D. Sutter, Z. Major, T. Metzger, and F. Krausz, "Third-generation femtosecond technology," *Optica* **1**(1), 45 (2014).
10. S.-S. Schad, T. Gottwald, V. Kuhn, M. Ackermann, D. Bauer, M. Scharun, and A. Killi, "Recent development of disk lasers at TRUMPF," *Proc SPIE* **9726**, 972615 (2016).
11. B. Deppe, G. Huber, C. Kränkel, and J. Küpper, "High-intracavity-power thin-disk laser for the alignment of molecules," *Opt. Express* **23**(22), 28491 (2015).
12. T. Gottwald, V. Kuhn, S.-S. Schad, C. Stolzenburg, and A. Killi, "Recent developments in high power thin disk lasers at TRUMPF Laser," *Proc SPIE* **8898**, 88980P (2013).
13. J.-P. Negel, A. Loescher, A. Voss, D. Bauer, D. Sutter, A. Killi, M. A. Ahmed, and T. Graf, "Ultrafast thin-disk multipass laser amplifier delivering 1.4 kW (47 mJ, 1030 nm) average power converted to 820 W at 515 nm and 234 W at 343 nm," *Opt. Express* **23**(16), 21064 (2015).
14. J.-P. Negel, A. Loescher, B. Dannecker, P. Oldorf, S. Reichel, R. Peters, M. A. Ahmed, and T. Graf, "Thin-disk multipass amplifier for fs pulses delivering 400 W of average and 2.0 GW of peak power for linear polarization as well as 235 W and 1.2 GW for radial polarization," *Appl. Phys. B* **123**(5), 156 (2017).
15. J. A. der Au, G. J. Spühler, T. Südmeyer, R. Paschotta, R. Hövel, M. Moser, S. Erhard, M. Karszewski, A. Giesen, and U. Keller, "16.2-W average power from a diode-pumped femtosecond Yb:YAG thin disk laser," *Opt. Lett.* **25**(11), 859 (2000).
16. C. J. Saraceno, F. Emaury, C. Schriber, A. Diebold, M. Hoffmann, M. Golling, T. Südmeyer, and U. Keller, "Toward Millijoule-Level High-Power Ultrafast Thin-Disk Oscillators," *IEEE J. Sel. Top. Quantum Electron.* **21**(1), 106 (2015).
17. A. Diebold, T. Zengerle, C. G. E. Alfieri, C. Schriber, F. Emaury, M. Mangold, M. Hoffmann, C. J. Saraceno, M. Golling, D. Follman, G. D. Cole, M. Aspelmeyer, T. Südmeyer, and U. Keller, "Optimized SESAMs for kilowatt-level ultrafast lasers," *Opt. Express* **24**(10), 10512 (2016).
18. C. J. Saraceno, F. Emaury, O. H. Heckl, C. R. E. Baer, M. Hoffmann, C. Schriber, M. Golling, T. Südmeyer, and U. Keller, "275 W average output power from a femtosecond thin disk oscillator operated in a vacuum environment," *Opt. Express* **20**(21), 23535 (2012).
19. J. Brons, V. Pervak, E. Fedulova, D. Bauer, D. Sutter, V. Kalashnikov, A. Apolonskiy, O. Pronin, and F. Krausz, "Energy scaling of Kerr-lens mode-locked thin-disk oscillators," *Opt. Lett.* **39**(22), 6442 (2014).

## References

---

20. C. J. Saraceno, F. Emaury, C. Schriber, M. Hoffmann, M. Golling, T. Südmeyer, and U. Keller, "Ultrafast thin-disk laser with 80  $\mu$ J pulse energy and 242 W of average power," *Opt. Lett.* **39**(1), 9 (2014).
21. T. Südmeyer, S. V. Marchese, S. Hashimoto, C. R. E. Baer, G. Gingras, B. Witzel, and U. Keller, "Femtosecond laser oscillators for high-field science," *Nat. Photonics* **2**(10), 599 (2008).
22. I. Pupeza, D. Sánchez, J. Zhang, N. Lilienfein, M. Seidel, N. Karpowicz, T. Paasch-Colberg, I. Znakovskaya, M. Pescher, W. Schweinberger, V. Pervak, E. Fill, O. Pronin, Z. Wei, F. Krausz, A. Apolonski, and J. Biegert, "High-power sub-two-cycle mid-infrared pulses at 100 MHz repetition rate," *Nat. Photonics* **9**(11), 721 (2015).
23. F. Emaury, A. Diebold, C. J. Saraceno, and U. Keller, "Compact extreme ultraviolet source at megahertz pulse repetition rate with a low-noise ultrafast thin-disk laser oscillator," *Optica* **2**(11), 980 (2015).
24. C. J. Saraceno, O. H. Heckl, C. R. E. Baer, C. Schriber, M. Golling, K. Beil, C. Kränkel, T. Südmeyer, G. Huber, and U. Keller, "Sub-100 femtosecond pulses from a SESAM modelocked thin disk laser," *Appl. Phys. B* **106**(3), 559 (2012).
25. A. Diebold, F. Emaury, C. Schriber, M. Golling, C. J. Saraceno, T. Südmeyer, and U. Keller, "SESAM mode-locked Yb:CaGdAlO<sub>4</sub> thin disk laser with 62 fs pulse generation," *Opt. Lett.* **38**(19), 3842 (2013).
26. O. Pronin, J. Brons, C. Grasse, V. Pervak, G. Boehm, M.-C. Amann, V. L. Kalashnikov, A. Apolonski, and F. Krausz, "High-power 200 fs Kerr-lens mode-locked Yb:YAG thin-disk oscillator," *Opt. Lett.* **36**(24), 4746 (2011).
27. C. J. Saraceno, O. H. Heckl, C. R. Baer, M. Golling, T. Südmeyer, K. Beil, C. Kränkel, K. Petermann, G. Huber, and U. Keller, "SESAMs for high-power femtosecond modelocking: power scaling of an Yb:LuScO<sub>3</sub> thin disk laser to 23 W and 235 fs," *Opt. Express* **19**(21), 20288 (2011).
28. S. Ricaud, A. Jaffres, K. Wentsch, A. Suganuma, B. Viana, P. Loiseau, B. Weichelt, M. Abdou-Ahmed, A. Voss, T. Graf, D. Rytz, C. Hönninger, E. Mottay, P. Georges, and F. Druon, "Femtosecond Yb:CaGdAlO<sub>4</sub> thin-disk oscillator," *Opt. Lett.* **37**(19), 3984 (2012).
29. C. J. Saraceno, C. Schreiber, O. H. Heckl, C. R. E. Baer, M. Golling, K. Beil, C. Kränkel, T. Südmeyer, G. Huber, and U. Keller, "25 W, 185 fs pulses from an Yb:Lu<sub>2</sub>O<sub>3</sub> modelocked thin disk laser," presented at Europhoton, Stockholm, Sweden, 2012.
30. C. J. Saraceno, S. Pekarek, O. H. Heckl, C. R. E. Baer, C. Schriber, M. Golling, K. Beil, C. Kränkel, G. Huber, U. Keller, and T. Südmeyer, "Self-referenceable frequency comb from an ultrafast thin disk laser," *Opt. Express* **20**(9), 9650 (2012).
31. C. Schriber, F. Emaury, A. Diebold, S. Link, M. Golling, K. Beil, C. Kränkel, C. J. Saraceno, T. Südmeyer, and U. Keller, "Dual-gain SESAM modelocked thin disk laser based on Yb:Lu<sub>2</sub>O<sub>3</sub> and Yb:Sc<sub>2</sub>O<sub>3</sub>," *Opt. Express* **22**(16), 18979 (2014).
32. C. Schriber, L. Merceron, A. Diebold, F. Emaury, M. Golling, K. Beil, C. Kränkel, C. J. Saraceno, T. Südmeyer, and U. Keller, "Pushing SESAM modelocked thin-disk lasers to shortest pulse durations," in *Advanced Solid State Lasers* (Optical Society of America, 2014), paper AF1A.4.
33. J. Zhang, J. Brons, M. Seidel, V. Pervak, V. Kalashnikov, Z. Wei, A. Apolonski, F. Krausz, and O. Pronin, "49-fs Yb:YAG thin-disk oscillator with distributed Kerr-lens mode-locking," in *European Quantum Electronics Conference* (Optical Society of America, 2015), paper PD\_A\_1.
34. J. Brons, V. Pervak, D. Bauer, D. Sutter, O. Pronin, and F. Krausz, "Powerful 100-fs-scale Kerr-lens mode-locked thin-disk oscillator," *Opt. Lett.* **41**(15), 3567 (2016).
35. U. Keller, K. J. Weingarten, F. X. Kärtner, D. Kopf, B. Braun, I. D. Jung, R. Fluck, C. Hönninger, N. Matuschek, and J. Aus der Au, "Semiconductor Saturable Absorber Mirrors (SESAM's) for Femtosecond to Nanosecond Pulse Generation in Solid-State Lasers," *IEEE J. Sel. Top. Quantum Electron.* **2**(3), 435 (1996).
36. R. Paschotta and U. Keller, "Passive mode locking with slow saturable absorbers," *Appl. Phys. B* **73**(7), 653 (2001).
37. F. X. Kärtner, I. D. Jung, and U. Keller, "Soliton mode-locking with saturable absorbers," *IEEE J. Sel. Top. Quantum Electron.* **2**(3), 540 (1996).
38. E. R. Thoen, E. M. Koontz, M. Joschko, P. Langlois, T. R. Schibli, F. X. Kärtner, E. P. Ippen, and L. A. Kolodziejski, "Two-photon absorption in semiconductor saturable absorber mirrors," *Appl. Phys. Lett.* **74**(26), 3927 (1999).

- 
39. R. Grange, M. Haiml, R. Paschotta, G. J. Spühler, L. Krainer, M. Golling, O. Ostinelli, and U. Keller, "New regime of inverse saturable absorption for self-stabilizing passively mode-locked lasers," *Appl. Phys. B* **80**(2), 151 (2005).
  40. S. V. Marchese, C. R. Baer, A. G. Engqvist, S. Hashimoto, D. J. Maas, M. Golling, T. Südmeyer, and U. Keller, "Femtosecond thin disk laser oscillator with pulse energy beyond the 10-microjoule level," *Opt. Express* **16**(9), 6397 (2008).
  41. D. E. Spence, P. N. Kean, and W. Sibbett, "60-fsec pulse generation from a self-mode-locked Ti:sapphire laser," *Opt. Lett.* **16**(1), 42 (1991).
  42. T. Brabec, C. Spielmann, P. F. Curley, and F. Krausz, "Kerr lens mode locking," *Opt. Lett.* **17**(18), 1292 (1992).
  43. H. A. Haus, "Theory of mode locking with a fast saturable absorber," *J. Appl. Phys.* **46**(7), 3049 (1975).
  44. J. Zhang, K. F. Mak, S. Gröbmeyer, D. Bauer, D. Sutter, V. Pervak, F. Krausz, and O. Pronin, "Generation of 220 fs, 20 W pulses at 2  $\mu\text{m}$  from Kerr-lens mode-locked Ho: YAG thin-disk oscillator," in *CLEO: Science and Innovations* (Optical Society of America, 2017), paper SM11-6.
  45. G. Cerullo, S. D. Silvestri, V. Magni, and L. Pallaro, "Resonators for Kerr-lens mode-locked femtosecond Ti:sapphire lasers," *Opt. Lett.* **19**(11), 807 (1994).
  46. I. P. Christov and V. D. Stoev, "Kerr-lens mode-locked laser model: role of space time effects," *JOSA B* **15**(7), 1960 (1998).
  47. T. Südmeyer, C. Kränkel, C. R. E. Baer, O. H. Heckl, C. J. Saraceno, M. Golling, R. Peters, K. Petermann, G. Huber, and U. Keller, "High-power ultrafast thin disk laser oscillators and their potential for sub-100-femtosecond pulse generation," *Appl. Phys. B* **97**(2), 281 (2009).
  48. P. Sévillano, G. Machinet, R. Dubrasquet, P. Camy, J.-L. Doualan, R. Moncorge, P. Georges, F. P. Druon, D. Descamps, and E. Cormier, "Sub-50 fs, Kerr-lens mode-locked Yb:CaF<sub>2</sub> laser oscillator delivering up to 2.7 W," in *Advanced Solid-State Lasers Congress (2013), Paper AF3A.6* (Optical Society of America, 2013), paper AF3A.6.
  49. J. Ma, H. Huang, K. Ning, X. Xu, G. Xie, L. Qian, K. P. Loh, and D. Tang, "Generation of 30 fs pulses from a diode-pumped graphene mode-locked Yb:CaYAlO<sub>4</sub> laser," *Opt. Lett.* **41**(5), 890 (2016).
  50. F. Druon, F. Balembois, P. Georges, A. Brun, A. Courjaud, C. Hönniger, F. Salin, A. Aron, F. Mougel, G. Aka, and others, "Generation of 90-fs pulses from a mode-locked diode-pumped Yb<sup>3+</sup>:Ca<sub>4</sub>GdO(BO<sub>3</sub>)<sub>3</sub> laser," *Opt. Lett.* **25**(6), 423 (2000).
  51. H. Liu, J. Nees, and G. Mourou, "Diode-pumped Kerr-lens mode-locked Yb:KY(WO<sub>4</sub>)<sub>2</sub> laser," *Opt Lett* **26**(21), 1723 (2001).
  52. F. Druon, S. Chenais, P. Raybaut, F. Balembois, P. Georges, R. Gaume, G. Aka, B. Viana, S. Mohr, and D. Kopf, "Diode-pumped Yb: Sr<sub>3</sub>Y(BO<sub>3</sub>)<sub>3</sub> femtosecond laser," *Opt. Lett.* **27**(3), 197 (2002).
  53. A. A. Lagatsky, A. R. Sarmani, C. T. A. Brown, W. Sibbett, V. E. Kisel, A. G. Selivanov, I. A. Denisov, A. E. Troshin, K. V. Yumashev, N. V. Kuleshov, V. N. Matrosov, T. A. Matrosova, and M. I. Kupchenko, "Yb<sup>3+</sup>-doped YVO<sub>4</sub> crystal for efficient Kerr-lens mode locking in solid-state lasers," *Opt. Lett.* **30**(23), 3234 (2005).
  54. Y. Zaouter, J. Didierjean, F. Balembois, G. L. Leclin, F. Druon, P. Georges, J. Petit, P. Goldner, and B. Viana, "47-fs diode-pumped Yb<sup>3+</sup>:CaGdAlO<sub>4</sub> laser," *Opt. Lett.* **31**(1), 119 (2006).
  55. A. Yoshida, A. Schmidt, H. Zhang, J. Wang, J. Liu, C. Fiebig, K. Paschke, G. Erbert, V. Petrov, and U. Griebner, "42-fs diode-pumped Yb:Ca<sub>4</sub>YO(BO<sub>3</sub>)<sub>3</sub> oscillator," *Opt. Express* **18**(23), 24325 (2010).
  56. A. Yoshida, A. Schmidt, V. Petrov, C. Fiebig, G. Erbert, J. Liu, H. Zhang, J. Wang, and U. Griebner, "Diode-pumped mode-locked Yb:YCOB laser generating 35 fs pulses," *Opt. Lett.* **36**(22), 4425 (2011).
  57. P. Sévillano, P. Georges, F. Druon, D. Descamps, and E. Cormier, "32-fs Kerr-lens mode-locked Yb:CaGdAlO<sub>4</sub> oscillator optically pumped by a bright fiber laser," *Opt. Lett.* **39**(20), 6001 (2014).
  58. F. Brunner, T. Südmeyer, E. Innerhofer, F. Morier-Genoud, R. Paschotta, V. E. Kisel, V. G. Shcherbitsky, N. V. Kuleshov, J. Gao, K. Contag, A. Giesen, and U. Keller, "240-fs pulses with 22-W average power from a mode-locked thin-disk Yb:KY(WO<sub>4</sub>)<sub>2</sub> laser," *Opt. Lett.* **27**(13), 1162 (2002).
  59. C. R. E. Baer, C. Kränkel, O. H. Heckl, M. Golling, T. Südmeyer, R. Peters, K. Petermann, G. Huber, and U. Keller, "227-fs pulses from a mode-locked Yb:LuScO<sub>3</sub> thin disk laser," *Opt. Express* **17**(13), 10725 (2009).

## References

---

60. R. C. Linares, "Growth of garnet laser crystals," *Solid State Commun.* **2**(8), 229 (1964).
61. R. Uecker, "The historical development of the Czochralski method," *J. Cryst. Growth* **401**(Supplement C), 7 (2014).
62. S. Uemura and K. Torizuka, "Sub-40-fs Pulses from a Diode-Pumped Kerr-Lens Mode-Locked Yb-Doped Yttrium Aluminum Garnet Laser," *Jpn. J. Appl. Phys.* **50**, 010201 (2011).
63. M. Tokurakawa and A. Shirakawa, "Numerical analysis of fast saturable absorber mode-locked Yb<sup>3+</sup> lasers under large modulation depth," *Opt. Express* **23**(20), 26288 (2015).
64. E. Innerhofer, T. Südmeyer, F. Brunner, R. Häring, A. Aschwanden, R. Paschotta, C. Hönninger, M. Kumkar, and U. Keller, "60-W average power in 810-fs pulses from a thin-disk Yb: YAG laser," *Opt. Lett.* **28**(5), 367 (2003).
65. F. Brunner, E. Innerhofer, S. V. Marchese, T. Südmeyer, R. Paschotta, T. Usami, H. Ito, S. Kurimura, K. Kitamura, G. Arisholm, and U. Keller, "Powerful red-green-blue laser source pumped with a mode-locked thin disk laser," *Opt. Lett.* **29**(16), 1921 (2004).
66. N. Kanda, A. A. Eilanlou, T. Imahoko, T. Sumiyoshi, Y. Nabekawa, M. Kuwata-Gonokami, and K. Midorikawa, "High-Pulse-Energy Yb: YAG Thin Disk Mode-Locked Oscillator for Intra-Cavity High Harmonic Generation," in *Advanced Solid State Lasers* (Optical Society of America, 2013), paper AF3A–8.
67. K. Hasse, T. Calmano, B. Deppe, C. Liebald, and C. Kränkel, "Efficient Yb<sup>3+</sup>:CaGdAlO<sub>4</sub> bulk and femtosecond-laser-written waveguide lasers," *Opt. Lett.* **40**(15), 3552 (2015).
68. C. R. E. Baer, C. Kränkel, C. J. Saraceno, O. H. Heckl, M. Golling, R. Peters, K. Petermann, T. Südmeyer, G. Huber, and U. Keller, "Femtosecond thin-disk laser with 141 W of average power," *Opt. Lett.* **35**(13), 2302 (2010).
69. B. Kreipe, J. Andrade, B. Deppe, C. Kränkel, and U. Morgner, "Kerr-lens mode-locked Yb<sup>3+</sup>:Lu<sub>2</sub>O<sub>3</sub> thin-disk laser," in *Conference on Lasers and Electro-Optics* (Optical Society of America, 2016), paper SM11.4.
70. R. Peters, C. Kränkel, K. Petermann, and G. Huber, "Broadly tunable high-power Yb:Lu<sub>2</sub>O<sub>3</sub> thin disk laser with 80% slope efficiency," *Opt. Express* **15**(11), 7075 (2007).
71. J. Petit, P. Goldner, and B. Viana, "Laser emission with low quantum defect in Yb:CaGdAlO<sub>4</sub>," *Opt. Lett.* **30**(11), 1345 (2005).
72. J. Boudeile, F. Druon, M. Hanna, P. Georges, Y. Zaouter, E. Cormier, J. Petit, P. Goldner, and B. Viana, "Continuous-wave and femtosecond laser operation of Yb:CaGdAlO<sub>4</sub> under high-power diode pumping," *Opt. Lett.* **32**(14), 1962 (2007).
73. W. Sibbett, A. A. Lagatsky, and C. T. A. Brown, "The development and application of femtosecond laser systems," *Opt. Express* **20**(7), 6989 (2012).
74. B. Weichelt, A. Voss, M. A. Ahmed, and T. Graf, "Enhanced performance of thin-disk lasers by pumping into the zero-phonon line," *Opt. Lett.* **37**(15), 3045 (2012).
75. R. Peters, C. Kränkel, S. T. Fredrich-Thornton, K. Beil, K. Petermann, G. Huber, O. H. Heckl, C. R. E. Baer, C. J. Saraceno, T. Südmeyer, and U. Keller, "Thermal analysis and efficient high power continuous-wave and mode-locked thin disk laser operation of Yb-doped sesquioxides," *Appl. Phys. B* **102**(3), 509 (2011).
76. R. Peters, C. Kränkel, K. Petermann, and G. Huber, "Crystal growth by the heat exchanger method, spectroscopic characterization and laser operation of high-purity Yb:Lu<sub>2</sub>O<sub>3</sub>," *J. Cryst. Growth* **310**(7–9), 1934 (2008).
77. S. Kitajima, Hi. Nakao, A. Shirakawa, Hi. Yagi, and T. Yanagitani, "CW Performance and Temperature Observation of Yb:Lu<sub>2</sub>O<sub>3</sub> Ceramic Thin-Disk Laser," in *Laser Congress 2017 (ASSL, LAC) (2017)* (Optical Society of America, 2017), paper JM5A.32.
78. A. M. Heuer, C. J. Saraceno, K. Beil, G. Huber, and C. Kränkel, "Efficient OPSSL-pumped mode-locked Yb:Lu<sub>2</sub>O<sub>3</sub> laser with 67% optical-to-optical efficiency," *Sci. Rep.* **6**, 19090 (2016).
79. M. Tokurakawa, A. Shirakawa, K. Ueda, H. Yagi, S. Hosokawa, T. Yanagitani, and A. A. Kaminskii, "Diode-pumped 65 fs Kerr-lens mode-locked Yb<sup>3+</sup>:Lu<sub>2</sub>O<sub>3</sub> and nondoped Y<sub>2</sub>O<sub>3</sub> combined ceramic laser," *Opt. Lett.* **33**(12), 1380 (2008).
80. M. Tokurakawa, A. Shirakawa, K. Ueda, R. Peters, S. T. Fredrich-Thornton, K. Petermann, and G. Huber, "Ultrashort pulse generation from diode pumped mode-locked Yb<sup>3+</sup>:sesquioxide single crystal lasers," *Opt. Express* **19**(4), 2904 (2011).



- 
81. B. Weichelt, K. S. Wentsch, A. Voss, M. A. Ahmed, and T. Graf, "A 670 W Yb:Lu<sub>2</sub>O<sub>3</sub> thin-disk laser," *Laser Phys. Lett.* **9**(2), 110 (2012).
  82. S. V. Marchese, C. R. E. Baer, R. Peters, C. Kränkel, A. G. Engqvist, M. Golling, D. J. H. C. Maas, K. Petermann, T. Südmeyer, G. Huber, and U. Keller, "Efficient femtosecond high power Yb:Lu<sub>2</sub>O<sub>3</sub> thin disk laser," *Opt. Express* **15**(25), 16966 (2007).
  83. C. R. Baer, C. Kränkel, C. J. Saraceno, O. H. Heckl, M. Golling, T. Südmeyer, R. Peters, K. Petermann, G. Huber, and U. Keller, "Femtosecond Yb:Lu<sub>2</sub>O<sub>3</sub> thin disk laser with 63 W of average power," *Opt. Lett.* **34**(18), 2823 (2009).
  84. U. Griebner, V. Petrov, K. Petermann, and V. Peters, "Passively mode-locked Yb:Lu<sub>2</sub>O<sub>3</sub> laser," *Opt. Express* **12**(14), 3125 (2004).
  85. C. J. Saraceno, C. Schreiber, O. H. Heckl, C. R. E. Baer, M. Golling, K. Beil, C. Kränkel, T. Südmeyer, G. Huber, and U. Keller, "25 W, 185 fs pulses from an Yb:Lu<sub>2</sub>O<sub>3</sub> modelocked thin disk laser," presented at Europhoton, Stockholm, Sweden, 2012.
  86. A.-L. Calendron, H. Çankaya, G. Cirmi, and F. X. Kärtner, "White-light generation with sub-ps pulses," *Opt. Express* **23**(11), 13866 (2015).
  87. E. T. J. Nibbering, G. Grillon, M. A. Franco, B. S. Prade, and A. Mysyrowicz, "Determination of the inertial contribution to the nonlinear refractive index of air, N<sub>2</sub>, and O<sub>2</sub> by use of unfocused high-intensity femtosecond laser pulses," *J. Opt. Soc. Am. B* **14**(3), 650 (1997).
  88. F. X. Kärtner, J. A. der Au, and U. Keller, "Mode-locking with slow and fast saturable absorbers-what's the difference?," *IEEE J. Sel. Top. Quantum Electron.* **4**(2), 159 (1998).
  89. H. A. Haus, "Mode-locking of lasers," *IEEE J. Sel. Top. Quantum Electron.* **6**(6), 1173 (2000).
  90. J. Brons, "High-power femtosecond laser-oscillators for applications in high-field physics," PhD Thesis, Ludwig-Maximilians-Universität München (2017).
  91. J. Brons, V. Pervak, E. Fedulova, D. Bauer, D. Sutter, V. Kalashnikov, A. Apolonskiy, O. Pronin, and F. Krausz, "Energy scaling of Kerr-lens mode-locked thin-disk oscillators," *Opt. Lett.* **39**(22), 6442 (2014).
  92. J. Herrmann, V. P. Kalosha, and M. Müller, "Higher-order phase dispersion in femtosecond Kerr-lens mode-locked solid-state lasers: sideband generation and pulse splitting," *Opt. Lett.* **22**(4), 236 (1997).
  93. S. Uemura and K. Torizuka, "Sub-40-fs Pulses from a Diode-Pumped Kerr-Lens Mode-Locked Yb-Doped Yttrium Aluminum Garnet Laser," *Jpn. J. Appl. Phys.* **50**, 010201 (2011).
  94. D. Bauer, I. Zawischa, D. H. Sutter, A. Killi, and T. Dekorsy, "Mode-locked Yb:YAG thin-disk oscillator with 41 µJ pulse energy at 145 W average infrared power and high power frequency conversion," *Opt. Express* **20**(9), 9698 (2012).
  95. S. V. Marchese, T. Südmeyer, M. Golling, R. Grange, and U. Keller, "Pulse energy scaling to 5 µJ from a femtosecond thin disk laser," *Opt. Lett.* **31**(18), 2728 (2006).
  96. M. Poetzlberger, J. Brons, J. Zhang, D. Bauer, D. Sutter, F. Krausz, and O. Pronin, "Towards Active Multi-pass Kerr-lens Mode-locked Yb:YAG Thin-disk Oscillators," in *CLEO Europe - EQEC 2017* (Optical Society of America, 2017), paper ca-7-2.
  97. I. J. Graumann, A. Diebold, C. G. E. Alfieri, F. Emaury, B. Deppe, M. Golling, D. Bauer, D. Sutter, C. Kränkel, C. J. Saraceno, C. R. Phillips, and U. Keller, "Peak-power scaling of femtosecond Yb:Lu<sub>2</sub>O<sub>3</sub> thin-disk lasers," *Opt. Express* **25**(19), 22519 (2017).
  98. J. Savolainen, S. Ahmed, and P. Hamm, "Two-dimensional Raman-terahertz spectroscopy of water," *Proc. Natl. Acad. Sci.* **110**(51), 20402 (2013).
  99. T. Petersen, J. D. Zuegel, and J. Bromage, "High-average-power, 2-µm femtosecond optical parametric oscillator synchronously pumped by a thin-disk, mode-locked laser," *Opt. Express* **25**(8), 8840 (2017).
  100. O. Pronin, M. Seidel, F. Lücking, J. Brons, E. Fedulova, M. Trubetskov, V. Pervak, A. Apolonski, T. Udem, and F. Krausz, "High-power multi-megahertz source of waveform-stabilized few-cycle light," *Nat. Commun.* **6**, 6988 (2015).
  101. D. T. Reid, C. M. Heyl, R. R. Thomson, R. Trebino, G. Steinmeyer, H. H. Fielding, R. Holzwarth, Z. Zhang, P. Del'Haye, T. Südmeyer, G. Mourou, T. Tajima, D. Faccio, F. J. M. Harren, and G. Cerullo, "Roadmap on ultrafast optics," *J. Opt.* **18**(9), 093006 (2016).

## References

---

102. U. Keller, "Ultrafast solid-state laser oscillators: a success story for the last 20 years with no end in sight," *Appl. Phys. B* **100**(1), 15 (2010).
103. P. Loiko, F. Druon, P. Georges, B. Viana, and K. Yumashev, "Thermo-optic characterization of Yb:CaGdAlO<sub>4</sub> laser crystal," *Opt. Mater. Express* **4**(11), 2241 (2014).
104. P. Loiko, J. M. Serres, X. Mateos, X. Xu, J. Xu, V. Jambunathan, P. Navratil, A. Lucianetti, T. Mocek, X. Zhang, U. Griebner, V. Petrov, M. Aguilo, F. Diaz, and A. Major, "Microchip Yb:CaLnAlO<sub>4</sub> lasers with up to 91% slope efficiency," *Opt. Lett.* **42**(13), 2431 (2017).
105. A. Greborio, A. Guandalini, and J. Aus der Au, "Sub-100 fs pulses with 12.5-W from Yb:CALGO based oscillators," *Proc SPIE* **8235**, 823511 (2012).
106. K. Beil, B. Deppe, and C. Kränkel, "Yb:CaGdAlO<sub>4</sub> thin-disk laser with 70% slope efficiency and 90 nm wavelength tuning range," *Opt. Lett.* **38**(11), 1966 (2013).
107. F. P. Druon, S. Ricaud, A. Jaffrès, K. S. Wentsch, A. Sukanuma, P. Loiseau, B. Weichelt, M. A. Ahmed, A. Voss, T. Graf, and others, "High power cw and fs Yb:CALGO thin-disk laser using diamond heat spreader," in *Advanced Solid State Lasers* (Optical Society of America, 2013), paper AF3A–7.
108. A. Agnesi, A. Greborio, F. Pirzio, G. Reali, J. Aus der Au, and A. Guandalini, "40-fs Yb<sup>3+</sup>:CaGdAlO<sub>4</sub> laser pumped by a single-mode 350-mW laser diode," *Opt. Express* **20**(9), 10077 (2012).
109. D. N. Papadopoulos, F. Druon, J. Boudeile, I. Martial, M. Hanna, P. Georges, P. O. Petit, P. Goldner, and B. Viana, "Low-repetition-rate femtosecond operation in extended-cavity mode-locked Yb:CALGO laser," *Opt. Lett.* **34**(2), 196 (2009).
110. J. Brons, V. Pervak, E. Fedulova, M. Seidel, D. Bauer, D. Sutter, V. Kalashnikov, A. Apolonskiy, O. Pronin, and F. Krausz, "High power Kerr-lens mode-locking of Yb:YAG and Yb:CALGO thin-disk oscillators," in *Advanced Solid State Lasers* (Optical Society of America, 2014), paper AF1A–5.
111. J. Zehetner, C. Spielmann, and F. Krausz, "Passive mode locking of homogeneously and inhomogeneously broadened lasers," *Opt. Lett.* **17**(12), 871 (1992).
112. F. Druon, M. Olivier, A. Jaffrès, P. Loiseau, N. Aubry, J. DidierJean, F. Balembos, B. Viana, and P. Georges, "Magic mode switching in Yb:CaGdAlO<sub>4</sub> laser under high pump power," *Opt. Lett.* **38**(20), 4138 (2013).
113. S. Ricaud, A. Jaffrès, P. Loiseau, B. Viana, B. Weichelt, M. Abdou-Ahmed, A. Voss, T. Graf, D. Rytz, M. Delaigue, E. Mottay, P. Georges, and F. Druon, "Yb:CaGdAlO<sub>4</sub> thin-disk laser," *Opt. Lett.* **36**(21), 4134 (2011).
114. H. R. Telle, G. Steinmeyer, A. E. Dunlop, J. Stenger, D. H. Sutter, and U. Keller, "Carrier-envelope offset phase control: A novel concept for absolute optical frequency measurement and ultrashort pulse generation," *Appl. Phys. B* **69**(4), 327 (1999).
115. D. J. Jones, S. A. Diddams, J. K. Ranka, A. Stentz, R. S. Windeler, J. L. Hall, and S. T. Cundiff, "Carrier-Envelope Phase Control of Femtosecond Mode-Locked Lasers and Direct Optical Frequency Synthesis," *Science* **288**(5466), 635 (2000).
116. A. Apolonski, A. Poppe, G. Tempea, C. Spielmann, T. Udem, R. Holzwarth, T. W. Hänsch, and F. Krausz, "Controlling the Phase Evolution of Few-Cycle Light Pulses," *Phys. Rev. Lett.* **85**(4), 740 (2000).
117. N. R. Newbury, "Searching for applications with a fine-tooth comb," *Nat. Photonics* **5**(4), 186 (2011).
118. S. Schiller, "Spectrometry with frequency combs," *Opt. Lett.* **27**(9), 766 (2002).
119. S. A. Diddams, L. Hollberg, and V. Mbele, "Molecular fingerprinting with the resolved modes of a femtosecond laser frequency comb," *Nature* **445**(7128), 627 (2007).
120. Jun Ye, H. Schnatz, and L. W. Hollberg, "Optical frequency combs: From frequency metrology to optical phase control," *IEEE J. Sel. Top. Quantum Electron.* **9**(4), 1041 (2003).
121. S. A. Diddams, T. Udem, J. C. Bergquist, E. A. Curtis, R. E. Drullinger, L. Hollberg, W. M. Itano, W. D. Lee, C. W. Oates, K. R. Vogel, and D. J. Wineland, "An Optical Clock Based on a Single Trapped 199Hg<sup>+</sup> Ion," *Science* **293**(5531), 825 (2001).
122. U. Sterr, C. Degenhardt, H. Stoehr, C. Lisdat, H. Schnatz, J. Helmcke, F. Riehle, G. Wilpers, C. Oates, and L. Hollberg, "The optical calcium frequency standards of PTB and NIST," *Comptes Rendus Phys.* **5**(8), 845 (2004).
123. T. W. Hänsch, "Nobel Lecture: Passion for precision," *Rev. Mod. Phys.* **78**(4), 1297 (2006).

- 
124. J. L. Hall, "Nobel Lecture: Defining and measuring optical frequencies," *Rev. Mod. Phys.* **78**(4), 1279 (2006).
  125. S. Schilt and T. Südmeyer, "Carrier-Envelope Offset Stabilized Ultrafast Diode-Pumped Solid-State Lasers," *Appl. Sci.* **5**(4), 787 (2015).
  126. J. M. Dudley, G. Genty, and S. Coen, "Supercontinuum generation in photonic crystal fiber," *Rev. Mod. Phys.* **78**(4), 1135 (2006).
  127. T. Popmintchev, M.-C. Chen, P. Arpin, M. M. Murnane, and H. C. Kapteyn, "The attosecond nonlinear optics of bright coherent X-ray generation," *Nat. Photonics* **4**(12), 822 (2010).
  128. F. Krausz and M. Ivanov, "Attosecond physics," *Rev. Mod. Phys.* **81**(1), 163 (2009).
  129. A. Ozawa, J. Rauschenberger, C. Gohle, M. Herrmann, D. R. Walker, V. Pervak, A. Fernandez, R. Graf, A. Apolonski, R. Holzwarth, F. Krausz, T. W. Hänsch, and T. Udem, "High Harmonic Frequency Combs for High Resolution Spectroscopy," *Phys. Rev. Lett.* **100**(25), 253901 (2008).
  130. A. Cingöz, D. C. Yost, T. K. Allison, A. Ruehl, M. E. Fermann, I. Hartl, and J. Ye, "Direct frequency comb spectroscopy in the extreme ultraviolet," *Nature* **482**(7383), 68 (2012).
  131. M. A. R. Reber, Y. Chen, and T. K. Allison, "Cavity-enhanced ultrafast spectroscopy: ultrafast meets ultra-sensitive," *Optica* **3**(3), 311 (2016).
  132. A. Ruehl, A. Marcinkevicius, M. E. Fermann, and I. Hartl, "80 W, 120 fs Yb-fiber frequency comb," *Opt. Lett.* **35**(18), 3015 (2010).
  133. T. R. Schibli, I. Hartl, D. C. Yost, M. J. Martin, A. Marcinkevičius, M. E. Fermann, and J. Ye, "Optical frequency comb with submillihertz linewidth and more than 10 W average power," *Nat. Photonics* **2**(6), 355 (2008).
  134. T. Saule, S. Holzberger, O. De Vries, M. Plötner, J. Limpert, A. Tünnermann, and I. Pupeza, "Phase-stable, multi- $\mu$ J femtosecond pulses from a repetition-rate tunable Ti:Sa-oscillator-seeded Yb-fiber amplifier," *Appl. Phys. B* **123**(1)(2017).
  135. I. Pupeza, T. Eidam, J. Kaster, B. Bernhardt, J. Rauschenberger, A. Ozawa, E. Fill, T. Udem, M. F. Kling, J. Limpert, Z. A. Alahmed, A. M. Azzeer, A. Tünnermann, T. W. Hänsch, and F. Krausz, "Power scaling of femtosecond enhancement cavities and high-power applications," *Proc SPIE* **7914**, 791411 (2011).
  136. O. Pronin, M. Seidel, J. Brons, F. Lücking, V. Pervak, A. Apolonski, T. Udem, and F. Krausz, "Carrier-envelope phase stabilized thin-disk oscillator," in *Advanced Solid-State Lasers Congress (2013), Paper AF3A.5* (Optical Society of America, 2013), paper AF3A.5.
  137. A. Klenner, F. Emaury, C. Schriber, A. Diebold, C. J. Saraceno, S. Schilt, U. Keller, and T. Südmeyer, "Phase-stabilization of the carrier-envelope-offset frequency of a SESAM modelocked thin disk laser," *Opt. Express* **21**(21), 24770 (2013).
  138. F. Emaury, A. Diebold, A. Klenner, C. J. Saraceno, S. Schilt, T. Südmeyer, and U. Keller, "Frequency comb offset dynamics of SESAM modelocked thin disk lasers," *Opt. Express* **23**(17), 21836 (2015).
  139. M. Seidel, J. Brons, F. Lücking, V. Pervak, A. Apolonski, T. Udem, and O. Pronin, "Carrier-envelope-phase stabilization via dual wavelength pumping," *Opt. Lett.* **41**(8), 1853 (2016).
  140. S. Hakobyan, V. J. Wittwer, P. Brochard, K. Gürel, S. Schilt, A. S. Mayer, U. Keller, and T. Südmeyer, "Full stabilization and characterization of an optical frequency comb from a diode-pumped solid-state laser with GHz repetition rate," *Opt. Express* **25**(17), 20437 (2017).
  141. G. Di Domenico, S. Schilt, and P. Thomann, "Simple approach to the relation between laser frequency noise and laser line shape," *Appl. Opt.* **49**(25), 4801 (2010).
  142. M. Hoffmann, S. Schilt, and T. Südmeyer, "CEO stabilization of a femtosecond laser using a SESAM as fast opto-optical modulator," *Opt. Express* **21**(24), 30054 (2013).
  143. S. Hakobyan, V. J. Wittwer, K. Gürel, A. S. Mayer, S. Schilt, and T. Südmeyer, "Carrier-envelope offset stabilization of a GHz repetition rate femtosecond laser using opto-optical modulation of a SESAM," *Opt. Lett.* **42**(22), 4651 (2017).
  144. A. McPherson, G. Gibson, H. Jara, U. Johann, T. S. Luk, I. A. McIntyre, K. Boyer, and C. K. Rhodes, "Studies of multiphoton production of vacuum-ultraviolet radiation in the rare gases," *JOSA B* **4**(4), 595 (1987).
  145. M. Ferray, A. L'Huillier, X. F. Li, L. A. Lompré, G. Mainfray, and C. Manus, "Multiple-harmonic conversion of 1064 nm radiation in rare gases," *J. Phys. B At. Mol. Opt. Phys.* **21**, L31 (1988).

## References

---

146. E. Constant, D. Garzella, P. Breger, E. Mével, C. Dorrer, C. Le Blanc, F. Salin, and P. Agostini, "Optimizing high harmonic generation in absorbing gases: Model and experiment," *Phys. Rev. Lett.* **82**(8), 1668 (1999).
147. J. Rothhardt, M. Krebs, S. Hädrich, S. Demmler, J. Limpert, and A. Tünnermann, "Absorption-limited and phase-matched high harmonic generation in the tight focusing regime," *New J. Phys.* **16**(3), 033022 (2014).
148. R. Klas, S. Demmler, M. Tschernajew, S. Hädrich, Y. Shamir, A. Tünnermann, J. Rothhardt, and J. Limpert, "Table-top milliwatt-class extreme ultraviolet high harmonic light source," *Optica* **3**(11), 1167 (2016).
149. F. Frank, C. Arrell, T. Witting, W. A. Okell, J. McKenna, J. S. Robinson, C. A. Haworth, D. Austin, H. Teng, I. A. Walmsley, J. P. Marangos, and J. W. G. Tisch, "Invited Review Article: Technology for Attosecond Science," *Rev. Sci. Instrum.* **83**(7), 071101 (2012).
150. M. D. Seaberg, D. E. Adams, E. L. Townsend, D. A. Raymondson, W. F. Schlotter, Y. Liu, C. S. Menoni, L. Rong, C.-C. Chen, J. Miao, and others, "Ultrahigh 22 nm resolution coherent diffractive imaging using a desktop 13 nm high harmonic source," *Opt. Express* **19**(23), 22470 (2011).
151. G. K. Tadesse, R. Klas, S. Demmler, S. Hädrich, I. Wahyutama, M. Steinert, C. Spielmann, M. Zürch, T. Pertsch, A. Tünnermann, J. Limpert, and J. Rothhardt, "High speed and high resolution table-top nanoscale imaging," *Opt. Lett.* **41**(22), 5170 (2016).
152. M. I. Stockman, M. F. Kling, U. Kleineberg, and F. Krausz, "Attosecond nanoplasmonic-field microscope," *Nat. Photonics* **1**(9), 539 (2007).
153. G. Sansone, F. Kelkensberg, J. F. Pérez-Torres, F. Morales, M. F. Kling, W. Siu, O. Ghafur, P. Johnsson, M. Swoboda, E. Benedetti, F. Ferrari, F. Lépine, J. L. Sanz-Vicario, S. Zherebtsov, I. Znakovskaya, A. L'Huillier, M. Y. Ivanov, M. Nisoli, F. Martín, and M. J. J. Vrakking, "Electron localization following attosecond molecular photoionization," *Nature* **465**(7299), 763 (2010).
154. B. Bergues, M. Kübel, N. G. Johnson, B. Fischer, N. Camus, K. J. Betsch, O. Herrwerth, A. Senftleben, A. M. Saylor, T. Rathje, T. Pfeifer, I. Ben-Itzhak, R. R. Jones, G. G. Paulus, F. Krausz, R. Moshhammer, J. Ullrich, and M. F. Kling, "Attosecond tracing of correlated electron-emission in non-sequential double ionization," *Nat. Commun.* **3**, 813 (2012).
155. C. M. Heyl, C. L. Arnold, A. Couairon, and A. L'Huillier, "Introduction to macroscopic power scaling principles for high-order harmonic generation," *J. Phys. B At. Mol. Opt. Phys.* **50**(1), 013001 (2017).
156. S. Hädrich, Jan Rothhardt, M. Krebs, S. Demmler, A. Klenke, A. Tünnermann, and J. Limpert, "Single-pass high harmonic generation at high repetition rate and photon flux," *J. Phys. B At. Mol. Opt. Phys.* **49**(17), 172002 (2016).
157. C. M. Heyl, J. Gütde, A. L'Huillier, and U. Höfer, "High-order harmonic generation with  $\mu$ J laser pulses at high repetition rates," *J. Phys. B At. Mol. Opt. Phys.* **45**(7), 074020 (2012).
158. J. Bouillet, Y. Zaouter, J. Limpert, S. Petit, Y. Mairesse, B. Fabre, J. Higuët, E. Mével, E. Constant, and E. Cormier, "High-order harmonic generation at a megahertz-level repetition rate directly driven by an ytterbium-doped-fiber chirped-pulse amplification system," *Opt. Lett.* **34**(9), 1489 (2009).
159. A. Vernaleken, J. Weitenberg, T. Sartorius, P. Russbuedt, W. Schneider, S. L. Stebbings, M. F. Kling, P. Hommelhoff, H.-D. Hoffmann, R. Poprawe, and others, "Single-pass high-harmonic generation at 20.8 MHz repetition rate," *Opt. Lett.* **36**(17), 3428 (2011).
160. C.-T. Chiang, A. Blättermann, M. Huth, J. Kirschner, and W. Widdra, "High-order harmonic generation at 4 MHz as a light source for time-of-flight photoemission spectroscopy," *Appl. Phys. Lett.* **101**(7), 071116 (2012).
161. R. J. Jones and J. Ye, "Femtosecond pulse amplification by coherent addition in a passive optical cavity," *Opt. Lett.* **27**(20), 1848 (2002).
162. A. K. Mills, T. J. Hammond, M. H. C. Lam, and D. J. Jones, "XUV frequency combs via femtosecond enhancement cavities," *J. Phys. B At. Mol. Opt. Phys.* **45**(14), 142001 (2012).
163. R. J. Jones, K. D. Moll, M. J. Thorpe, and J. Ye, "Phase-Coherent Frequency Combs in the Vacuum Ultraviolet via High-Harmonic Generation inside a Femtosecond Enhancement Cavity," *Phys. Rev. Lett.* **94**(19), 193201 (2005).
164. C. Gohle, T. Udem, M. Herrmann, J. Rauschenberger, R. Holzwarth, H. A. Schuessler, F. Krausz, and T. W. Hänsch, "A frequency comb in the extreme ultraviolet," *Nature* **436**(7048), 234 (2005).

- 
165. I. Hartl, T. R. Schibli, A. Marcinkevicius, D. C. Yost, D. D. Hudson, M. E. Fermann, and J. Ye, "Cavity-enhanced similariton Yb-fiber laser frequency comb:  $3 \times 10^{14}$  W/cm<sup>2</sup> peak intensity at 136 MHz," *Opt. Lett.* **32**(19), 2870 (2007).
  166. J. Lee, D. R. Carlson, and R. J. Jones, "Optimizing intracavity high harmonic generation for XUV fs frequency combs," *Opt. Express* **19**(23), 23315 (2011).
  167. A. Ozawa, Z. Zhao, M. Kuwata-Gonokami, and Y. Kobayashi, "High average power coherent vuv generation at 10 MHz repetition frequency by intracavity high harmonic generation," *Opt. Express* **23**(12), 15107 (2015).
  168. D. C. Yost, A. Cingöz, T. K. Allison, A. Ruehl, M. E. Fermann, I. Hartl, and J. Ye, "Power optimization of XUV frequency combs for spectroscopy applications [Invited]," *Opt. Express* **19**(23), 23483 (2011).
  169. C. Benko, T. K. Allison, A. Cingöz, L. Hua, F. Labaye, D. C. Yost, and J. Ye, "Extreme ultraviolet radiation with coherence time greater than 1 s," *Nat. Photonics* **8**(7), 530 (2014).
  170. H. Carstens, M. Högner, T. Saule, S. Holzberger, N. Lilienfein, A. Guggenmos, C. Jocher, T. Eidam, D. Esser, V. Tosa, V. Pervak, J. Limpert, A. Tünnermann, U. Kleineberg, F. Krausz, and I. Pupeza, "High-harmonic generation at 250 MHz with photon energies exceeding 100 eV," *Optica* **3**(4), 366 (2016).
  171. H. Carstens, S. Holzberger, J. Kaster, J. Weitenberg, V. Pervak, A. Apolonski, E. Fill, F. Krausz, and I. Pupeza, "Large-mode enhancement cavities," *Opt. Express* **21**(9), 11606 (2013).
  172. N. Lilienfein, H. Carstens, S. Holzberger, C. Jocher, T. Eidam, J. Limpert, A. Tünnermann, A. Apolonski, F. Krausz, and I. Pupeza, "Balancing of thermal lenses in enhancement cavities with transmissive elements," *Opt. Lett.* **40**(5), 843 (2015).
  173. G. Winkler, J. Fellingner, J. Seres, E. Seres, and T. Schumm, "Non-planar femtosecond enhancement cavity for VUV frequency comb applications," *Opt. Express* **24**(5), 5253 (2016).
  174. N. Lilienfein, C. Hofer, S. Holzberger, C. Matzer, P. Zimmermann, M. Trubetskov, V. Pervak, and I. Pupeza, "Enhancement cavities for few-cycle pulses," *Opt. Lett.* **42**(2), 271 (2017).
  175. S. Holzberger, N. Lilienfein, M. Trubetskov, H. Carstens, F. Lücking, V. Pervak, F. Krausz, and I. Pupeza, "Enhancement cavities for zero-offset-frequency pulse trains," *Opt. Lett.* **40**(10), 2165 (2015).
  176. D. R. Carlson, J. Lee, J. Mongelli, E. M. Wright, and R. J. Jones, "Intracavity ionization and pulse formation in femtosecond enhancement cavities," *Opt. Lett.* **36**(15), 2991 (2011).
  177. T. K. Allison, A. Cingöz, D. C. Yost, and J. Ye, "Extreme Nonlinear Optics in a Femtosecond Enhancement Cavity," *Phys. Rev. Lett.* **107**(18), 183903 (2011).
  178. S. Holzberger, N. Lilienfein, H. Carstens, T. Saule, M. Högner, F. Lücking, M. Trubetskov, V. Pervak, T. Eidam, J. Limpert, A. Tünnermann, E. Fill, F. Krausz, and I. Pupeza, "Femtosecond Enhancement Cavities in the Nonlinear Regime," *Phys. Rev. Lett.* **115**(2), 023902 (2015).
  179. E. Seres, J. Seres, and C. Spielmann, "Extreme ultraviolet light source based on intracavity high harmonic generation in a mode locked Ti:sapphire oscillator with 9.4 MHz repetition rate," *Opt. Express* **20**(6), 6185 (2012).
  180. J. Zhang, J. Brons, N. Lilienfein, E. Fedulova, V. Pervak, D. Bauer, D. Sutter, Z. Wei, A. Apolonski, O. Pronin, and F. Krausz, "260-megahertz, megawatt-level thin-disk oscillator," *Opt. Lett.* **40**(8), 1627 (2015).
  181. K. J. Schafer and K. C. Kulander, "High Harmonic Generation from Ultrafast Pump Lasers," *Phys. Rev. Lett.* **78**(4), 638 (1997).
  182. C. J. Saraceno, C. Schriber, M. Mangold, M. Hoffmann, O. H. Heckl, C. R. Baer, M. Golling, T. Südmeyer, and U. Keller, "SESAMs for High-Power Oscillators: Design Guidelines and Damage Thresholds," *IEEE J. Sel. Top. Quantum Electron.* **18**(1), 29 (2012).
  183. C. G. E. Alfieri, A. Diebold, F. Emaury, E. Gini, C. J. Saraceno, and U. Keller, "Improved SESAMs for femtosecond pulse generation approaching the kW average power regime," *Opt. Express* **24**(24), 27587 (2016).
  184. J. Neuhaus, J. Kleinbauer, A. Killi, S. Weiler, D. Sutter, and T. Dekorsy, "Passively mode-locked Yb:YAG thin-disk laser with pulse energies exceeding 13  $\mu$ J by use of an active multipass geometry," *Opt. Lett.* **33**(7), 726 (2008).
  185. D. C. Yost, "Development of an Extreme Ultraviolet Frequency Comb for Precision Spectroscopy," PhD Thesis, University of Colorado (2011).

## References

---

186. J. L. Krause, K. J. Schafer, and K. C. Kulander, "High-order harmonic generation from atoms and ions in the high intensity regime," *Phys. Rev. Lett.* **68**(24), 3535 (1992).
187. I. Pupeza, X. Gu, E. Fill, T. Eidam, J. Limpert, A. Tünnermann, F. Krausz, and T. Udem, "Highly sensitive dispersion measurement of a high-power passive optical resonator using spatial-spectral interferometry," *Opt. Express* **18**(25), 26184 (2010).
188. E. D. Palik, *Handbook of Optical Constants of Solids* (1985).
189. D. C. Yost, T. R. Schibli, and J. Ye, "Efficient output coupling of intracavity high-harmonic generation," *Opt. Lett.* **33**(10), 1099 (2008).
190. Y.-Y. Yang, F. Süßmann, S. Zherebtsov, I. Pupeza, J. Kaster, D. Lehr, H.-J. Fuchs, E.-B. Kley, E. Fill, X.-M. Duan, Z.-S. Zhao, F. Krausz, S. L. Stebbings, and M. F. Kling, "Optimization and characterization of a highly-efficient diffraction nanograting for MHz XUV pulses," *Opt. Express* **19**(3), 1954 (2011).
191. K. D. Moll, R. J. Jones, and J. Ye, "Output coupling methods for cavity-based high-harmonic generation," *Opt. Express* **14**(18), 8189 (2006).
192. J. Wu and H. Zeng, "Cavity-enhanced noncollinear high-harmonic generation for extreme ultraviolet frequency combs," *Opt. Lett.* **32**(22), 3315 (2007).
193. O. Pronin, V. Pervak, E. Fill, J. Rauschenberger, F. Krausz, and A. Apolonski, "Ultrabroadband efficient intracavity XUV output coupler," *Opt. Express* **19**(11), 10232 (2011).
194. I. Pupeza, E. E. Fill, and F. Krausz, "Low-loss VIS/IR-XUV beam splitter for high-power applications," *Opt. Express* **19**(13), 12108 (2011).
195. I. Pupeza, S. Holzberger, T. Eidam, H. Carstens, D. Esser, J. Weitenberg, P. Rußbüldt, J. Rauschenberger, J. Limpert, T. Udem, A. Tünnermann, T. W. Hänsch, A. Apolonski, F. Krausz, and E. Fill, "Compact high-repetition-rate source of coherent 100 eV radiation," *Nat. Photonics* **7**(8), 608 (2013).
196. I. Pupeza, M. Högner, J. Weitenberg, S. Holzberger, D. Esser, T. Eidam, J. Limpert, A. Tünnermann, E. Fill, and V. S. Yakovlev, "Cavity-Enhanced High-Harmonic Generation with Spatially Tailored Driving Fields," *Phys. Rev. Lett.* **112**(10), 103902 (2014).
197. D. Esser, J. Weitenberg, W. Bröring, I. Pupeza, S. Holzberger, and H.-D. Hoffmann, "Laser-manufactured mirrors for geometrical output coupling of intracavity-generated high harmonics," *Opt. Express* **21**(22), 26797 (2013).
198. S. Hädrich, M. Krebs, A. Hoffmann, A. Klenke, J. Rothhardt, J. Limpert, and A. Tünnermann, "Exploring new avenues in high repetition rate table-top coherent extreme ultraviolet sources," *Light Sci. Appl.* **4**(8), e320 (2015).
199. N. Kanda, N. Kanda, T. Imahoko, K. Yoshida, A. A. Eilanlou, Y. Nabekawa, T. Sumiyoshi, M. Kuwata-Gonokami, M. Kuwata-Gonokami, K. Midorikawa, and K. Midorikawa, "Multi-port Intra-Cavity High Harmonic Generation in a Yb:YAG Thin Disk Mode-Locked Oscillator with MHz Repetition Rate," in *Frontiers in Optics 2017* (2017), *Paper LW5F.4* (Optical Society of America, 2017), paper LW5F.4.

# Curriculum Vitae

Name: Clément Paradis  
Date of Birth: July 1, 1989 (France)  
Citizenship: French



## Education

- Oct. 2013 – Dec. 2017: **PhD studies** in the group of Prof. Thomas Südmeyer, Laboratoire Temps-Fréquence (LTF), University of Neuchâtel, Switzerland.
- Sept. 2009 – Nov. 2013: **Diplôme d'ingénieur (Master's degree)**, ENSTA ParisTech (École Nationale Supérieure de Techniques Avancées - ParisTech), France.
- Oct. 2012 – Nov. 2013: **Master of Science with Distinction in Applied Photonics**, Imperial College of London, United Kingdom.
- Sept. 2011 – Sept. 2012: **Master of Science (M.Sc.) Degree Program in Photonics**, Friedrich-Schiller University, Jena, Germany.

## Research Experience

- 2013 – 4 years: **PhD studies** in the Laboratoire Temps-Fréquence (LTF), Physics department, University of Neuchâtel, Switzerland.  
*Development of novel ultrafast high-power thin-disk laser oscillators and applications for metrology and XUV generation*
- 2013 – 6 months: **Master Thesis** in the Quantum Optics and Laser Science (QOLS) research group, Imperial College of London, United Kingdom.  
*Progress in hollow-fiber pulse compression for high-energy few-cycle pulses with double-differential pumping system*
- 2012 – 3 months: **Lab internship** in the Institute of Applied Physics (IAP), Abbe Center of Photonics, Friedrich-Schiller University, Jena, Germany.  
*Femtosecond laser nanostructuring and doping of silicon surfaces*
- 2011 – 3 months: **Lab internship** in the Institute of Electronic Structure and Laser (IESL), Foundation for Research and Technology – Hellas (FORTH), Heraklion, Greece.  
*Building of nonlinear optical setups: non-collinear optical parametric amplifier (NOPA) and intensity autocorrelator.*

## Awards and honors

- 2018: Co-author of the paper "Frequency Comb Stabilization of a 4 W, 50-fs Thin-Disk Laser Oscillator," **awarded outstanding result prize** in the student paper competition at *32<sup>nd</sup> European Frequency and Time Forum (EFTF 2018)*.
- 2017: Co-author of the paper "Towards Few-Cycle Ultrafast Thin-Disk Lasers," awarded **outstanding student poster presentation prize** at *Laser Congress 2017 (ASSL, LAC)*.
- 2011: **Erasmus Mundus Scholarship** to pursue the Erasmus Mundus Master course OPSCITECH (Optics in Science and Technology).



# ***Acknowledgments***

Such work could not have been accomplished without the participation and the help of a great number of people. Unfortunately, these few lines are not enough to cite and thank everybody. I already regret that too many names might be missing from this list.

Firstly, I would like to thank Prof. Thomas Südmeyer for giving me the opportunity to realize my PhD studies in his research group in Neuchâtel. I appreciated the trust and freedom you granted me to conduct my work, whether it was to build the new lab or to initiate research in a new direction and to investigate a technology outside the expertise of the lab. I will keep in mind that doing a lot of karaoke is one of the best ways to train for presentations! I am also grateful to Valentin for accepting being a member of the jury and for his contribution to this thesis and to the lab work in general. Thank you for being authentic and helpful even though sometimes we were not even able to see you behind the pill of work that was waiting for you. I would like to give my special thanks to Norbert who contributed greatly to the experimental work and without whom, the laser development would not have been pushed to this level. Thank you for sharing with me many of the “funny” night shifts. I am very grateful to Stephane who had the patience to read this manuscript and corrected many mistakes, though, he is not the one to blame for the remaining ones.

Then I would like to thank all the current/former/newest colleagues of the group for the lab work, office fun and entertaining leisure events. Maxim, François, Norbert, Olga, Jakub: our high-power team rocks, that’s for sure! Nayara, Kutan, Sargis, Loïc: our office was never really quiet, and I had a good time sharing with you so many jokes. I would like to add more thanks to all other members of the group, Pierre, Antoine, Renaud, Christophe, William, Florian, Matthieu, Nil, Gaetano, Bertrand...

My special acknowledgment goes to Christian Kränkel for the fruitful discussions and his honesty. I will always keep in mind this advice concerning publication or presentation that you gave me once (ok, probably two times): “you should better start again from scratch”. This turned out to be really productive! I am also grateful to Clara Saraceno for sharing her passion of continuously pushing the ultrafast TDL oscillator technology further. Besides, I would like to thank Martin Saraceno for the nice time we spent in Neuchâtel as colleagues, as well as for all the illustrations that he kindly allowed me to use in this manuscript.

## Acknowledgments

---

I am also grateful to my previous professors, mentors, supervisors who provided me such an outstanding education. I owe you a lot and I hope to be worthy of the time you spent on me. Amongst all, I would like to acknowledge Prof. Karsten Plamann (ENSTA ParisTech), Prof. Stelios Tzortzakis (IESL-FORTH), and Prof. John Tisch (Imperial College of London), without whom I would probably do something completely different today.

Besides the scientific research, the PhD studies are a great human adventure shared with many colleagues. Many of them are working in the shadow, their names will not appear on the publications and they will not be in the bright light of the spot on the stage. Even though their impact is often underestimated, these people are part of the key to the success. During my work at the university of Neuchâtel, I am grateful to have benefited from the support of wonderful engineers and technicians: Patrick, Marc, Christian, Isidro, André, Thierry, Daniel, Dominique; as well as marvelous administrative staff: Natacha, Joelle, Sandrine, Patricia. Natacha, I miss your smile and happiness.

Finally, I am very thankful to all my friends who encouraged me during all these years whether they were in Neuchatel with me, in France or somewhere else in the world. You were the light at the end of the tunnel which helped me to keep it up. I enjoyed so many life adventures outside the lab with you. I am looking forward for the next ones. Additionally, I would like to thank my family for their unconditional support during all these years of efforts. None of this could have been possible without you and I owe you a lot. I would like to give my last grateful word to Rica. Thank you for being so wonderful every day by my side.

Neuchâtel, April 2018

Clément Paradis



In this work, recent achievements in the field of ultrafast thin-disk lasers (TDLs) are discussed. The novel ultrafast Yb-based TDL oscillators presented in this thesis show improved performance at sub-100-fs pulse duration. Benefiting from the fruitful combination of the Kerr lens mode locking scheme and the broad emission of the gain materials, TDL oscillators reach new pulse duration limits as well as record-high average powers from any TDL oscillator in both sub-100-fs and sub-50-fs pulse duration regimes. The influence of key laser parameters is investigated for the generation of powerful ultrashort laser pulses. This proof-of-principle study opens avenues for average- and peak-power scaling towards the generation of sub-100-fs pulses from simple one-box lasers with hundred watts of average power and multi-ten microjoules of pulse energy. These results confirm the potential for compact ultrafast Yb-based TDL oscillators to replace complex amplifier systems and Ti:sapphire-based lasers for an extensive range of applications.

These innovative sources aim at directly driving exciting new applications in the fields of spectroscopy and high-field physics. An initial experiment has been realized to highlight the potential and reliability of these lasers and demonstrates the first fully-stabilized optical frequency comb based on a TDL. Additionally, this thesis reports on the proof-of-principle realization of intra-cavity HHG inside a SESAM mode-locked TDL oscillator as a table-top pulsed source of XUV laser light.

About the author:

**Clément Paradis** received a “diplôme d’ingénieur”, in 2013, from ENSTA ParisTech (Ecole Nationale Supérieure de Techniques Avancées, member of the ParisTech network - Université Paris-Saclay), France. He pursued additional master studies in the framework of the European Erasmus Mundus program Optics in Science and Technology (OpSciTech) and received, in 2013, two M.S. degrees in photonics from the Friedrich-Schiller University of Jena, Germany and from the Imperial College of London, United Kingdom, respectively. The same year, he joined the research group of Prof. Dr. Thomas Südmeyer, Time and Frequency Laboratory (LTF), at the University of Neuchâtel, Switzerland. His research interests focus on the development of high-power ultrafast laser sources based on thin-disk laser oscillators and subsequent applications enabled by these novel driving laser sources.